THE EFFECTIVENESS OF TOPICAL TOFACITINIB VS TOPICAL MINOXIDIL ON HAIR GROWTH IN MICE

BY

MISS JINDAPA THUMMAKRIENGKRAI

A THESIS SUBMITTED IN PARTIAL FULFILLMENT OF
THE REQUIREMENTS FOR THE DEGREE OF
MASTER OF SCIENCE (DERMATOLOGY)
CHULABHORN INTERNATIONAL COLLEGE OF MEDICINE
THAMMASAT UNIVERSITY
ACADEMIC YEAR 2016
COPYRIGHT OF THAMMASAT UNIVERSITY

Ref. code: 25595829040418WTR

THE EFFECTIVENESS OF TOPICAL TOFACITINIB VS TOPICAL MINOXIDIL ON HAIR GROWTH IN MICE

BY

MISS JINDAPA THUMMAKRIENGKRAI

A THESIS SUBMITTED IN PARTIAL FULFILLMENT OF
THE REQUIREMENTS FOR THE DEGREE OF
MASTER OF SCIENCE (DERMATOLOGY)
CHULABHORN INTERNATIONAL COLLEGE OF MEDICINE
THAMMASAT UNIVERSITY
ACADEMIC YEAR 2016
COPYRIGHT OF THAMMASAT UNIVERSITY

Ref. code: 25595829040418WTR

THAMMASAT UNIVERSITY
CHULABHORN INTERNATIONAL COLLEGE OF MEDICINE

THESIS

BY

MISS JINDAPA THUMMAKRIENGKRAI

ENTITLED

THE EFFECTIVENESS OF TOPICAL TOFACITINIB VS TOPICAL MINOXIDIL ON HAIR GROWTH IN MICE

was approved as partial fulfillment of the requirements for
the degree of Master of Science (Dermatology)

on April 10, 2017

Chairman Poonkiat Suchonwanit
(Poonkiat Suchonwanit, M.D.)

Member and Advisor Jitlada Meephansan
(Assistant Professor Jitlada Meephansan, M.D., Ph.D.)

Member and Co-advisor
(Saranyoo Ponnikorn, Ph.D.)

Member Sattvachai Prasopdee
(Sattrachai Prasopdee, D.V.M., Ph.D.)

Director, Graduate Studies
(Professor Kesara Na-Bangchang, Ph.D.)

Dean
(Associate Professor Kammal Kumar Pawa, M.D.)

Ref. code: 25595829040418WTR

Thesis Title	THE EFFECTIVENESS OF TOPICAL TOFACITINIB VS TOPICAL MINOXIDIL ON HAIR GROWTH IN MICE
Author	Miss Jindapa Thummakriengkrai
Degree	Master of Science
Major Field/Faculty/University	Dermatology Chulabhorn International College of Medicine Thammasat University
Thesis Advisor	Asst. Prof. Jitlada Meephansan, M.D., Ph.D.
Thesis Co-Advisor	Saranyoo Ponnikorn, Ph.D.
Academic Years	2016

ABSTRACT

Tofacitinib is a JAK3 inhibitor, and belongs to a new class of immunomodulatory agents that target the JAK-STAT signaling pathway. It possesses immunosuppressive, anti-inflammatory, anti-allergic, anti-thrombotic and anti-leukemic effects. Recent studies using mice models and clinical trials in humans have shown that inhibition of JAK-STAT pathway promotes hair growth.

This study compares the stimulatory effect of topical tofacitinib with that of topical minoxidil on hair growth in mice.

Twenty-one eight-week-old male C57BL/6 mice were divided equally into three groups and treated with tofacitinib, minoxidil, DMSO or ethanol via topical application over a coated area on the dorsal side once daily for 21 days. Photographs were taken weekly to determine area hair growth, hair length, and hair growth rate using digital camera and digital microscope. Tissue samples from the treated area were collected at experimental endpoint for histopathological evaluation and determination of cell growth factors expression including VEGF and IGF-1 by RT-PCR and further quantitatively interpretation of VEGF protein by ELISA technique.

Tofacitinib-treated group exhibited significantly more hair regrowth than the minoxidil-treated group (P=0.002) since day 7. As treatment continued from day 14 through 21, distinct hair regrowth was observed (P=0.004 and P=0.012, respectively).

Ref. code: 25595829040418WTR

At experimental endpoint, tofacitinib-treated group demonstrated almost full area of regrown hair (98.5%) as compared to partial area of regrown hair in minoxidil-treated group (61.58%). Mice treated with topical tofacitinib also promoted rapid rate of hair growth in comparison with topical minoxidil (P=0.003). Accordingly, histopathology showed significant increase in the mean number of hair follicles mostly in the anagen phase in tofacitinib-treated group (43.43) as compared to the mean number of hair follicles in the anagen and catagen phase in minoxidil-treated group (28.43), P=0.015. Tofacitinib-treated group demonstrated the least inflammatory cells infiltration among all treatment groups. Besides, newly formed small-sized capillaries were found more in tofacitinib-treated group, whereas slightly dilated completely formed capillaries were more often found in minoxidil-treated group. In case of cell growth factors, the median expression of VEGF mRNA in tofacitinib-treated group (117.45) showed significantly higher in value as compared to that of minoxidil (25.415), P=0.033. Correspondingly, mean VEGF concentration of tofacitinib-treated group (904.77 pg/mL) also demonstrated significantly higher than minoxidil-treated group (562.20 pg/mL), P=0.046. Despite, the median expression of IGF-1 mRNA in minoxidil-treated group (175.46) revealed higher in comparison to tofacitinib-treated group (15.23), P=0.039.

Topical tofacitinib is significantly more efficient in promoting hair growth than topical minoxidil, with faster onset of growth, more rapid rate of hair regrowth, and better outcome. The increasing in VEGF expression which promoted by tofacitinib and its anti-inflammatory effect on hair follicle microinflammation suggest to play a particular role in hair growth promoting mechanism. Our findings allow an open access to use tofacitinib in human clinical trials, which will be beneficial in developing a new therapeutic option for non-scarring alopecia.

Keywords: JAK3 inhibitor, Tofacitinib, Minoxidil, Non-scarring alopecia, Hair growth, VEGF, Hair follicle microinflammation

ACKNOWLEDGEMENTS

First of all, I would like to express my gratitude to Asst. Prof. Jitlada Meephansan, M.D., Ph.D., my advisor, for her helpful support, valuable suggestion, and her dedicated spirit as a role model teacher. Also, I am grateful to my co-advisor, Saranyoo Ponnikorn, Ph.D., for his advice especially in laboratory consultation together with Rungrawee Mongkolrob, Ph.D. for laboratory supervision in protein extracting process. In addition, I would like to acknowledge my gratitude to the committee members, Poonkiat Suchonwanit, M.D. and Sattrachai Prasopdee, D.V.M., Ph.D. for their assistance in providing useful comments through the course of this research, which greatly improved the thesis quality. I am also immensely grateful to Sawang Kesdangsakonwut, D.V.M., Ph.D. and Raksawan Deenonpoe, D.V.M., Ph.D. for the histopathological consultation, and Weerayut Yingmeema, D.V.M. and his colleagues for their assistance during the research experiments carried out at the Center of Animal Research at Thammasat University.

Moreover, the thesis would not achieved this completion without all comments and encouragement from all lecturers in Chulabhorn International College of Medicine. And I would like to extend my thanks to all my classmates for the help and support during the experimental period. Likewise, thank you to those whose names are not mentioned here but were greatly assisted throughout the research course.

Finally, I would like to take this opportunity to explicit my passionate gratitude to my family which always provide me their kind support in everything. And lastly, thank you Sangchai Hongyangyuen, M.D. for all helpful assistance and encouragement whenever I need.

Miss Jindapa Thummakriengkrai

Ref. code: 25595829040418WTR

TABLE OF CONTENTS

Ref. code: 25595829040418WTR

Ref. code: 25595829040418WTR

Ref. code: 25595829040418WTR

Ref. code: 25595829040418WTR

Ref. code: 25595829040418WTR

LIST OF TABLES

Ref. code: 25595829040418WTR

LIST OF FIGURES

Ref. code: 25595829040418WTR

Ref. code: 25595829040418WTR

Ref. code: 25595829040418WTR

LIST OF ABBREVIATIONS

Symbols/Abbreviations	Terms
α	alpha
β	beta
γ	gamma
%	Percent
µL	Microliter(s)
µm	Micrometer(s)
°C	Degree(s) Celsius
/	per
AA	Alopecia areata
ACVRL1	Activin A receptor like type 1
AGA	Androgenetic alopecia
ALADIN	Alopecia areata disease activity index
AT	Alopecia totalis
AU	Alopecia universalis
BAX	B-cell lymphoma 2-associated X protein
Bcl-2	B-cell lymphoma 2
Bcl2L11	Bcl2-like11
Bcl-XL	B-cell lymphoma-extra large
BDNF	Brain derived neurotrophic factor
bFGF	Basic fibroblast growth factor
BMP	Bone morphogenetic protein
BMPR1a	Bone morphogenetic protein receptor type 1a
CASP12	Caspase12
cDNA	Complementary DNA
CI	Confidence interval
cm	Centimeter(s)

Ref. code: 25595829040418WTR

CNTF	Ciliary neurotrophic factor
CO_2	Carbon dioxide
CT-1	Cardiotrophin-1
DHT	Dihydrotestosterone
DLE	Discoid lupus erythematosus
DMSO	Dimethyl sulfoxide
DP	Dermal papilla
EAE	Experimental allergic encephalomyelitis
EDA2R	Ectodysplasin A2 receptor
EGF	Epidermal growth factor
ELISA	Enzyme-linked immunosorbent assay
ERK	Extracellular signal-regulated protein kinase
FDA	Food and drug administration
FERM domain	four-point-one, ezrin, radixin, moesin domain
FFA	Frontal fibrosing alopecia
FGF	Fibroblast growth factor
FGFR1	Fibroblast growth factor receptor 1
GAS	Interferon-gamma activated sequence
GM-CSF	Granulocyte macrophage colony-stimulating factor
HDL	High-density lipoprotein
H&E	Haematoxylin and eosin
HGF	Hepatocyte growth factor
HS	Hair shaft
IFN	Interferon
IFNAR-1	IFNα/β receptor, the α subunit
IFNAR-2	IFNα/β receptor, the β subunit
IFNGR-1	IFNγRα subunit
IFNGR-2	IFNγRβ subunit

IgE	Immunoglobulin E
IGF-1	Insulin-like growth factor 1
IGFR1	Insulin-like growth factor 1 receptor
IL	Interleukin
IRF	Interferon regulatory factor
IRS	Inner root sheath
IRSE	Interferon-stimulated regulatory element
ISRE	Interferon-stimulated response element
JAK	Janus kinase
JH	Janus kinase homology
KIR	Kinase-interacting region
LDL	Low-density lipoprotein
LEF1	Lymphoid enhancer-binding factor 1
LIF	Leukemia inhibitory factor
LLLT	Low-level laser light therapy
LPP	Lichen planopilaris
LPS	Lipopolysaccharides
MD	Mean difference
mg	Milligram(s)
mL	Milliliter(s)
mm	Millimeter(s)
mTOR	Mammalian target of rapamycin
NFkB	Nuclear factor kappa-light-chain-enhancer of activated B cell
ORS	Outer root sheath
OSMR	Oncostatin M receptor
PASI	Psoriasis area and severity index
PDGF	Platelet-derived growth factor
pg	Picogram(s)
PGA	Physician’s global assessment

Ref. code: 25595829040418WTR

PIAS	Protein inhibitors of activated signal transducer and activator of transcription
PKC	Protein kinase C
PlGF	Placental growth factor
PLSS	Psoriatic lesion severity sum
PRP	Platelet-rich plasma
PTGFR	Prostaglandin F receptor
PTP	Protein tyrosine phosphatases
RR	Relative risk
RT-PCR	Real-time polymerase chain reaction
SAP	SAF-A/B, acinus and protein inhibitors of activated signal transducer and activator of transcription
SCID	Severe combined immunodeficiency
SD	Standard deviation
SEM	Standard error of mean
SH	Src homology
SHH	Sonic hedgehog
SOCS	Suppressor of cytokine signaling
STAT	Signal transducer and activator of transcription
TE	Telogen effluvium
TGF	Transforming growth factor
Th	T helper
TNF	Tumor necrosis factor
Tpo	Thrombopoietin
OD	Optical density
UVB	Ultraviolet B
VEGF	Vascular endothelial growth factor
VS	Versus

Ref. code: 25595829040418WTR

CHAPTER 1
INTRODUCTION

1.1 Background and rationale

Hair loss is one of the most common dermatological condition seen by dermatologists worldwide. It can be categorized into scarring and non-scarring alopecia. Androgenetic alopecia (AGA) is the most common form of hair loss in non-scarring alopecia group. It is characterized by progressive hair loss due to miniaturization of hair follicles and is affected both men and women with distinctive patterns of hair loss. The onset often begins around puberty and effects on the individual's self-esteem and quality of life. Its main cause known to result from androgen-dependent process and genetic transmission with associated to suspected pathogenic factors including microbial flora, stress and microinflammation. Moreover, AGA implies a process of shortened anagen phase associated with premature catagen phase which has been advocated to occur as a consequence of decreased in anagen maintaining factors expression, including insulin-like growth factor 1 (IGF-1), basic fibroblast growth factor (bFGF) and vascular endothelial growth factor (VEGF), together with increasing in cytokines promoting apoptosis expression, including transforming growth factor (TGF) -β1, interleukin (IL) -1 α and tumor necrosis factor (TNF) -α. In contrast to its high prevalence and widely influence of AGA, the approved therapeutic options are still limited. Current standard treatment modalities for AGA are oral finasteride and topical solution of minoxidil. Finasteride acts as a potent competitive inhibitor of type II 5α-reductase and inhibits the conversion of testosterone to dihydrotestosterone (DHT). Topical minoxidil, an adenosine-triphosphate-sensitive potassium channel opener and vasodilator, which its mechanism known to extend the duration of anagen phase of hair follicles. In contrast to their efficacy on hair growth promotion, undesirable adverse events seem to be frequently concerned. Accordingly, we are interested in doing research on a new group of medication in the purpose of improving alternative modalities of treatment for non-scarring alopecia patient. Recently, the discovery of tofacitinib as Janus kinase (JAK) 3 inhibitor, a new class of

Ref. code: 25595829040418WTR

immunomodulatory agent has been proposed. It has crucial role in driving autoimmunity on Type I/II cytokines receptors in γc family, as well as cytokines receptors that signal via JAK1 and also disrupts T-helper (Th) 1 and Th2 differentiation together with impaired inflammatory Th17 cells production. Interestingly, previous study shows that inhibitory of JAK-STAT signal could stimulates the activation and/or proliferation of hair follicle stem cells, resulting in promotion of hair growth. However, the mechanism of tofacitinib is still not completely clear, hence further study should be done. In considering, we examine the efficacy in promoting hair growth in mice models of topical tofacitinib as JAK3 inhibitor in comparable to topical minoxidil as standard treatment for AGA. The results will be beneficial in applying to develop a new alternative therapeutic agent for patient whom suffered from non-scarring alopecia in the near future.

1.2 Research question

JAK3 inhibitor, a new class of immunomodulatory agents, provides immunosuppressive, anti-inflammatory, anti-allergic, anti-thrombotic and anti-leukemic effects. It has important role in driving autoimmunity on Type I/II cytokines receptors in γc family, as well as disrupts Th1 and Th2 differentiation and impaired inflammatory Th17 cells production. Moreover, recent studies showed that inhibits JAK-STAT signal could promotes hair growth by activation and proliferation of hair follicle stem cells.

Alopecia is one of the most common condition concerned among patients. The prevalence ranges around 16-96% depend on age, race, and severity of the disease. According to the pathophysiological condition, we could categorized alopecia into scarring and non-scarring subgroup. Therapeutic agents have crucial role targeted in non-scarring alopecia group because of its potential ability in promoting hair growth. AGA, the most common form of non-scarring alopecia, affects wide range group of patients in both sex and all ages. It is characterized by progressive hair loss due to miniaturization of hair follicles, results from androgen-dependent process and genetic predisposition with suspected association of microinflammatory process of dermal

Ref. code: 25595829040418WTR

papilla. The role of JAK3 inhibitors in non-scarring alopecia has not been clearly elucidated.

Concurrently, this study will demonstrate the efficacy in hair growth promotion of tofacitinib as JAK3 inhibitor compare with minoxidil as standard treatment for AGA and also demonstrate another feasible mechanism of JAK3 inhibitor in promoting hair growth in non-scarring alopecia.

1.3 Specific objective

The primary objective is to compare the promoting effect of 2% topical tofacitinib to 5% topical minoxidil on hair growth in mice model.

The secondary objective is to determine and compare the level of VEGF and IGF-1 after treatment of 2% topical tofacitinib to 5% topical minoxidil in mice model.

1.4 Hypothesis

2% topical tofacitinib might be as effective as 5% topical minoxidil on hair growth promotion in mice model.

1.5 Keywords

JAK3 inhibitor
Tofacitinib
Minoxidil
Non-scarring alopecia
Hair growth
VEGF
Hair follicle microinflammation

Ref. code: 25595829040418WTR

1.6 Operation definition

Male C57BL/6 mice aged 8 weeks.

1.7 Ethical consideration

The study protocol was approved by Thammasat University's Animal Ethical Committee and conducted according to Ethical Principals and Guidelines for the Use of Animals for Scientific Purpose.

1.8 Limitation

Duration of the study.

1.9 Expected benefits and application

Non-scarring alopecia, especially the most common form, AGA, has been one of frequently seen conditions in dermatological clinic worldwide. It effects on the individual's self-esteem and quality of life. Despite its high prevalence and widely influence, still has limitations on the efficacy of its therapeutic agents together with problems on adverse events. This research will prove tofacitinib efficacy in comparable to minoxidil on hair growth promotion and also help us in better understanding the mechanism of tofacitinib as hair growth promoter, which would be beneficial in applying the use in patients whom suffered from non-scarring alopecia as an alternative therapeutic treatment.

1.10 Obstacles and strategies to solve the problems

The concentration of DMSO was exorbitant resulting in dermatitis on the dorsal back coated area of mice treated with DMSO and tofacitinib (use DMSO as a solvent). The problem was solved by decreasing DMSO concentration or use other appropriate solvents instead.

Ref. code: 25595829040418WTR

Table 1.1 Administration and time schedule

	2016												2017					
	JAN	FEB	MAR	APR	MAY	JUN	JUL	AUG	SEP	OCT	NOV	DEC	JAN	FEB	MAR	APR	MAY	JUN
Research proposal																		
Research ethics																		
Experiment																		
Data analysis																		
Manuscript preparation																		
Publication																		

Ref. code: 25595829040418WTR

CHAPTER 2
REVIEW OF LITERATURE

JAK3 inhibitors, a new class of immunomodulatory agents, provides immunosuppressive, anti-inflammatory, anti-allergic, anti-thrombotic and anti-leukemic effects (1).

Tofacitinib (former CP-690,550), a drug of the JAK inhibitor class, inhibits JAK3 and JAK1 with lesser effects on JAK2 (2, 3). Among JAK inhibitors family, tofacitinib has high specificity compared to others. It has crucial role in driving autoimmunity on Type I/II cytokines receptors in γc family : IL-2, IL-4, IL-7, IL-9, IL-15 (2, 4), as well as cytokines receptors that signal via JAK1. Accordingly, tofacitinib disrupts Th1 and Th2 differentiation and also impaired inflammatory Th17 cells production (4). The drug has been widely used in clinical trials in many settings of rheumatoid arthritis (2, 5–7), inflammatory bowel disease (8), psoriasis (9), organ transplantation (1, 10) to corneal inflammation and dry eyes (11, 12). Subsequently, tofacitinib is approved by Food and Drug Administration (FDA) for the treatment of rheumatoid arthritis since 2012 and currently in clinical trials for treatment of psoriasis (13), vitiligo (14) and alopecia areata (AA) (15, 16).

Recently, Xing et al. demonstrated that pharmacological inhibition of the Janus kinase signal transducer and activator of transcription (STAT) pathway promotes hair regrowth in AA. JAK inhibitors could block interferon (IFN) -γ, IL-2, and IL-15Rβ prevented the development of AA, decreasing the $CD8^{+}NKG2D^{+}$ T cells accumulation in the skin and the response of dermal IFN in AA mice model (15). Accordingly, Harel et al. demonstrated that JAK inhibitors treatment resulted in rapid onset of hair growth in mice by the process of activates WNT and Sonic hedgehog (SHH) signaling pathways (3) which mimics the mechanisms of normal anagen initiation (17, 18). Moreover, JAK-STAT inhibition causes hair follicle progenitor cells activate (3) from the evidence that hair germ compartment (P-cadherin+) of drug-treated hair follicles was proliferated (19). And also enhanced pathways, such as Rho and integrin signaling, involved in cell motility and migration which responsible in the transition between telogen and anagen (3). Furthermore, they also examined the effect of JAK inhibition

Ref. code: 25595829040418WTR

on hair growth in human tissue (grafted human fetal scalp skin onto severe combined immunodeficient mice). The results suggested that tofacitinib treatment promotes hair elongation rate and enhances effect on inductivity of human dermal papilla. These were followed from the process evidence from repressed in receptors that involved in the modulation of dermal papilla inductivity, such as fibroblast growth factor receptor 1 (FGFR1), activin A receptor like type 1 (ACVRL1), insulin-like growth factor 1 receptor (IGFR1), oncostatin M receptor (OSMR) and prostaglandin F receptor (PTGFR) (20–23) collocate with down-regulated of proapoptotic genes included Bcl2-associated X protein (BAX), Bcl2-like11 (Bcl2L11) and Caspase12 (CASP12). In addition, genes up-regulated by tofacitinib treatment involved the members of the TGF-β pathway and the bone morphogenetic protein (BMP) pathway, which formerly shown to have a critical role in dermal papilla (DP) inductivity (23–26). Besides, lymphoid enhancer-binding factor 1 (LEF1), another key regulators of the WNT pathway, which control dermal-epidermal interactions (27, 28) together with the NOTCH pathway members, which control hair follicle fate (29) were also overexpression in tofacitinib treatment (3).

In summary, from their findings can be concluded that JAK-STAT signal inhibition stimulates the activation and/or proliferation of hair follicle stem cells, resulting in promotion of hair growth (3).

Despite the aspect of successful therapeutic options for alopecia areata and variants with tofacitinib and ruxolitinib (JAK2/JAK1 inhibitors), another aspect is the potential risks of these medications if taken in oral form, Craiglow et al. were concerned about this matter. They decided to pursue a trial of topical ruxolitinib on a failure treatment alopecia universalis (AU) patient. Then finally reported a first case of successful treatment of alopecia universalis with topical ruxolitinib as JAK inhibitor. While further studies are needed to confirm the efficacy, safety and tolerability (30).

Nowadays, the problem of hair loss has been increasingly concerned by patients, which can be categorized into scarring and non-scarring alopecia. Examples of the diseases organized in scarring alopecia group are lichen planopilaris (LPP), frontal fibrosing alopecia (FFA), and discoid lupus erythematosus (DLE). Meanwhile, AGA, AA, and telogen effluvium (TE) are in non-scarring alopecia group.

Ref. code: 25595829040418WTR

AA is a non-scarring loss of hair on scalp or other area of the body, affects approximately up to 2% of population. Its pathogenesis is involved multifactorial autoimmune associated with unknown etiology. AA is characterized by one or more well-defined hair-less non-scarring patches, which it could be progressed to more severe form as involved whole scalp or body hair. In spite of multiple treatments available including steroids, photochemotherapy and immunotherapy, AA could be spontaneously resolved within 1 year, whereas up to 25% developed to severe form.

TE, defined by loss of telogen hair, results from abnormal hair cycling. Possible causes of TE including systemic illness, drug induced, loss of weight, nutritional deficiency, delivery, oral contraceptives interruption and scalp inflammation. As same as AA, TE could spontaneously be resolved, after treated underlying causes (31).

AGA is known to be the most common form of non-scarring alopecia. According to a previous study in Thailand reported the prevalence of baldness reaching 61.78% at 70 years of age (32). It mainly results from androgen-dependent process and genetic transmission, in associated with suspected pathogenic factors such as microbial flora, stress (endogenous and exogenous), and microinflammation (33). The hallmark characteristics of AGA is vellus-like hair transformation in correspond to miniaturization of hair follicles during repeated hair cycles with premature termination of anagen (34). In male AGA, commonly known to be associated with increasing in 5-alpha reductase activity propagate to an increase in DHT production, which may be results in hair follicle loss, yet the mechanism is not clearly known (35).

Apart from genetic predisposition and androgens main theories, suspected noticeably coincidence from scalp biopsy has shown that the miniaturization of terminal hairs is oftenly associated with perifollicular lymphocytic infiltration, and fibrosis (36). Subsequently, this may be one of the credible reasons encourages microscopic follicular inflammation theory.

In the focus on hair follicle cycling, AGA implies a process of shortened anagen phase associated with premature catagen phase. Catagen has been advocated to occur as a consequence of decreased in anagen maintaining factors expression, including IGF-1 (37), bFGF (38), and VEGF (39), associated with increasing in

Ref. code: 25595829040418WTR

cytokines promoting apoptosis expression, including TGF-β1 (25, 34), IL-1α, and TNF-α (33, 40).

The goal of treatment in AGA is to increase in hair number on the scalp and to delay progression of hair thinning. Current available treatment modalities for AGA with proven efficacy (FDA approved) are oral finasteride (dose 1 mg/day) and topical solution of minoxidil (dose 2% for women, 5% for men).

Finasteride acts as a potent competitive inhibitor of type II 5α-reductase and inhibits the conversion of testosterone to DHT (41, 42), which is involved in miniaturization process of hair follicle in AGA. In the focus on drug efficacy, according to a systematic review of twelve studies showed moderate-quality evidence that daily use of oral finasteride increased the mean hair count from baseline in comparison to placebo treatment, reported as a percentage of the initial count in each patient, at short term (mean difference (MD) 9.42%, 95% confidence interval (CI) 7.95%-10.90%, I^2 50%) and at long term (MD 24.3%, 95% CI 17.92%-30.60%, I^2 0%) and also increased in the proportion of patients reported as improved by investigator assessment in the short term (relative risk (RR) 1.80, 95% CI 1.43-2.26) (43). In contrast to its efficacy, adverse effects of finasteride are increasingly concerned especially on sexual functions (reported in clinical trials at rates of 2.1% to 38%) (44), which leads to poor compliance problem. Moreover, Thompson et al. reported that taking finasteride may associate with increased risk of high-grade prostate cancer (6.4 % and 5.1 % in the finasteride treated group compared to placebo group respectively, $P<0.001$; RR 1.67, 95% CI 1.44%-1.93%) due to it prevented or delayed the onset of cancer (45), but long term follow-up of the same subjects proved no significant difference in the rate of overall survival or survival after the diagnosis of prostate cancer (the 10-year survival rate was 73.0% with 95% CI 68.1%-78.0% and 73.6% with 95% CI 68.3%-78.9% in finasteride-treated group and placebo group respectively, among those with high-grade prostate cancer) (46). Nevertheless, further study is required to conclude the association between the use of finasteride and prostate cancer. Another limitation of finasteride is its slow onset and must be in long term use which may increase risk of adverse effects. Finasteride is contraindicated in who are or may potentially be pregnant because of the risk in impair virilization of a male fetus (47).

Ref. code: 25595829040418WTR

Topical minoxidil, an adenosine-triphosphate-sensitive potassium channel opener and vasodilator (33), which feasible mechanism is to extend the duration of anagen phase of hair follicles by induces cell growth factors including VEGF, hepatocyte growth factor (HGF), IGF-1 and activates uncoupled sulfonylurea receptor on dermal papilla plasma membrane leading to HGF and IGF-1 enhancement, as well as inhibits TGF-β which acts as hair matrix cells apoptosis inducer, and lastly dilates hair follicle arteries and increases blood flow in dermal papilla (48). In the aspect of clinical use, Olsen et al. reported that 5% topical minoxidil was significantly greater in efficacy to 2% topical minoxidil and placebo in increasing hair regrowth in AGA patient (5% topical minoxidil treated group showed 45% more hair regrowth than 2% topical minoxidil treated group at week 48, P=0.025). The adverse events using topical minoxidil are dose-dependent, commonly from dermatologic nature such as pruritus, itching, burning and other symptoms of scalp dermatitis, but no systemic effects has been reported (49). Another important adverse event of patient using topical minoxidil is that it provokes a transitory TE. TE is characterized by increased hair shedding, in case of minoxidil use, the condition caused by mechanism of fast reentry to anagen phase of the hair follicles. Although acute TE from minoxidil treatment is reversible and transient, but the condition causes psychoemotional stress which leads to the main cause of concern and the reason for seeking medical advice (50).

Since clinical success rate of the treatment of AGA with modulators of androgen metabolism or hair growth promoters is still limited. In spite of the standard treatment of AGA which are oral finasteride and topical minoxidil, still some problems on adverse events which leads to drop out of patient. Thus, we are interested in doing research on a new group of medication in purpose of improved alternative modalities of treatment for non-scarring alopecia patient. As mentioned above, tofacitinib as JAK3 inhibitor, a new class of immunomodulatory agent, provides multiple therapeutic effects. In the focus on hair promoting effect, inhibitory of JAK-STAT signal could leads to initiate anagen phase of hair cycle, and also activates hair follicle stem cells. In considering, another possible mechanism in promoting hair growth of tofacitinib maybe take part in the process of hair follicle microinflammation, due to its anti-inflammatory effect. However, the mechanism of tofacitinib is still not completely clear, hence further study should be done. In this research, we are interested in the treatment of tofacitinib

Ref. code: 25595829040418WTR

on its efficacy in promoting hair growth in mice, in comparable to topical minoxidil which has been approved as standard treatment for AGA, the most common form of non-scarring alopecia. The process of determining therapeutic mechanism of tofacitinib in the study which involved clinical, histopathology and cytokine protein expression would lead to further understanding in the mechanism of tofacitinib and probably be beneficial in developing an alternative group of drug for patient with non-scarring alopecia in the near future.

Ref. code: 25595829040418WTR

CHAPTER 3
JAKS AND STATS

3.1 JAKs and STATs

We all known that cytokines and IFN are cell-to-cell messengers inducing a lot of important biological responses in target cells. Recent years, a new signaling pathway has been clarified. This extraordinary pathway involves proteins families, designated as JAKs and STATs (51). This pathway has been constitutive to both type I (IFNα/β) and type II (IFNγ) interferons and also cytokines within type I cytokine receptors superfamily members including IL-2, IL-3, IL-4, IL-5, IL-6, IL-7, IL-9, IL-11, IL-13, IL-15, granulocyte macrophage colony-stimulating factor (GM-CSF), OSM, ciliary neurotrophic factor (CNTF), cardiotrophin-1 (CT-1), growth hormone, prolactin, erythropoietin, and thrombopoietin. The JAK-STAT pathway is a signaling system which immensely rapid transfer from membrane to nucleus and could be induced by different cytokines to elucidate signals (52).

3.1.1 JAKs characteristics

JAKs are comparatively large kinases (approximately 1150 amino acids) with approximately 120–130 kDa of molecular weight. Two transcription of JAK2 have been identified, while multiple spliced forms of JAK3 have been identified, including variation that lacks a part of the catalytic domain (53). These variant transcripts is not well understood of its functional significance, but it is fascinating to theorize that a normally occurring dominant negative form of JAK3 may have regulatory function (52).

3.1.2 Structure of JAKs

The JAK family consists of 4 members including JAK1, JAK2, JAK3, and TYK2. The JAK family of protein kinases are structurally in having tandem kinase and pseudokinase domains which refers name to JAK family. The catalytic domain is named C-terminal kinase, and the definite function of pseudokinase domain is not yet to be clearly determined. The termed JAK homology (JH) domains are used to define regions of homology shared by JAKs. While C-terminal–to–N-terminal named in Src homology (SH) domains (54). The JH1 domain is the kinase domain and

Ref. code: 25595829040418WTR

the JH2 domain is the pseudokinase domain. These two JH domains characterize the most unique feature of the protein because of having extensive homology to tyrosine kinase domains. The JH1 domain is a functional tyrosine kinase domain with an essential YY motif in the activation loop, hence JH1 plays a critical role in catalytic activity (55). The JH2 domain, a kinase-like or pseudokinase domain, plays an important role in regulation of JAK family proteins activation and cytokine-induced signaling. The previous theoretical model strongly suggested that the JH2 domain has a negative effect on the JH1 domain kinase activity (56). The JH5 to JH7 (as well as segment of the JH4) domains consist of the four-point-one, ezrin, radixin, moesin (FERM) domain regulating the catalytic activity and associated with receptors and other proteins mediation. Activation of JAK1 mutants requires intact FERM domain in order to support type I IFN signaling (57). Moreover, in the JAK2 FERM domain, tyrosine 913 mutation also has been shown to result in the kinase activation though the cytokine stimulation is absent (58). In case of JAK3, the FERM domain mutations could influence function of protein, which these proteins were shown to be lack of kinase activity and the association with receptors were failed (59). The binding of JAKs and box 1/proline-rich region of cytokine receptors has been mediated by residues that located in the JH7 region (60), which this interaction eventually regulates localization and turnover of receptor (61). The JAKs N-terminal is associated with cytokine receptor subunits. STATs have a preserved tyrosine which the process of phosphorylation could allow dimerization of STAT. The STAT dimerization mediates by SH2 domain, also an N-terminal region takes part in the dimerization process of STAT. The N and C-terminal regions of STATs bind with interacting proteins on both sides.

Ref. code: 25595829040418WTR

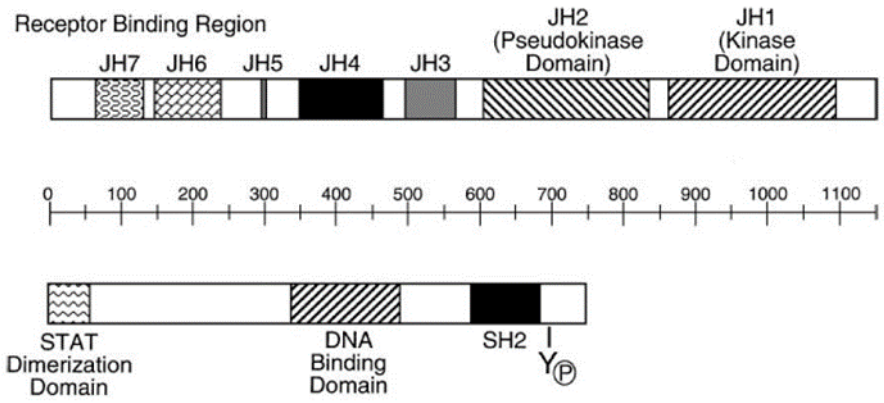

Figure 3.1 Structure of JAKs and STATs (52)

3.1.3 Cytokine receptor signaling via JAKs

Many cytokines and growth factors signals mediate by JAKs. Precisely, JAK1 and TYK2 are required for IFNα/β signaling, while IFNγ required JAK1 and JAK2 (62). Moreover, erythropoietin and growth hormone have been shown to activate JAK2 (63, 64), while IL-6 activated JAK1, JAK2, and TYK2 (65). JAK2 also accomplices with βc which shared subunit of the IL-3, IL-5, and GM-CSF receptors (66). In case of JAK3, it could only be activated by cytokines receptors in γc family including IL-2, IL-4, IL-7, IL-9, and IL-15 (2, 4), as well as cytokines receptors that signal via JAK1 (the particular receptor subunits of cytokines in γc family (e.g. IL-2Rβ) associate with JAK1) (67). Subsequently, all type I cytokines activated JAKs (summarized in Table 3.1). Alike, the IFNα/β receptor, the α subunit (IFNAR-1), is associated with TYK2, whereas the β subunit (IFNAR-2) is corresponded with JAK1 (68). For the IFNγRα subunit (IFNGR-1) associates with JAK1 and IFNγRβ (IFNGR-2) associates with JAK2. The β1 subunit of IL-12R associates with TYK2, while the β2 subunit associates with JAK2 (69). In conclusion, JAKs are integrally associated with receptors and could be amplified by ligand in multiple receptor systems.

Ref. code: 25595829040418WTR

Table 3.1 Cytokines activate JAKs and STATs (52)

Type I Cytokines	Jaks	STATs
Cytokines whose receptors share γc		
IL-2, IL-7, IL-9, IL-15	Jak1, Jak3	Stat5a, Stat5b, Stat3
IL-4	Jak1, Jak3	Stat6
IL-13*	Jak1, Jak2, Tyk2	Stat6
Cytokines whose receptors share β_c		
IL-3, IL-5, GM-CSF	Jak2	Stat5a, Stat5b
Cytokines whose receptors share gp130		
IL-6, IL-11, OSM, CNTF, LIF, CT-1	Jak1, Jak2, Tyk2	Stat3
IL-12^{+}	Jak2, Tyk2	Stat4
Leptin^{+}		Stat3
Cytokines with homodimeric receptors		
Growth hormone	Jak2	Stat5a, Stat5b, Stat3
Prolactin	Jak2	Stat5a, Stat5b
Erythropoietin	Jak2	Stat5a, Stat5b
Thrombopoietin	Jak2	Stat5a, Stat5b
Type II Cytokines	Jaks	STATs
Interferons		
IFNα, IFNβ	Jak1, Tyk2	Stat1, Stat2
IFNγ	Jak1, Jak2	Stat1
IL-10$^{\#}$	Jak1, Tyk2	Stat3

*IL-13 does not share γc but uses IL-4Rα.

$^{+}$IL-12 and leptin do not share gp130, but their receptors are related to gp130.

$^{\#}$IL-10 is not an interferon, but its receptor is a type II cytokine receptor.

Primarily, ligand binding with receptor results in dimerization/oligomerization which leads to the JAKs juxtapositioning through homodimeric or heterodimeric interactions. The recruitment results in phosphorylation

Ref. code: 25595829040418WTR

of JAKs via autophosphorylation and/or transphosphorylation by either tyrosine kinases families or other JAKs. As a result, JAK kinase activity increases activation, then phosphorylate receptors on tyrosine residues, which these targets act as docking sites that allow other SH2 domain–containing signaling molecules to bind including STATs, protein phosphatases, Src kinases, Shc, Grb2, and PI-3 kinase (70).

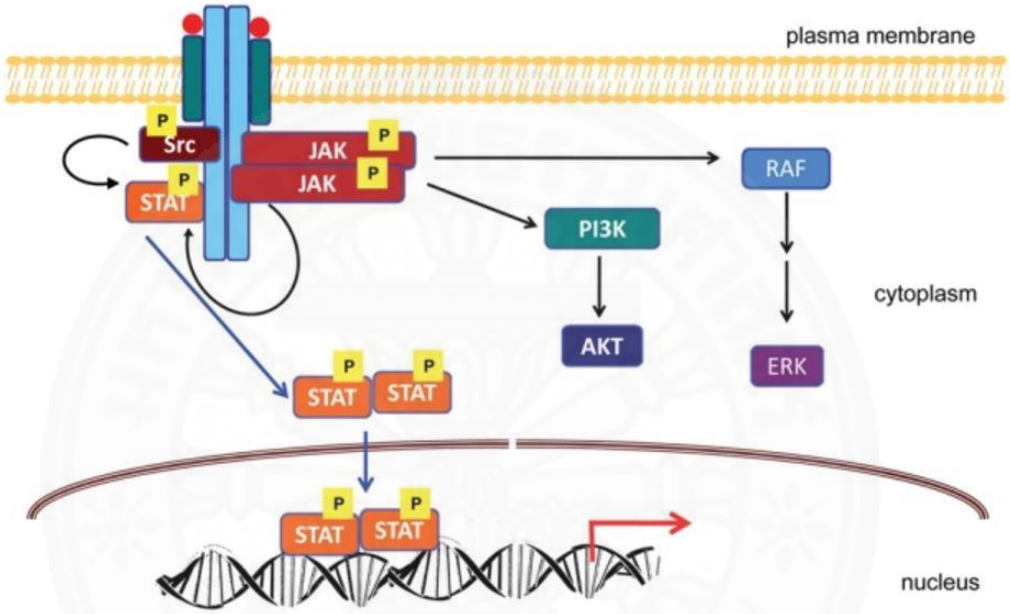

Figure 3.2 Signaling pathways mediated by JAKs (71)

3.1.4 JAK1

Previous studies have designated that JAK1 is convoluted in signaling by members of the IL-2 receptor family (IL-2R, IL-7R, IL-9R, and IL-15R), the IL-4 receptor family (IL-4R and IL-13R), the gp130 receptor family (IL-6R, IL-11R, LIF-R, OSM-R CT-1R, CNTF-R, NNT-1R/BSF-3R, and Leptin-R), and cytokine receptors class II (type I IFN-R, type II IFN-R, IL-10R) (72). According to these receptors function pleiotropism, Rodig et al. reported that JAK1 knockout mice displayed an early postnatal lethal phenotype (73) that accomplished them in suckling defect from a neurological lesion caused by losing in leukemia inhibitory factor (LIF) function (74). Corresponding to this, LIF and IL-6 response was considerably decreased in $JAK1^{-/-}$

Ref. code: 25595829040418WTR

tissues. Also, JAK1$^{-/-}$ mice exerted defects in production of thymocyte and B cell, which associated in responses to IL-7 defection, which is critical in development of early lymphocyte (75). Moreover, JAK1 nonattendance leads to seriously abnormalities in type I and type II interferons biological response. Defect in response to IL-10 also occurs in JAK1$^{-/-}$ mice. In conclusion, JAK1 exhibits an important role in biological responses to several cytokine receptor families mediation (76).

3.1.5 JAK2

JAK2 is extensively expressed and is elaborated in signaling by the common β chain family, and the class II receptor cytokine family certain members. Defect of the murine JAK2 gene caused erythropoiesis failure which lead to embryonic lethality at day 12.5 (77). According to the cells harvested from these mice showed that JAK2 is necessary for IL-3, GM-CSF, IL-5, thrombopoietin (Tpo), and IFN-γ, exception of IL-6 and IFNα/β signaling. However, JAK2 is not crucial for development of T cell from the evidence that normal thymic subsets occured after JAK2$^{-/-}$ fetal liver cells were transfered into irradiated JAK3$^{-/-}$ recipients (78).

3.1.6 TYK2

At first, TYK2 was identified as a crucial component in a screen for mutants in IFN-α signaling (79). Remarkable that profound defects in IFN-α/β signaling were found in TYK2$^{-/-}$ mice (80). Cells harvested from these mice are insensitive to type I IFNs in low doses but antiviral responses are rather normal. IL-10 signaling is found normal and responses of IL-12 were defective, but not totally absent. In response to IL-6, there was no defect observed. Unexpectedly, response to lipopolysaccharides (LPS) was defect in correspond to macrophages with ineffective TYK2, although the mechanism of this defect still not be clarified (81). Consequently, TYK2 shows to be the most important in IL-12 and LPS biological response mediation (76, 78).

3.1.7 JAK3

The previous biochemical studies indicated that JAK3 signals through all receptors that enroll the common γC receptor family including IL-2R, IL-4R, IL-7R, IL-9R, IL-15R, and IL-21R (52). JAK3$^{-/-}$ mice exhibit severe lymphopoiesis defects, similarly to that observed in γC-deficient mice (82). Due to a critical role in IL-2 signaling of JAK3, JAK3 with ineffective T cells have problems in negative selection and the functional peripheral T cells maintenance (83). In contrast to murine, in human,

Ref. code: 25595829040418WTR

these patients are severe combined immunodeficiency (SCID), which characterize in defective profound T cell, with normal B cells (52). SCID is a primary disastrous immunodeficiency that results in an illness with severe recurrent infection such as diarrhea, atopic dermatitis, and failure to thrive in children. Lately, the crucial immunopathologic enigma was discovered when the common γ chain or γc mutations were found to regulate X-linked SCID (84). In case of lacking of this receptor subunit, lymphocytes would be incapable to respond to IL-2, IL-4, IL-7, IL-9, IL-15, and IL-21 leading to T cells development, NK cells, and B cells function defect. Due to the selectivity of JAK3 to γc, JAK3 mutations would bring out similar sequelae (85). This contrast has been credited to IL-7 that is necessary for mice pre-B cell growth, but null in humans. Consequently, JAK3 plays a crucial role in development of lymphoid. Mice with $JAK3^{-/-}$ defect in IL-2, IL-4, and IL-7 response, leading to SCID phenotype (76).

3.2 Signal transducers and activators of transcription

Signal transducers and activators of transcription, or STATs are transcription factors that triggered by multiple cytokines and growth factors and having important roles in signal transduction pathways (86). The seven mammalian STAT proteins have been identified consist of STAT1, STAT2, STAT3, STAT4, STAT5a, STAT5b, and STAT6. Additional forms of STATs 1 and 3 result from splicing alternation or posttranslational proteolytic cleavage (87). Also, STAT-4 has 2 forms denoted STAT-4α and STAT-4β and STAT-5 has 2 isoforms which are STAT-5a and STAT-5b that encoded by isolated tandem-linked genes (88). Most STATs are 750 to 800 amino acids in approximate length, while approximately 850 amino acids for STAT2 and STAT6.

STATs display a modular structure and harbor 7 well-defined domains made up of an N-terminal, a coiled-coil, a DNA binding, a linker region, an SH2, a tyrosine activation, and a C-terminal transactivation domain. The amino-terminal region is important for STAT function, if there are small missing or deletions in this region, STATs would be unable phosphorylated. Nuclear import, export, receptor binding, and collocates with the DNA binding domain also the domain important functions. Furthermore, during inactive state, the amino-terminal region also regulates

Ref. code: 25595829040418WTR

STATs dimerization (89). The coiled-coil domain, an α-helical configuration, associates with regulatory proteins, and has receptor binding functions. The DNA binding domain is a β-barrel with an immunoglobulin fold which lies carboxy-terminal to the coiled-coil domain. In the most proximal half of γ-activated sequence (GAS) elements, each STAT component recognizes bases. The DNA binding cooperation is at least probably important in transcriptional activity effectiveness (76). The linker domain is a spacer that maintains proper construction between the DNA binding domains and dimerization. The SH2 domain is the most highly preserved domain among the STATs, functions in STAT signaling, important to recruit the STATs in order to activate receptor complexes and for the collaboration with Src and JAK kinases. Moreover, STAT homodimerization and heterodimerization also require this domain, which demanding for nuclear localization and DNA binding activities. The transactivation domain is variety in among family members, it regulates the target genes transcriptional activation. C-terminally abbreviated STATs 3, 4, and 5 isoforms behave as dominant-negative proteins according to previous report (72).

Ref. code: 25595829040418WTR

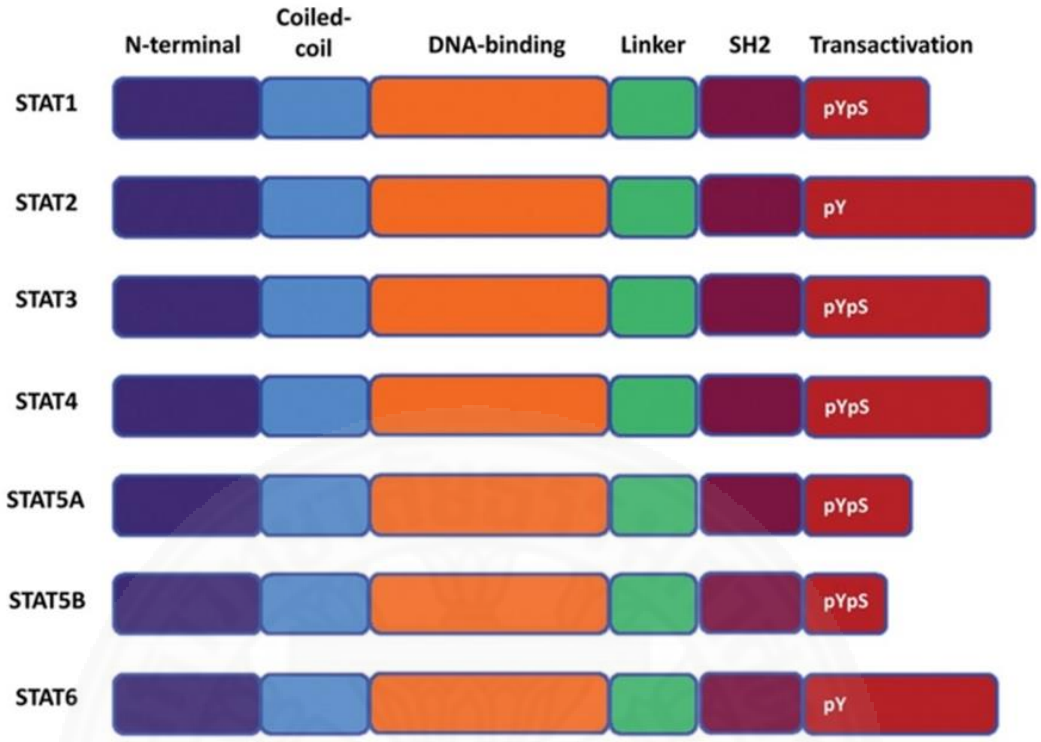

Figure 3.3 STAT proteins structure (71)

STATs are inactive within cells in unstimulated condition, the cytosolic proteins exhibit an unphosphorylated state. During cytokine stimulation, phosphorylated form of tyrosine residues on the receptor are induced then contributed to STATs docking sites via their SH2 domains. Bounding the receptor, in response to cytokine stimulation, STAT family members become tyrosine phosphorylated. This phosphorylated tyrosine residue seems to be attained by growth factor receptors as well as Src and JAK kinases, up to cell type and ligand/receptor interactions nature. In this case, the phosphorylation stimulates STAT proteins reorientation and homo/heterodimerization along the interaction between the SH2 domain of one STAT molecule and the phosphotyrosine residue of another. And after phosphorylated, the process of dimerized STATs translocate to the nucleus occur (90). In the nucleus, normally, the STAT homo/heterodimers can directly bind to DNA, but not the case of activation by type I interferons (IFNα and IFNβ). STAT1-STAT2 heterodimer which is activated by type I interferons requires p48, a DNA binding protein, to bind DNA.

Ref. code: 25595829040418WTR

The STAT1-STAT2-p48 complex recognizes a comparatively nonpalindromic, AGTTTNCNTTTCC (91), interferon-stimulated response element (ISRE) motif, while other STAT complexes contribute to bind semipalindromic motifs, TTCNNNGAA or TTCNNNNGAA. Nevertheless, it is obviously known that such sequences can also be perceived by several other STATs.

3.2.1 Cytokine and growth factor receptors involved in STAT activation

According to the studies of multiple hematopoietin receptors from the cytokine family reveal that the active form of the dimerized receptors are promoted by ligand binding. The activation is considered to generate close resemblance of cytoplasmic receptor tails and leads the transphosphorylation of the receptor-associated JAKs to be enabled. Then, activated JAKs phosphorylate specific tyrosine motifs in turning mediate recruited STATs to their appropriate receptor, which require the STAT SH2 domains ability to perceive a phosphotyrosine residue and 4–5 carboxy-proximal amino acids (has been known as the receptor STAT recruitment motif). Corresponding to the recruited STATs nature and the similarities of structure, divide the hematopoietin receptors into multiple relevant families, including the IFN/IL-10 receptor family, IFN-γ receptor, IFN-α receptor, IL-10 receptor and IL-10 related receptors, Gp130 receptor family, IL-2 receptor family, IL-3 receptor family, single chain receptor family, and non-cytokine receptors (receptor tyrosine kinases (RTks) and G-protein-coupled receptors) (76).

Table 3.2 The recruitment of specific STATS is mediated by implicated cytokine receptor tyrosine motifs (76).

STAT	Receptor	STAT-binding tyrosine motif[a]
Stat1	IFN-γ	YDKPH
Stat2	IFN-α	YVFFP
Stat3	IL-6, LIF, IL-10	YXXQ
Stat1, Stat3	IL-6	YXPQ
Stat4	IL-12	YLPSNID

Ref. code: 25595829040418WTR

Table 3.2 The recruitment of specific STATS is mediated by implicated cytokine receptor tyrosine motifs (76). (Cont.)

STAT	Receptor	STAT-binding tyrosine motif[a]
Stat5	IL-2	YLSLQ
		YCTFP
		YFFFH
	IL-7	YVTMS
	IL-9	YLPQE
	EPO	YLVLD
		YTILD
	PRL	YLDPT
		YVEIH
	GH	YVSTD
		YFCEA
		YITTE
		YTSIH
	GM-CSF	YLSLP
		YLCLP
		YVSSA
		YVELP
		YCFLP
Stat 6	IL-4	YKAFS
		YKPFQ

a The tyrosine is not conserved in the murine system.

3.2.2 STAT family members

More from the critical developmental role in primitive eukaryotes of STAT, previous studies reveal that STATs predominantly evolved to host responses

Ref. code: 25595829040418WTR

mediation to stress in mammals (72, 88). These studies enlightened a significant level of specificity in STAT function. For instance, type I and type II IFNs are mainly transduced signals by STAT1 and STAT2. Whereas, STAT4 and STAT6 importantly enact in the naive T cells polarization into Th1 and Th2 cells, respectively. Nonetheless, STAT3 and STAT5 have more pleiotropic function, and are induced by even more cytokines in their activation. Due to this, they present to be more closely correlate with the STATs within lower species eukaryotes.

3.2.2.1 STAT1

STAT1 homodimers are activated by IFNγ initiating GAS-driven genes transcription. Type I IFNs induce STAT1 homodimers and STAT1/STAT2 heterodimers formation. The later complex links with p48 then induce ISRE-driven genes transcription. Recent studies enlightening of IFN-γ roles against chemically induced and spontaneous tumors in mice, according to evidence that deficiency of STAT1 and IFN-γ mice lead to develop chemically induced tumors more frequently and rapidly than normal mice. Furthermore, RAG2/STAT1 double knockout mice seem to develop cancer spontaneously at higher frequency than $RAG2^{-/-}$ mice, thus, these are evidence of an IFN-γ/STAT1 dependent tumor immune surveillance system (93). Moreover, some studies have proposed that STAT1 affects apoptosis via caspases regulation (94). This hypothesis has been supported by many studies that inactive STAT1 (e.g. $STAT1^{Y701F}$) conserves cells from apoptosis (95).

3.2.2.2 STAT2

Role in IFN-α/β signaling is the main function of STAT2 by complexes with interferon regulatory factor (IRF) 9 and STAT1 binding interferon-stimulated regulatory elements (IRSEs). Correspondingly, STAT2 knockout mice are viable and fertile but viral infections are vulnerable (96). In cells with deficiency of STAT2 found that upregulated-STAT1 in response of IFN-α is impaired. Consequently, of GAS-dependent genes, the IFN-α induction, which are apparently not directly STAT2 dependent, is impaired. Nonetheless, lacking response of GAS-driven genes IFN-α is not supposed in $STAT2^{-/-}$ macrophages, while in STAT1 express normal levels (78).

Ref. code: 25595829040418WTR

3.2.2.3 STAT3

Primarily described as an acute-phase response factor, activated by IL-6 and multiple other cytokines. STAT3 targeted deletion cause lethal in embryo at day 7.5. STAT3 has an important role in biological functions diversity for example growth of cell, induction and suppression of apoptosis, and also cell sensitivity (97). T cells and hepatocytes with STAT3 deficiency response to IL-6 poorly, while deficiency of STAT3 in macrophages and neutrophils causes IL-10 response impairment, which leads to amplify cytokines production. STAT3 deletion in mammary glands brings about delayed programmed cell death that happens during involution of cyclical mammary gland. In keratinocytes, STAT3 lacking still allows normal development of skin and hair initiation, but after that disruption of hair cycle tends to occur. Also, wound healing, migration of epidermal cells in vitro, and thymic architecture are disturbed (98). Activation of STAT3 and STAT5 are usually upon engagement of growth factor receptors and promote expansion of cell by transactivating genes encoding proteins which they enhance survival of cell (including B-cell lymphoma 2 (Bcl-2) and B-cell lymphoma-extra large (Bcl-X_L)). Activation of STAT3 and STAT5 are also usually activated in cells that can be transform several oncogenes (v-src and BCR-abl for example). In conclusion, STAT3 and STAT5 function in an aspect of growth promotion and/or transformed cells surveillance, contrast with STAT1, which suppresses these functions. It has been hypothesized that STAT1 and STAT3 maintain an important biological balance in regulation of normal cells growth, thus, a cellular phenotype transformation and/or oncogenesis may occur if the balance disruption (78).

3.2.2.4 STAT4

Wurster et al. reported that IL-12 activates STAT4 and STAT4 knockout mice phenotype is identical to IL-12 or IL-12R subunits lacking mice, which known to be impaired Th1 differentiation, IFN-γ production, and cell-mediated immunity (99). As predictable, mice with STAT4 deficiency are resistant to autoimmune diseases described by responsiveness to Th1, such as arthritis, diabetes, and experimental allergic encephalomyelitis (EAE) models (100). In contrast, deficiency of IL-12, IL-12 receptor, and STAT4 in mice seems to provoke higher susceptibility to intracellular infection. And possibly, STAT4 may have both anti- or

Ref. code: 25595829040418WTR

pro-inflammatory effects. Furthermore, IL-23 can also activate STAT4 and, in human, STAT4 phosphorylation can be induced by IFN-α/β (101).

3.2.2.5 STAT5

STAT5a and STAT5b genes are chromosomally linked and closely similar (>90% identical). Activation of STAT5a and STAT5b genes are induced by multiple cytokines. Abnormality in development of Prolactin-mediated mammary gland has been reported to be found in STAT5a knockout mice, while STAT5b knockout mice develop sexually dimorphic growth retardation. Conversely, many STAT5a/b-deficient mice die within just few weeks after birth, have defective in corpus luteum development leading infertility, and have mammary gland development disruption. Either male or female STAT5a/b knockout mice have smaller fat pads size and the level of IGF-1 is declined. Moreover, these double knockout mice also develop lymphopenia, neutrophilia, anemia, thrombocytopenia, and hypocellular bone marrow (98, 99). Roughly, myeloid development is normal in STAT5a/b-deficient mice, but cytokine-dependent proliferation in vitro, survival, and in vivo myeloid cells migration to inflammatory sites are impaired (104). B cell precursors and mature B cells numbers are reduced in these mice and also decreased in IL-7 response, in contrast to immunoglobulins number that still intact. Absence of NK cells are reported in these mice but developmental of thymus is normal, nonetheless, in vitro peripheral T cells seem to be impaired proliferation. Apparently, STAT5a/b$^{-/-}$ mice, similar to IL-2$^{-/-}$ mice, establish autoimmunity, and the pathology is contributed (78).

3.2.2.6 STAT6

STAT6 is activated by IL-4 and IL-13, and is important for Th2 differentiation. STAT6 associates to the expression of GATA-3 and c-maf regulation, which are two transcription factors involved in Th2 function. STAT6 is necessary for chromatin in the IL-4 locus remodeling because of its function on Th2 differentiation (105). In addition, deficiency of STAT6 B cells are incapable to withstand class switching and surely unable to produce IgE. Previously known IL-4 inhibits Th1 responses also through STAT6. As predicted, STAT6$^{-/-}$ mice are defected in helminthic parasites expulsion, reduced pathology in asthma models, and exacerbate Th1 diseases like EAE severity (100). Tumor immunity is intensified in STAT6 deficiency (106).

Ref. code: 25595829040418WTR

3.3 Cytokine signaling negative regulation

Multiple protein tyrosine phosphatases (PTP) such as SHP-1, CD45, and PTP1b have been proved to be cytokine signaling negative regulators. CD45 negatively regulates proliferation of IL-3-mediated cell, erythropoietin-dependent haematopoiesis, and antiviral responses (107). Binding of PTP1b with JAK2 and TYK2 via phosphorylated activation loop then discourages signaling, but JAK1 and JAK3 are probably unregulated by this phosphatase. Finally, after nucleus translocation, dephosphorylation of STATs occur. Binding of dimerized STATs with protein inhibitors of activated STAT (PIAS) members, which known to be SUMO E3 ligases, the represented STATs sumoylation, nevertheless, is an unproven, although feasible, probability. In addition, transcription of SH2 family containing proteins (suppressor of cytokine signaling or SOCS proteins) is induced by cytokine stimulation. SOCS proteins prohibit signaling in several ways including to bind and inhibit JAKs, bind to cytokine receptors then block recruitment of STATs, and ubiquitination promotion and JAK/receptor complex degradation. Dephosphorylation of STATs occurs in the nucleus, but the integrity of dominating nuclear STAT phosphatase still unclear (78).

Ref. code: 25595829040418WTR

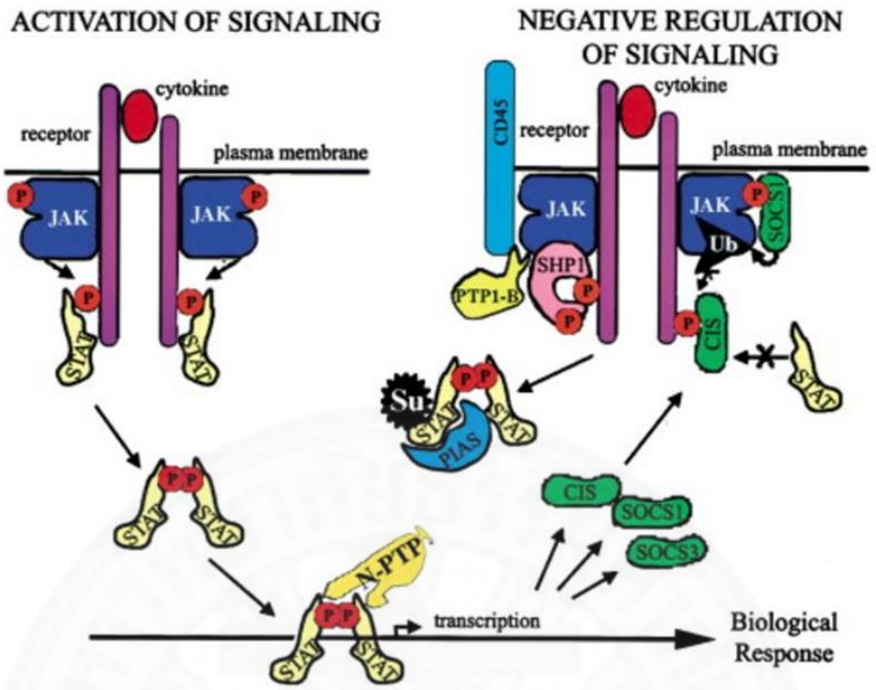

Figure 3.4 Positive and negative regulation of cytokine signaling (78)

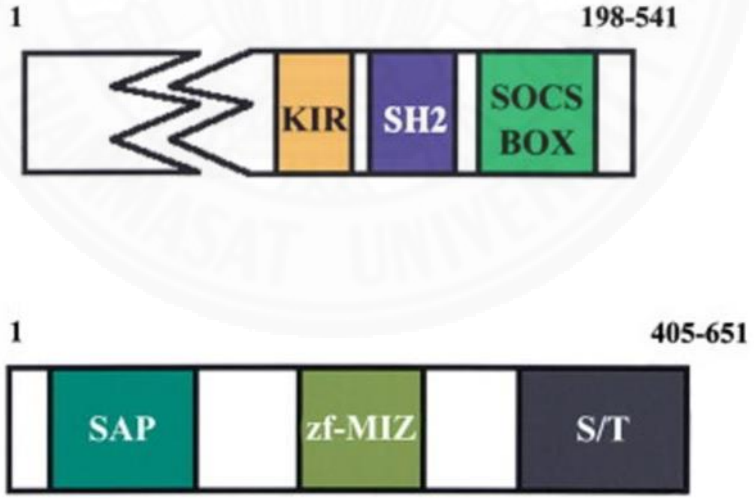

Figure 3.5 This figure shows SOCS and PIAS family member structure. SOCS proteins contains SH2 domain in the middle and SOCS box at C-terminal, likewise, SOCS1 and SOCS3 consist of a kinase-interacting region (KIR). PIAS proteins compose of SAP (SAF-A/B, Acinus and PIAS) domain, ring-finger domain, and serine/threonine rich region at C-terminal (78).

Ref. code: 25595829040418WTR

CHAPTER 4
JAK INHIBITORS

4.1 JAK inhibitors

Cytokine receptors targeted has been an effective therapeutic modality in treating immune-related diseases. In the past few years, many researches directly effort towards intracellular cytokines signaling pathways especially an important one, the JAK-STAT signaling pathway. At first, researchers tried heading toward the development of therapeutic drugs in treating cancer, then, they clarified that the intracellular protein kinases and their receptors targeted is one of the most important and attractive probability in treating autoimmune diseases.

Recently, first generation of JAK inhibitors were launched out in 2011 and being approved for clinical use with still a problem of less specificity. Thereafter, second generation of JAK inhibitors have been launched and appeared to be more specific. In spite of the selectivity might not results in increasing the efficacy, but hypothesizes that it might be more favorable in diseases with very few involved cytokines (108).

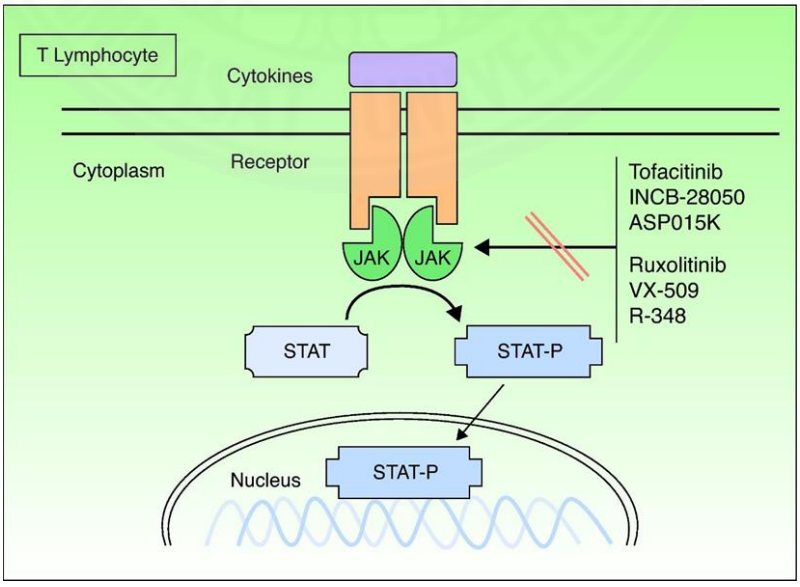

Figure 4.1 JAK inhibitors mechanism of action (109)

Ref. code: 25595829040418WTR

4.1.1 Ruxolitinib

Ruxolitinib (Jakafi®) is a JAK2/JAK1 inhibitor, with also some activity on JAK3 and TYK2. JAK3 deletion disrupts the development of lymphocyte due to its essential function in cγc cytokine signaling. Nonetheless, JAK1 gene targeting also consequences SCID phenotype. Thus, from this aspect, it would be hypothesized that this group of first-generation JAK inhibitor drugs might share similar mechanisms of action, up to the cytokines that have been blocked (2). Ruxolitinib is currently approved in treating intermediate to high-risk myeloproliferative disorders including post-essential thrombocythemia myelofibrosis and primary myelofibrosis post-polycythemia vera myelofibrosis (110). Ruxolitinib diminishes systemic symptoms and splenomegaly, thus also improves overall survival rate. According to phase I/II clinical trial data led to upcoming and ongoing clinical trials in United States of America and Europe. Closely monitoring of drug dosing can help preventing adverse events from erythropoiesis and thrombocytopoiesis reduction. Moreover, inhibitory of JAK1 from ruxolitinib has led to an inflammatory cytokine signaling inhibition, which benefits in patients with rheumatoid arthritis and psoriasis (111). Recently, in 2016, Craiglow et al. decided to pursue a trial of topical ruxolitinib on a failure treatment alopecia universalis patient. Then finally reported a first case of successful treatment of alopecia universalis with topical ruxolitinib as JAK inhibitor. While further studies are needed to confirm the efficacy, safety and tolerability (30). In September 2016, Mackay-Wiggan et al. has proposed another open-label clinical trial of using oral ruxolitinib in patients with moderate-to-severe AA. At the endpoint, patients at least 50% achieved hair regrowth as compare to baseline and the mean hair growth was reported in high percentage with neither serious adverse events nor discontinuation of therapy required from patients was reported (112), as fully described in Chapter 6, JAK Inhibitors and Hair Growth. In conclusion, ruxolitinib has shown therapeutic efficacy in a wide range of disorders according to its property of JAK-STAT inhibition.

4.1.2 Baricitinib

Baricitinib is also a JAK1/JAK2 inhibitor. It has been proved to have efficacy in a highly active rheumatoid arthritis patient who resist to modifying and biologics drugs by treating with high dose (up to 4 or 8 mg once daily in 2 weeks period). Adverse effects are dose dependent including hemoglobin and neutrophil count

Ref. code: 25595829040418WTR

decreasing and increase of low density lipoprotein (LDL) and creatinine (2). In psoriasis, oral baricitinib resulted in improvement of moderate to severe psoriasis after treatment for 12 weeks (113).

4.1.3 Tofacitinib

Tofacitinib (CP-690,550, Xeljanz®) is a selective JAK3 inhibitor with nanomolar potency and has kinome selectivity in high degree. Tofacitinib has exhibited γc-cytokine signaling potent inhibition by blocking T cell proliferation driven by IL-2 and selectively functions over JAK2-mediated GM-CSF-driven proliferation of HUO3 cells (114). Moreover, tofacitinib has been demonstrated to inhibit both JAK3- and JAK1-dependent STAT activation potently with specificity through JAK2 pathways mediation (115). IL-21, also uses common γ chain, is an important cytokine that acts as an immunoregulator, which has crucial functions on T cells, B cells, and NK cells. Tofacitinib reported to disturb IL-21 signaling in mice and human $CD4^+$ T cells proving by STAT3 and STAT1 phosphorylation inhibition in mice and STAT phosphorylation induced by IL-2, IL-4, IL-7, IL-15, and IL-21 was blocked in human. This reaffirm that in both mouse and human T cells tofacitinib affects downstream signaling pathways of JAK3-dependent γc-cytokine receptors. More from this, tofacitinib was found inhibiting phosphorylation of STAT3 and STAT1 driven by IL-6 in $CD4^+$ T cells of mice, as same as in human, the results were similar. They further examined and found that JAK3-deficient mice totally suppressed STAT5 phosphorylation mediated by IL-7. They concluded that not just T cells, but both STAT1 driven by IL-6 and STAT pathways activated by cytokines in γc family are JAK1 dependent. Tofacitinib also suppressed phosphorylation of STAT1 driven by IL-12. From these evidences, tofacitinib interferes with multiple JAKs and thus influential to multiple cytokine signaling cascades in T cells. Furthermore, Th cells differentiation is also affected by inhibition of JAK3. The expression of Th2 cytokines and GATA3 were inhibited by tofacitinib, in contrast not affected to proliferation of Th cells mediated by T cell receptor. The production of IL-2 was augmented, and by STAT5-activated, IL-2 could limit Th1 and Th2 cells production (116). In Th2 cells, expression of IL-4 mRNA was detectable and suppressed in the existence of tofacitinib. Of which, the findings correlate with tofacitinib efficacy in Th2-mediated allergic disease models (117). In case of Th1, tofacitinib strongly inhibited T-bet expression and the IFN-γ-

Ref. code: 25595829040418WTR

producing Th1 cells differentiation, but the proliferation was not affected. This inhibition had similar quantity as in IFN-γ neutralizing antibody or T cells with STAT1 deficiency. They suggested that the mechanism by which tofacitinib inhibits Th1 differentiation is to inhibit STAT1 signaling mediated by IFN-γ- and IL-12 (4). Kamran et al. has shown that generation of Th17 cells can be occur from naïve T cells in the condition of absence of TGF-β signaling if using IL-23, IL-1β, and IL-6 (118). Tofacitinib potently inhibited IL-17A, IL-17F, and IL-22 expression while the generation of Th17 cells occurred in the absence of TGF-β1. But if TGF-β1 presence, tofacitinib did not affect IL-17A or IL-17F expression, though affected IL-22-production. IL-21, another key cytokine generated by Th17 and follicular Th cells, tofacitinib potently suppressed its production, no matter how Th17 cells were generated. Thus, tofacitinib can induce the production of IL-17 in TGF-β1-induced Th17 cells, although in pathogenic IL-23-induced Th17 cells, it inhibits the production of IL-17. Tofacitinib also blocks Rorγt expression, T-bet, and IL-23R (4). Kamran et al. also examined whether tofacitinib could affect the established arthritis in mice and found that arthritis was significant reduction within 48 hours (day 50) after initiating tofacitinib treatment which the symptoms continue to improve until the experimental endpoint. Interestingly, within 4 hours of initial tofacitinib administration, the inflammatory mediator expression was significantly reduced. Due to the data that tofacitinib effectively inhibited the activation of STAT1 in T cells in response to IL-6, IFN-γ, and IL-12. Continuation of using tofacitinib further inhibited STAT1-responsive genes expression to approximate normal levels as disease resolved. Correlatively, after 7 days of treatment, the arthritis severity score, histopathology, and immunohistochemistry demonstrate significantly reduced inflammation (4). Of note inhibition of JAK1 and JAK3 property of tofacitinib is responsible for the anti-inflammatory activity regulation. In sepsis model, which known to be IFN-γ dependent, the production of TNF and IL-1 was blocked by tofacitinib. Hence, the production and action of TNF can be disturbed by tofacitinib (4).

Ref. code: 25595829040418WTR

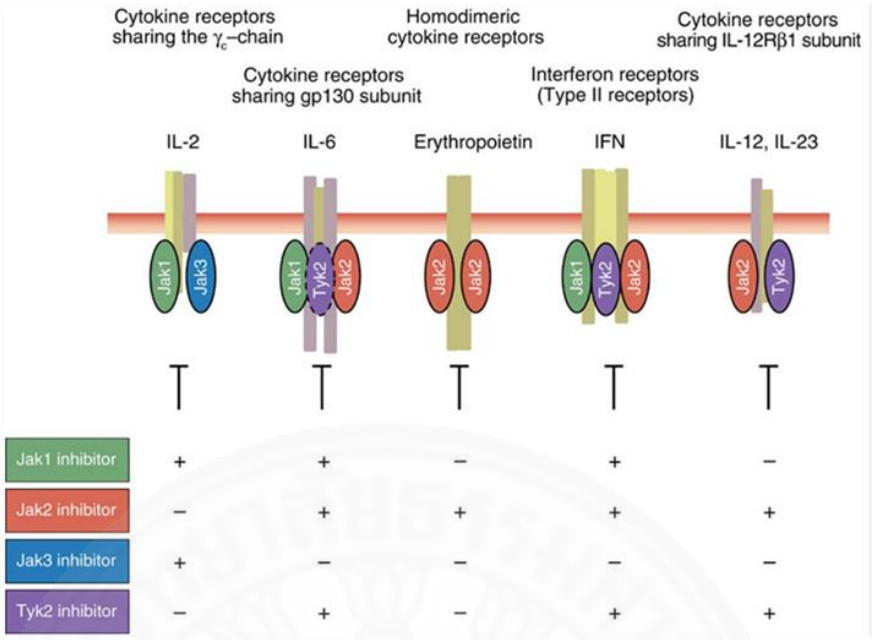

Figure 4.2 The inhibition of various JAKs by selected cytokines impact signaling (119)

Subsequently, tofacitinib has been widely used in clinical trials in many settings of rheumatoid arthritis (2, 5–7), inflammatory bowel disease (8), psoriasis (9), organ transplantation (1, 10) to corneal inflammation and dry eyes (11, 12). Recently, in November 2012, tofacitinib has been approved by FDA in treating rheumatoid arthritis with 5 mg twice daily dose recommended.

In dermatological condition, tofacitinib has been used in many clinical settings. Psoriasis is one of the common inflammatory skin diseases found in out-patient dermatological department. Boy et al. reported that in phase 1, randomized, dose escalation, double-blind study, 59 patients with mild-to-moderate psoriasis were taken a 14-day course of oral tofacitinib 5 mg, 10 mg ,20 mg, 30 mg and 50 mg twice daily and 60 mg once daily. The results demonstrated that the improvement of Psoriatic Lesion Severity Sum (PLSS) score in tofacitinib treatment was higher than placebo ($P<0.01$), with exception of the 5 mg twice daily dose. Also, the physician's global assessment (PGA) score in 50 mg twice daily group was significantly improved more in tofacitinib-treated group compared to placebo ($P<0.05$) (9). In phase 2b, of 197 patients, after twelve weeks of treatment, the proportion of patients achieving 75% or Psoriasis Area and Severity Index (PASI75) reduction was significantly higher in

Ref. code: 25595829040418WTR

tofacitinib-tread group (2 mg, 5mg, and 15 mg twice daily) than in placebo (120). In phase III, double-dummy, placebo-controlled, 12-week trial, in 1,106 patients with moderate-to-severe plaque type psoriasis comparing the effectiveness oral tofacitinib 5 mg, 10 mg twice daily, subcutaneous etanercept 50 mg twice weekly, and placebo. The results demonstrated that of tofacitinib dose 10 mg twice daily was not inferior to etanercept and superior to placebo (13). Others similar design studies seem to results in the same way that tofacitinib affects the improvement of PASI75 superiorly to placebo and non-inferiorly to standard therapeutic treatment. Rates of serious adverse events including infections and malignancies were low (121). Latest in 2016, Papp et al. reported that longer term (2 years) efficacy in treating psoriasis of tofacitinib (5mg, 10 mg twice daily) was maintained, of note 10 mg twice daily had higher efficacy than 5 mg twice daily. The overall rate of adverse effects, serious adverse effects, or adverse effects lead to discontinuation was not dose-related through week 52 and those rates were not significantly different comparing to that of other drugs treating psoriasis. The most common adverse effects is infection (122). Apart from oral form, topical form of tofacitinib also has been in clinical trials. 81 patients with plaque type psoriasis were recruited to intra-subject, left-right, randomized, controlled study. After matching left and right psoriatic plaques, then randomized applying 2%, 0.2%, or 0.02% tofacitinib or vehicle solution once or twice daily. Unfortunately, after 1 month of application without supervised, the primary end point was not reached by any treatment group (123). In the most recently published journal of Papp et al. reported that, in phase 2b randomized, double-blind study using 1% and 2% tofacitinib ointment compared with vehicle in 435 adult plaque psoriasis patients, at 8 weeks application of 2% tofacitinib ointment once daily and twice daily demonstrated higher in efficacy than vehicle. The tolerability and safety were acceptable (124).

Another example in dermatological condition, vitiligo, a common hypopigmenting or depigmenting skin disorder, which affects the patients' self-esteem and quality of life. Craiglow et al. reported a case of a 50-year-old woman suffered from widespread and progressive vitiligo for at least 1 year with failure treatment of topical steroid, tacrolimus, and narrowband ultraviolet B (UVB) phototherapy. After using 5 mg every other day of oral tofacitinib for 3 weeks, then increasing dosage to 5 mg daily for 2 months partial repigmentation of the face and upper extremities was

Ref. code: 25595829040418WTR

observed. After 5 months, the forehead and hands depigmented skin become repigmented (125).

Moreover, tofacitinib has been proved to be beneficial in many other dermatological disorders such as atopic dermatitis (126) and dermatomyositis (127). Interestingly, in hair loss condition or alopecia, especially non-scarring form, tofacitinib (both in oral and topical form) has been widely mentioned and involved in multiple successful clinical trials, which will be fully described in Chapter 6, JAK Inhibitors and Hair Growth.

4.1.4 Second-generation JAK inhibitors

Second generation JAK inhibitors has been developed to be more specific including GLPG0634 is proved to be selectively JAK1, while Vertex's VX-509 is reported as JAK3 specific. In spite of the selectivity, still curious that whether this affects the efficacy. Currently, phase 2 trials have shown these second-generation JAK inhibitors efficacy in treating rheumatoid arthritis. However, further studies have to be done in order to expand the knowledge, to confirm the results, and to evaluate those possible adverse events.

4.2 Adverse events of JAK inhibitors

The most common adverse events of JAK inhibitors is infection. Most infections have been urinary tract infection, upper respiratory tract infection, and viral gastroenteritis. Nonetheless, serious or opportunistic infection has been reported such as Mycobacterial tuberculosis, Pneumocystis carinii pneumonia, and Cytomegalovirus. Treatment with tofacitinib has been reported of increasing frequency of Herpes zoster which may follow from the reduction of NK cells by inhibitory of JAK1 or JAK3. In case of hematologic side effects, anemia, thrombocytopenia, and lymphopenia have been reported, possible from inhibitory of JAK2, which known to be crucial for erythropoietin signaling and colony stimulating factors activation. The use of JAK inhibitors also related with hypercholesterolemia suggesting that high level of LDL, triglycerides, and high density lipoprotein (HDL) may result from the inhibitory of IL-6 signaling mediation. Accordingly, cardiovascular adverse effects have been reported. Elevations of transaminases or creatinine have also been noted. In case of malignancy,

Ref. code: 25595829040418WTR

a seriously concerned side effect, has been noted after treated with tofacitinib, may be due to its primary effects on JAK1 and JAK2, which known to be critical in the signaling of IFN and for immunoediting of cancer (2, 128).

Ref. code: 25595829040418WTR

CHAPTER 5
HAIR

Hair is one of the most important parts of human which defines our characteristic. It helps keeping most mammals warm and protecting from harmness. Hair has diversity of style, colour, shape, and growth pattern. Normally, human hair has been changed in many ways due to disorder, aging, and external precipitating environment. Among hair structures, the hair follicle serves as a feasible model system. The producing segment of hair follicle sustains cyclic regeneration in the adult from an enthusiastic stem cell pool. This chapter aims to describe hair biology and hair cycle of human and murine model.

Hair bulk consists of keratinocytes, the epithelial cells that form into hair shaft, and also the inner root sheath and outer root sheath that are encircled. The dermal papilla (DP), functions directly in the keratinocytes activities forming the follicle and finally generating the hair shaft (129).

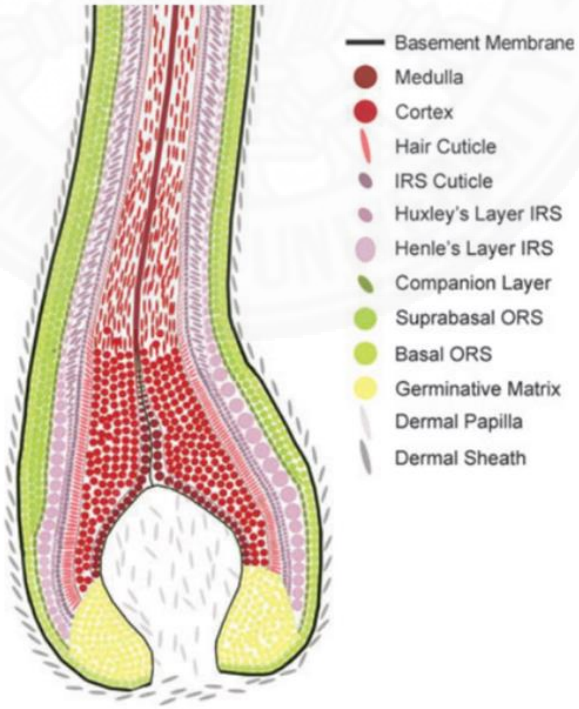

Figure 5.1 The hair follicle bulb cellular compartments (130)

Ref. code: 25595829040418WTR

5.1 Hair morphogenesis

During embryo, the beginning of skin tissue is just a single layer of epidermal stem cells. Then after that, mesenchymal cells occupy the skin to generate the underlying collagenous dermis. Underneath epidermal layer, the particular dermal cells directly coordinate in small clusters, stimulating the above epithelial stem cells in to downward growth manner and finally generate a hair follicle. The epithelium is connected together composing the continuation of the follicle. Both structures are detached from the dermis by in between basement membrane consisting of quantity extracellular matrix and growth factors which synthesized and predominantly deposited by epithelial cells. Along the chemotactic tract, the follicle sprouts down. The differentiation of the inner layers occurs generating the concentric-shaped cylinders and finally form the central hair shaft (HS) and the surrounding IRS. The DP, an inductive mesenchymal cluster, develop into the follicle base permanent component (131). It navigates along with the downgrowth of epithelium, then becomes enfolded by the hair bulb. Approximately as it bulb situates the bottom of dermis, the follicle becomes totally mature. During this time (in the dorsal skin of mice at approximate postnatal day 6), at the base of follicle, the division of proliferative cells continue, generating the progenitor cells that finally differentiate to form the mature growing hair on the skin surface.

Ref. code: 25595829040418WTR

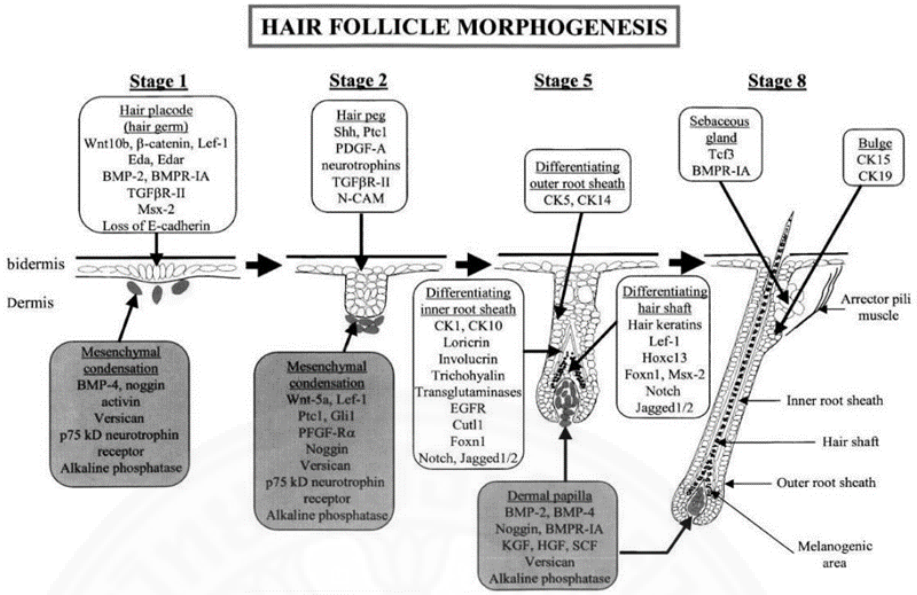

Figure 5.2 Hair follicle morphogenesis (132)

5.2 The hair cycle

Human hair needs cyclic regeneration of new hairs during lifetime. In order to produce new hairs, follicles that are existing have to go through the cycles of growth (anagen phase), regression (catagen phase) and rest (telogen phase). The hair cycle performs a striking model of the stem cell quiescent and activated regulatory, likewise the proliferation of transit-amplifying cell, choice of cell-fate, differentiation, and apoptosis in an epithelial tissue that is able to regeneration.

5.2.1 Anagen

Anagen hair follicles are straight and long, but in order to lie parallel to the skin surface, they have to be angled. The proliferating matrix cells take about 18 hours for a cell cycle length (133). Daughter cells move in upward direction, meanwhile from outermost to innermost, recruiting one of six genealogies of the IRS and HS, including the layers of Henley, Huxley and cuticle of the IRS, and the cuticle, medulla and cortex of the HS. Terminally, when HS cells differentiate, their organelles are extruded, then becoming firmly packed with 10-nm filaments bundles which organized from hair keratins containing large amount of cysteine. They assemble together and

Ref. code: 25595829040418WTR

crosslink to provide higher tensile strength and flexibility of the hair shaft. During the process of differentiation, the IRS also keratinizes to provide tightly support and benefit in HS guidance. When the HS reaches the upper follicle, its dead cells degenerate, thus releasing its end out and continues through the surface of skin. The length of hair is determined by anagen phase duration and also depends on the continuation of follicle base matrix cells differentiation and proliferation.

5.2.2 The transition from anagen to catagen

Before differentiation, the matrix cells sustain the process of cell divisions so called "transit-amplifying cells". When deterioration of the matrix cells supply occurs, the differentiation of HS and IRS slowdown and finally the follicle enters a disruptive phase called catagen. The first catagen onset time varies up to races in human and strains of mice and varies upon the skin region. In case of mice, the color of their skin can indicate the catagen phase progression. During anagen, the color of mice dorsal skin changes from dark grey to black and in telogen, changes to pale pink. Normally, the first catagen initiates as a wave pattern, growing from the head region cordially towards the tail region and down the animal lateral sides. From midline of the dorsal skin, the first catagen onset ranges from postnatal day 14 at the upper part of the dorsal back region to postnatal day 18 at the lower part of the dorsal back region. In mice, catagen lasts for about 3-4 days.

The molecular mediators of the transition from anagen to catagen have been described, although the completely clarified mechanism or how it regulates the transitional process is not yet understood. The growth factors including fibroblast growth factor (FGF) 5 and epidermal growth factor (EGF), neurotrophins including brain derived neurotrophic factor (BDNF) and probably the p53, p75-neurotrophin receptor and members of TGF-family pathway including TGF-1 and bone morphogenetic protein receptor type 1a (BMPRIa) stimulate the catagen transition (134–137).

5.2.3 Catagen

The process of transition from anagen to telogen is critically dynamic, is called catagen. It takes only a few days during this phase. During catagen, the lower part of each hair follicle turns to the phase regression, till entirely the process includes apoptosis of the bulb epithelial cells and ORS (138). The differentiation of HS ceases,

Ref. code: 25595829040418WTR

then the lower part of the HS bursts off and turn into a club. The club then moves upward till it reaches the non-cycling upper follicle, and remains there during telogen phase. As the lower follicle diminishes, the epithelial strand, a temporary structure of catagen forms. The epithelial strand provides the connection between DP and the upper part of the hair follicle which contains a lot of apoptotic cells. Finally, when DP reaches the cells surrounded the club hair remnant, it is then totally eradicated.

5.2.4 Telogen

The phase of telogen follows the catagen, the hair follicles lie in resting manner. In mice model, the first telogen starts in approximately postnatal day 19 to 21 at the middle part of dorsal back, and is quite short in duration, just a few days lasting. And for the second telogen begins at around postnatal day 42 and lasts longer for about 2 weeks or more (18).

5.2.5 The compartment of follicular stem cell

After birth, though no new hair follicle is produced, the lower segment of the hair follicle regenerates, thus a new hair can be reproduced. Due to this objective and for the purpose of the epidermis and sebaceous gland maintaining, during the process of development, the multipotent epithelial stem cells reservoirs are settled as a part in hair follicle. These cells locate in the lowest permanent part of the hair follicle, named "hair bulge" (139). At the phase of transition from telogen to anagen, the activation of follicle stem cells begins in order to reinitiate a new round of hair cycle.

5.2.6 The transition from telogen to anagen

During the telogen-to-anagen transition, the activation of quiescent stem cells at the telogen follicle base occurs in order to generate a new hair growth (140). The proliferation of stem cells occurs rapidly to become the transit-amplifying daughter cells which impending to generate a new hair follicle. Once the new hair follicle has already formed, it is adjoining to the former segment that docks the club hair, which finally will be shed off as exogen. This process constructs into the hair bulge which then adds to the reservoir of stem cells. As same as the old hair, the new hair turns up from the similar upper orifice. In case of initiating anagen, WNT and SHH signaling pathways activation are necessity (17, 18), while BMP signaling pathway known to be involved in hair follicle differentiation (141) and DP inductivity (23, 26).

Ref. code: 25595829040418WTR

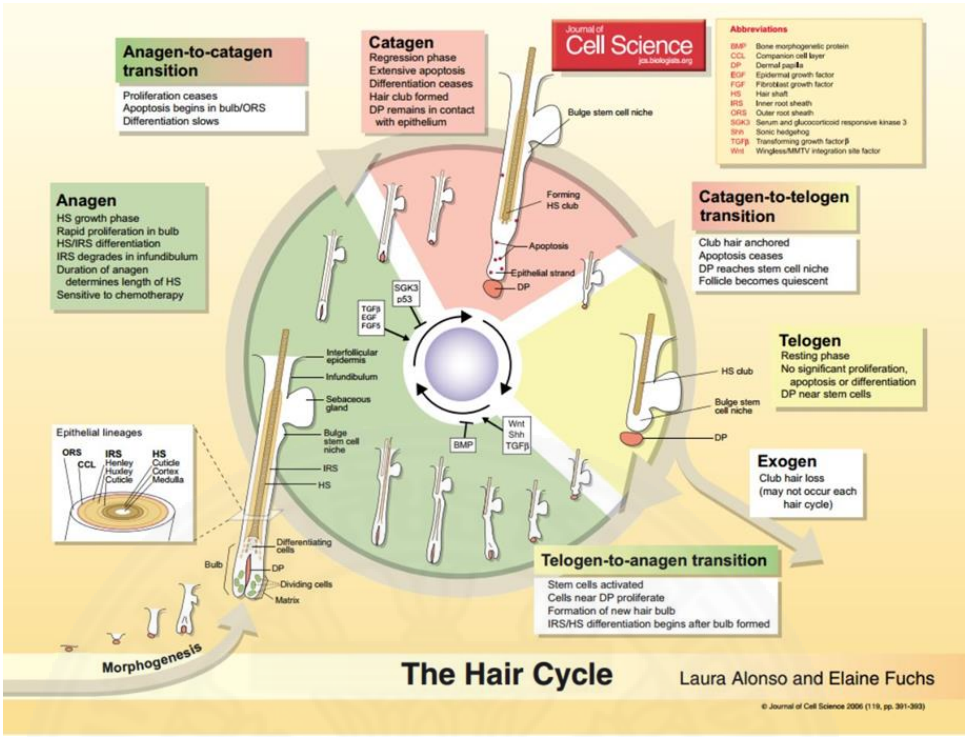

Figure 5.3 The hair cycle (18)

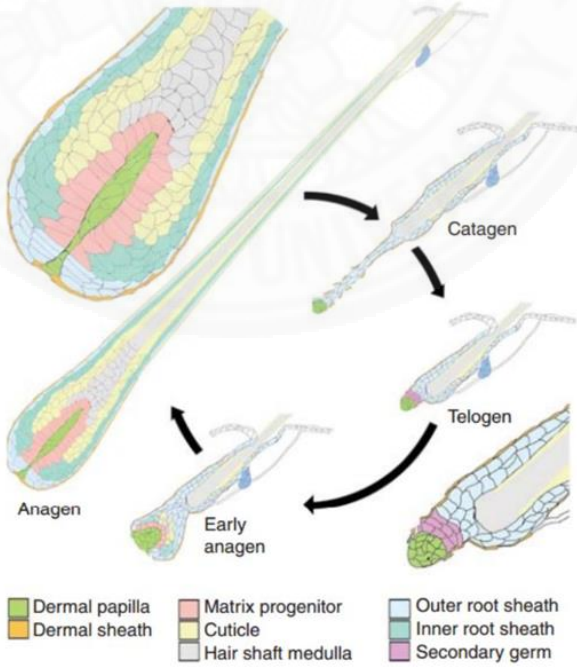

Figure 5.4 The hair follicle structure at different stages of hair cycle (129)

Ref. code: 25595829040418WTR

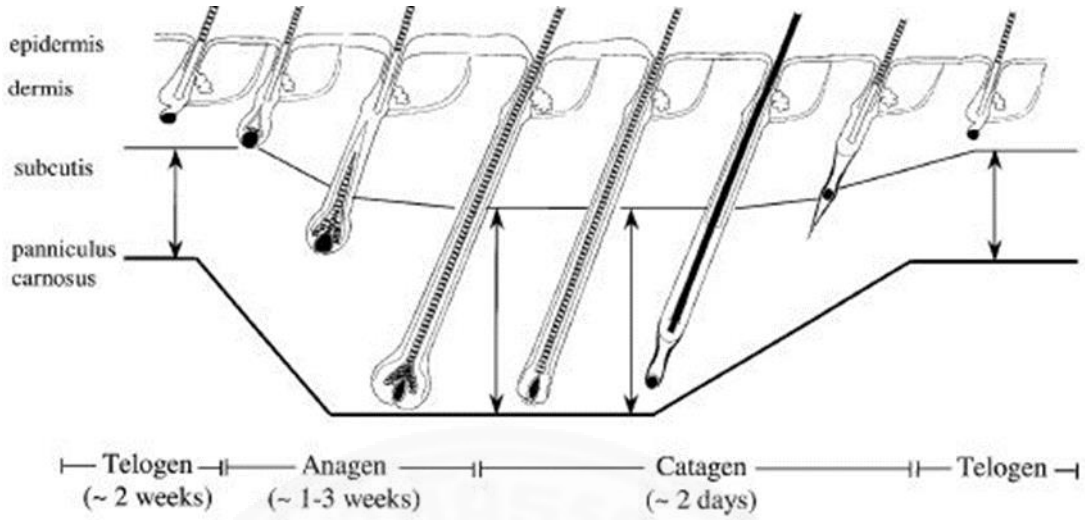

Figure 5.5 This schematic represents the HF length and the correlation with subcutaneous tissue during the different phase of hair cycle (142).

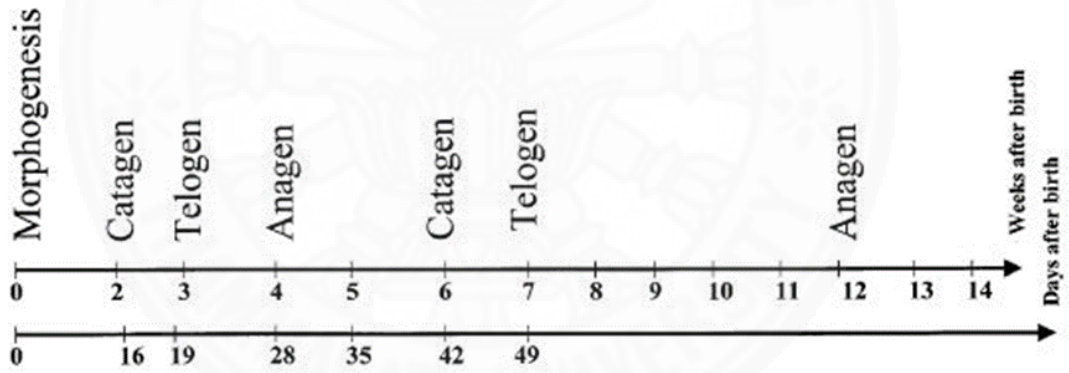

Figure 5.6 The hair cycle timeline ranging at birth until 14 weeks after birth in C57BL/6 female mice (142)

5.3 Hair loss

Currently, hair loss problem has been increasingly concerned by patients. Hair loss disorder can be categorized into scarring and non-scarring alopecia. Examples of diseases organised in scarring alopecia group are LPP, FFA, and DLE. The diseases in this group usually have to suffer from permanently hair loss, the current knowledge

Ref. code: 25595829040418WTR

still unable to induce the regrowth of hair. Meanwhile, the diseases of non-scarring alopecia group including AGA, AA and TE are able to induce hair regrowth. Thus, drugs function as hair growth promoter aim to have target and play a therapeutic role in non-scarring alopecia. This chapter will be scoped in non-scarring alopecia because of its able to treat property. Understanding in the detail especially the mechanism of diseases would be beneficial applying the knowledge in therapeutic purpose.

5.3.1 Non-scarring alopecia

Look closer at the lesion on scalp using a magnifying glass or a dermoscope is the common and easy way to differentiate scarring and non-scarring alopecia. In non-scarring alopecia, follicular orifices are usually present. Moreover, other signs and symptoms on scalp, pattern of hair loss, and also relevant systemic symptoms need to be assessed in order to differentiate the specific disease. Carefully asking the patient's clinical history is also necessary for example asking for potential triggers of hair loss from 3 months before the initiation of hair shedding, including systemic disease, drug, and stress. In female patient, information on gynecologic history and hormonal evaluation are crucial. Family history of hair loss also essential in differentiation of AGA. And sometimes, laboratory tests including the level of iron, vitamin D and thyroid function test are important to be evaluated.

5.3.1.1 Alopecia areata

AA is a form of non-scarring loss of hair on scalp or other area of the body. It affects approximately up to 2% of population. The pathogenesis is involved multifactorial autoimmune associated with unclear etiology for example genetics and environmental contributors (143). AA patients usually present with a sudden loss of hair. It is characterized by one or more well-defined hair-less non-scarring patches, which it could be progressed to more severe form as involved whole scalp (alopecia totalis, AT) or body hair (AU). AA can be correlated with other autoimmune diseases, such as atopy, thyroid disease, celiac disease, and vitiligo (144). AA first episode often spontaneously improve without any medical interference, but the first episode severity is related to the prognosis. AA can be spontaneously resolved within 1 year, whereas up to 25% developed to severe form.

Currently available medications may induce hair regrowth but do not change the disease course. Intralesional steroids are possibly one of the most

Ref. code: 25595829040418WTR

effective treatments for AA. Systemic steroids can also be prescribed in AA, but the success rate is vary according to the pattern of AA (145). Moreover, the relapse rate is quite high after cessation of treatment or tapering, thus limited use of systemic steroids in AA (146). Occlusive treatment of topical steroids with high potency are also effective in AT and AU, with benefit nearly 15% of patients in long-term study (147). Topical diphenylcyclopropenone or squaric acid dibutylester, as an immunotherapy, is also a beneficial modality in severe form of AA due to its mechanism of inducing hair regrowth by provoke contact dermatitis (148).

Latest in 2016, many studies have conducted clinical trials of using JAK inhibitors in the promotion of hair growth in AA and the report of those successful results has been launched, which will be fully described in Chapter 6, JAK Inhibitors and Hair Growth.

5.3.1.2 Telogen effluvium

TE refers to the loss of telogen hair which results from abnormal hair cycling. Approximately 100–200 telogen hairs shed off a day is typically found in TE. If the duration of active hair loss lasts less than 6 months, then categorizes as acute TE, but if longer, as chronic TE. Acute TE usually present with thinning of hair rather than visible alopecia due to nearly half of hair is often lost before the alopecic patch is clearly seen. Possible causes of TE including systemic illness, drug induced, loss of weight, nutritional deficiency, delivery, oral contraceptives interruption and scalp inflammation. Similarly to AA, TE could spontaneously be resolved, after treated underlying causes (31).

5.3.1.3 Androgenetic alopecia

AGA is the most common form of non-scarring alopecia. The previous study in Thailand reported the prevalence of baldness reaching 61.78% at 70 years of age (32), despite the high percentage of AGA patients in Thailand, the AGA prevalence in Turkey and Caucasians was even higher (149).

Vellus-like hair is the typical characteristic of AGA, this transformation of hair is due to the hair follicles miniaturization with premature termination of anagen (34). Patients with AGA usually present by losing hair length, pigmentation, and also diameter. Unfortunately, the process becomes progressively worse by increasing of age. In female, AGA often develops diffuse hair thinning on the

Ref. code: 25595829040418WTR

crown region with intact frontal hairline (Ludwig pattern). Whereas male pattern is represented by frontal hairline bitemporal recession, followed by diffuse hair thinning at the vertex area.

The pathogenesis of AGA is mainly results from androgen-dependent process and genetic transmission. AGA is acclaimed of the genetic inheritance which the recent findings indicate that the main AGA locus is an X-chromosome region consisting of androgen receptor and ectodysplasin A2 receptor (EDA2R) genes (150). The four genomes that have been identified as significant risk loci for AGA are on chromosomes 2q35, 3q25.1, 5q33.3, and 12p12.1. The substantial corporation signal was achieved for rs7349332 ($P = 3.55 \times 10^{-15}$) on chromosome 2q35, which is intronically placed in WNT10A (151). Another associated pathogenic factors of AGA including microbial flora, stress (both endogenous and exogenous), drugs, and microinflammation (33). Example of drugs associated with androgenetic effects include oral contraceptives that contain progestins and hormone replacement therapy for the menopause, may aggravate or worsen AGA. In male, AGA is commonly known to be associated with increasing in 5-alpha reductase activity propagate to DHT production excess, which may be results in hair follicle loss, yet the mechanism is not clearly known (35).

More from genetic predisposition and androgens main theories, suspected noticeably coincidence from scalp biopsy has shown that the miniaturization of terminal hairs is oftenly associated with perifollicular lymphocytic infiltration and fibrosis (36). Subsequently, this may be one of the credible reasons encourages microscopic follicular inflammation theory.

In the focus on hair follicle cycling, AGA implies a process of shortened anagen phase associated with premature catagen phase. Catagen has been advocated to occur as a consequence of decreased in anagen maintaining factors expression, IGF-1 (37), bFGF (38) and VEGF (39), associated with increasing in cytokines promoting apoptosis expression, including TGF-β1 (25, 34), IL-1α and TNF-α (33, 40).

The goal of treatment in AGA is to increase in hair number on the scalp and to delay progression of hair thinning. Current available treatment

Ref. code: 25595829040418WTR

modalities that FDA approved for AGA are oral finasteride (dose 1 mg/day) and topical solution of minoxidil (dose 2% for women and 5% for men).

Finasteride acts as a potent competitive inhibitor of type II 5α-reductase and inhibits the conversion of testosterone to DHT (41, 42), which is involved in miniaturization process of hair follicle in AGA. In the focus on drug efficacy, according to a systematic review of twelve studies showed moderate-quality evidence that daily use of oral finasteride increased the mean hair count from baseline in comparison to placebo treatment, reported as a percentage of the initial count in each patient, at short term (MD 9.42%, 95% CI 7.95%-10.90%, I^2 50%) and at long term (MD 24.3%, 95% CI 17.92%-30.60%, I^2 0%) and also increased in the proportion of patients reported as improved by investigator assessment in the short term (RR 1.80, 95% CI 1.43-2.26) (43). In contrast to its efficacy, adverse effects of finasteride are increasingly concerned especially on sexual functions (reported in clinical trials at rates of 2.1% to 38%) (44), which leads to poor compliance problem. Moreover, Thompson et al. reported that taking finasteride may associate with increased risk of high-grade prostate cancer (6.4 % and 5.1 % in the finasteride treated group compared to placebo group respectively, P<0.001; RR 1.67, 95% CI 1.44%-1.93%) due to it prevented or delayed the onset of cancer (45), but long term follow-up of the same subjects proved no significant difference in the rate of overall survival or survival after the diagnosis of prostate cancer (the 10-year survival rate was 73.0% with 95% CI 68.1%-78.0% and 73.6% with 95% CI 68.3%-78.9% in finasteride-treated group and placebo group respectively, among those with high-grade prostate cancer) (46). Nevertheless, further study is required to conclude the association between the use of finasteride and prostate cancer. Another limitation of finasteride is its slow onset and must be in long term use which may increase risk of adverse effects. Finasteride is contraindicated in who are or may potentially be pregnant because of the risk in impair virilization of a male fetus (47).

Topical minoxidil, an adenosine-triphosphate-sensitive potassium channel opener and vasodilator (33), which feasible mechanism is to extend the duration of anagen phase of hair follicles by induces cell growth factors including VEGF, HGF, and IGF-1 and activates uncoupled sulfonylurea receptor on dermal papilla plasma membrane leading to HGF and IGF-1 enhancement, as well as inhibits

Ref. code: 25595829040418WTR

TGF-β which acts as hair matrix cells apoptosis inducer, and lastly dilates hair follicle arteries and increases blood flow in dermal papilla (48). In the aspect of clinical use, Olsen et al. reported that 5% topical minoxidil was significantly greater in efficacy to 2% topical minoxidil and placebo in increasing hair regrowth in AGA patient (5% topical minoxidil treated group showed 45% more hair regrowth than 2% topical minoxidil treated group at week 48, P=0.025). The adverse events using topical minoxidil are dose-dependent, commonly from dermatologic nature such as pruritus, itching, burning and other symptoms of scalp dermatitis, but no systemic effects has been reported (49). Another important adverse event of patient using topical minoxidil is that it provokes a transitory TE. TE is characterized by increased hair shedding, in case of minoxidil use, the condition caused by mechanism of fast reentry to anagen phase of the hair follicles. Although acute TE from minoxidil treatment is reversible and transient, but the condition causes psychoemotional stress which leads to the main cause of concern and the reason for seeking medical advice (50).

In the present, low-level laser light therapy (LLLT) is one of the effective modalities in treatment of AGA. Seeking for new alternative treatment options has brought many patients to withstand treatment with topically-administered blood components, including platelet-rich plasma (PRP). PRP is a part of the plasma fraction from autologous blood with higher in platelet concentration. It has potential in regenerative property according to the activation of platelet α-granules which leads to the releasing of growth factors. In hair cycle, PRP seems to prolong the anagen phase, inhibit apoptotic process which increase follicular cells survival rate, activate differentiation of stem cell, and enhance the vascular plexus at perifollicular, via VEGF and platelet-derived growth factor (PDGF) (152).

Ref. code: 25595829040418WTR

CHAPTER 6
JAK INHIBITORS AND HAIR GROWTH

6.1 JAK inhibitors and hair growth

According to the wide range therapeutic effect of JAK inhibitors, as immunoregulators, they have been used successfully in many clinical trials. Apart from the major immunoregulatory functions, JAK inhibitors also have the interesting property on hair growth promotion. In AA, Xing et al. has proved that cytotoxic $CD8^+NKG2D^+$ T cells are essential for AA induction in mice models of the disease. Due to global transcriptional profiling in AA skin of mice and human affirmed gene expression signatures suggestive of cytotoxic T cell infiltration, the response of IFN-γ and several γ_c cytokines upregulation known to stimulate IFN-γ–producing $CD8^+NKG2D^+$ effector T cells activation and survival. Therapeutically, systemic JAK inhibitors administration could decrease function of the IFN-γ and γ_c cytokine receptors, eradicate the IFN signature and lastly led to AA prevention. Whereas topical form could promote hair regrowth and recover the disease (15). Another interesting finding was that the JAK inhibitors in topical form induced more robust hair growth than systemic form, since it raises the drug local concentration in microenvironment of hair follicle, granting the interactions to ensue (3).

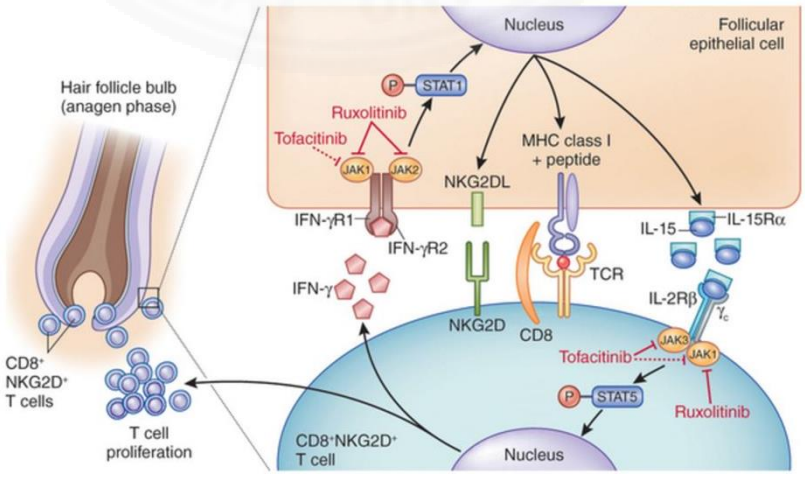

Figure 6.1 Mechanism of the JAK inhibitors on hair follicle in AA (153)

Ref. code: 25595829040418WTR

Correspondingly, Harel et al. demonstrated that JAK inhibitors treatment resulted in rapid onset of hair growth in mice by the process of activates WNT and SHH signaling pathways (3) which mimics the mechanisms of normal anagen initiation (17, 18), evidenced from the results that JAK inhibitors promoted hair growth with similar kinetics to SHH agonist. Moreover, in order to examine the effect on stem cell activation, mice in telogen phase treated with JAK inhibitors within 4 days period were experimented, they next demonstrated that the hair germ compartment (P-cadherin+) of the treated hair follicle was significantly proliferated, concluding that JAK-STAT inhibition causes hair follicle progenitor cells activation (19). However, JAK-STAT inhibition is sufficient in hair growth promotion during telogen in late stages, but is unable to abrogate the quiescence microenvironment of the telogen in early stages, which this correspond to Geyfman et al.'s study that described the progression concept of telogen phase initiating from refractory to competent state (before-to-after 8 weeks) for anagen phase induction (154). The results from 4 days treating 8.5-week-old mice with JAK inhibitors and vehicle as a control group on microarray experiments encouraged that inhibitory of JAK-STAT signal allows the hair cycle upon its normal progression. Ruxolitinib-treated group enhanced the mammalian target of rapamycin (mTOR) and nuclear factor kappa-light-chain-enhancer of activated B cell (NFkB) pathways, which previously known to be essential in regulatory of the hair cycle (155, 156), while tofacitinib enhanced pathways that involved in cell motility and migration, such as Rho and integrin signaling, which responsible in the transition from telogen to anagen.

Genes expression that related to the JAK-STAT pathway measuring by real-time polymerase chain reaction (qPCR) array demonstrated that the JAK-STAT pathway key genes including STAT5a/b, STAT3, JAK1, JAK3, and SOCS2/3 were upregulated in catagen and telogen phase and were declined in early anagen phase. According to the hair follicle immunofluorescence studies in anagen, catagen, and telogen phase reaffirmed that phosphorylated STAT3 is asserted in the DP and other extrafollicular cells. Phosphorylated-STAT3 can also be found expressing in the hair germ cells during catagen and telogen phase. During all phases of the hair cycle, phosphorylated-STAT5 is highly activated in the DP, with especially highest peak

Ref. code: 25595829040418WTR

during catagen phase. Consequently, this indicates a potentially feasible role in the quiescence regulation (3).

Legrand et al. also submitted that the phosphorylated-STAT5 in the DP may take part in the transition from telogen to anagen in murine hair follicles. With the immunofluorescent studies, they revealed that the phosphorylated-STAT5 activation, an active JAK-STAT signaling marker, is upregulated in the hair follicles DP during late catagen and sustained through telogen till early anagen. In vivo, the DP with STAT5 deficiency showed to delay onset of the anagen phase, especially in the adult hair cycle on the second phase. Correspondingly, in ex vivo, deficiency of STAT5 led to downregulation of WNT6, FGF7, and FGF10 which previously known to be correlated in the anagen phase induction and the WNT inhibitors, including Dkk3 and Dlk1, are upregulated. Nevertheless, in vivo, the phosphorylated-STAT5 is unable to aggravate these anagen-inducing factors production, because STAT5 activation is occurred during late catagen, sustaining phosphorylated throughout telogen, next in early anagen, the up-regulated WNT6, FGF7, and FGF10 genes then express many weeks later. Thus, this maybe assume that, apart from phosphorylated-STAT5, there are several other molecular events mediate the anagen-promoting factors activation. In hair follicle stem cell compartments, it seems that the interaction of signals among several pathways might be the crucial factor that determine the quiescence or activation of the hair follicles stem cell (157).

Nonetheless, the previous study has also demonstrated that, in the hair follicle stem cells and the ORS, phosphorylated-STAT3 and STAT5 are activated in telogen phase, and during early telogen phase, phosphorylated-STAT3 is seldom found in the DP (3), advocating that topical JAK inhibitors may be promoting anagen through several other pathways apart from those have been described.

Furthermore, Harel et al. also examined the effect of JAK inhibitors on hair growth in human tissue (grafted human fetal scalp skin onto severe combined immunodeficient mice). Different from mice, the growth pattern of human hair follicle is asynchronous and when randomly picks a hair from human scalp, found that at any given time almost 90% categorized as anagen hair (158). Thus, in humans, it is quite hard to evaluate the transition process from telogen to anagen. According to Harel et al.'s study in human tissue, the results suggested that tofacitinib treatment promotes hair

Ref. code: 25595829040418WTR

elongation rate and induces significantly higher in overall hair follicles number, suggesting that tofacitinib or in another word inhibition of JAK1/3 signaling enhances effect on inductivity of human dermal papilla. These were followed from the process evidence from repressed in receptors that involved in the modulation of dermal papilla inductivity, such as FGFR1, ACVRL1, IGFR1, OSMR, and PTGFR (20–23). Proapoptotic genes including BAX, Bcl2L11, and CASP12 were demonstrated downregulation in tofacitinib treatment, whereas upregulation in ruxolitinib treatment. In addition, genes up-regulated by tofacitinib treatment involved the members of the TGF-β pathway (TGF-β2) and the BMP pathway (BMP6), corresponding to the previous study showed that up-regulation of TGF-β2, FGF7, and FGF10 in the DP inclines BMP signaling in the quiescence/activation process which committed to the initiation of early anagen phase (23–26). Besides, LEF1, another key regulators of the WNT pathway, which control dermal-epidermal interactions (27, 28) together with the NOTCH pathway members, which control hair follicle fate (29) were also overexpression in tofacitinib treatment. Inhibiting BMP and activating WNT also drive over telogen phase, declining the hair follicle stem cell activation threshold (159). Cooperatively, this suggests that treating with tofacitinib helps in inductive promotion by mediating either the inductive function or the cultured DP surveillance. In case of comparing DP inductivity in response to tofacitinib treatment, the authors investigated the differences in molecule between newly isolated human DP, cultured DP, and cultured dermal spheroids, and tried to identify the unique genes that correlated with each state. By co-expression, the genes are categorized into four territories. They hypothesized that since treatment with tofacitinib could enhance hair growth, when comparing tofacitinib-treated to control groups, the genes expression within four territories should be enhanced in a statistically significant manner. But the results contrastingly revealed that not all genes within four territories expressed in the hypothesized manner, suggesting that, by tofacitinib treatment, the inductive restoration may not be entirely complete. Surprisingly, in contrast to tofacitinib, treatment with ruxolitinib did not enhance the human DP spheres inductivity, although the rate of growth in the organ culture model was increased. This maybe explain by the study findings that proapoptotic signals were down-regulated in tofacitinib-treated spheres

Ref. code: 25595829040418WTR

resulting in hair growth enhancement by the process of survival promotion, but this process was not found in ruxolitinib-treated spheres (3).

In conclusion, the findings from previous studies suggest that the activation of JAK-STAT signals can be promoted by multiple pathways in different compartments, and possibly that the dynamic interaction among these signals leads to the initiation of hair growth. Thus, spotting on the pharmacological importance of these pathways may beneficial in expediting the discovery of new alternative therapeutic treatment in treating several forms of alopecia.

6.2 JAK inhibitors and hair disorders

According to the variety of therapeutic modalities of JAK inhibitors, focusing especially on hair growth effects, many clinical trials reported of multiple successful cases in response to ruxolitinib and tofacitinib, and interestingly that many of them are still ongoing for further studies which will be gradually launched in the very near future.

6.2.1 Alopecia areata

Currently, there is still none of the FDA-approved drug for AA. Due to the fact that AA has complicated pathogenesis, thus it quite challenges to design clinical trials in order to develop new therapeutic treatments for it. Despite AA can be spontaneous remission but its course is unpredictable and the disease characteristics suffer the patients, so several group of therapies are available for AA, and the treatment of choices depend on the disease activity, duration, and the patient age group. Apart from treatments for AA that has been previously described in Chapter 5, Hair (part 5.3.1.1 Alopecia areata), JAK inhibitors have been used in clinical trials for AA and multiple of them are now successfully launched.

Craiglow et al. has reported an AU case with failure of treatment from intralesional and topical steroid, sulfasalazine, topical squaric acid dibutylester, and topical anthralin. After 12 weeks of using 0.6% topical ruxolitinib, a JAK1/2 inhibitor, applying twice daily to the scalp and eyebrow, found that eyebrows were regrowth to nearly normal and 10% of scalp hair with numerous 5- to 10-mm darkly pigmented hairs were seen. Neither adverse event nor abnormal lab value has been reported

Ref. code: 25595829040418WTR

according to this case (30). Then, in September 2016, Mackay-Wiggan et al. has proposed another successful open-label clinical trial of using oral ruxolitinib 20 mg twice daily for 3–6 months in 12 patients with moderate-to-severe AA. At the endpoint, patients at least 50% achieved hair regrowth assessing by the SALT score compared with baseline. 75% (9 out of 12) of patients demonstrated significant scalp hair regrowth. The mean hair growth was shown as high as 92%. And reported no serious adverse events, with none discontinuation of therapy required from patients (112).

More from ruxolitinib, there is also a successful reported case from the use of tofacitinib, a JAK3 inhibitor, in treating AU, an AA severe form. Gupta et al. reported of two cases suffered from AU. The first case was an otherwise healthy male patient presented with AA at age 10 years, then progressed to AU around his thirties, with failure of treatment from steroids, sulfasalazine, and minoxidil. After prescription of oral tofacitinib at dosage of 5 mg twice daily for 3 months, significant hair regrowth was observed on the beard and scalp. And by 6 months, hair regrowth was clearly visible almost full of the body. Followed by eyebrows and eyelashes were then exhibited by 8 months after initiating tofacitinib treatment, without any serious side effects was reported. The second case was also a healthy male with first diagnosed as AA and finally progressed to AU. He has been prescribed topical and oral steroids, vitamins D3, biotin and multivitamin, but after a month passed, the clinical was just minimal improved. Thus, his physician determined prescribing oral tofacitinib at 5 mg twice daily dosage, but at 1 month, the treatment was contemporary paused due to viral infections, which during that time, his scalp hair had already noticeable of thickening in hair density, while leg hair and eyebrow had initiated visibly regrowth. After a month, the therapy was re-prescribed and by 4 months from the first start, hair regrowth was significantly observed on scalp, eyelash, eyebrow, and beard. And by 8 months after tofacitinib treatment, axillary and leg hair were noted the regrowth.

Another interesting study to prove oral tofacitinib efficacy for AA has been proposed by Jabbari et al. in August 2016 as an open-label pilot study. A case of Caucasian female whom suffered from moderate to severe AA was recruited to the study. 5 years prior to the enrolment, her AA initiated on the scalp and spontaneously resolved within 1 year during the pregnancy. But within few months after delivery, her AA became recurrent and progressed to involve eyelashes, eyebrows, and entire body

Ref. code: 25595829040418WTR

hairs, with failure of anthralin cream, topical, and intralesional corticosteroids treatment. Oral tofacitinib 5 mg twice daily was prescribed to the patient, then after a month of treatment, hair regrowth was observed and improved gradually at month 2 and 3 with 62.5% and 94% of scalp hair regrowth, respectively. Her eyebrows and eyelashes were obviously regrowth. Finally, scalp hair was completely regrowth at 4 months after starting treatment. Neither side effects nor laboratory abnormalities was reported. Furthermore, blood sample was drawn and punch biopsy of the scalp was performed at baseline and at 4 weeks after treatment in order to evaluate gene expression and the changes of biomarker level. According to the drawn blood sample, CXCL10, a chemokine that induced by IFN typically found high levels in AA skin (15), declined after 4 weeks of tofacitinib treatment. Additionally, the skin biopsy samples were further analyzed using microarray. At baseline, the patient expressed high levels of IFN and cytotoxic T lymphocyte (15), which found to be declined by 4 weeks after treatment, based on the AA Disease Activity Index (ALADIN) (160). As a result, tofacitinib is one of the efficient drug for AA which improved clinical outcome with affirming by gene expression and the changes in level of biomarker.

6.2.2 Androgenetic alopecia

Up to date, not yet any clinical trials of using the JAK inhibitors in treating AGA has been published.

Ref. code: 25595829040418WTR

CHAPTER 7
RESEARCH METHODOLOGY

7.1 Materials

7.1.1 Animals

Seven-week-old male C57BL/6 mice procure from National Laboratory Animal Center. A total of studied mice will be randomly assigned to tofacitinib-treated group (N=7), minoxidil-treated group (N=7) and control group (N=7). During the experiments, the animals will be housed under strict hygienic conventional standard, maintain under controlled environmental conditions (12-hour light/dark cycle, temperature approximately 23°C), and provided with standard laboratory food and water ad libitum. Study protocol was approved by Thammasat University's Animal Ethical Committee and conducted according to Ethical Principals and Guidelines for the Use of Animals for Scientific Purpose.

7.1.1.1 Sample size

A total of 21 eight-week-old male C57BL/6 mice are recruited for this study.

▪ Program G* Power 3.1.7 (161) :

Effect size f = 0.8

α error probability = 0.05

Power (1-β error probability) = 0.80

Number of groups = 3

Total sample size = 21

7.1.1.2 Inclusion criteria

Male C57BL/6 mice aged 8 weeks.

7.1.1.3 Exclusion criteria

- Mice are in seriously ill condition, weight loss >20%, moan with pain or soundless, reject food or water.

- Death during the experiment.

Ref. code: 25595829040418WTR

7.1.2 Drugs

Tofacitinib was purchased from Abmole Bioscience (catalog no.477600-75-2), then dissolved in dimethyl sulfoxide (DMSO) into 2% concentration. 5% topical minoxidil was purchased from drug industry and dissolved in ethanol base into 60-65% concentration, was used in comparable to topical tofacitinib.

7.2 Research design

7.2.1 Animal experiment

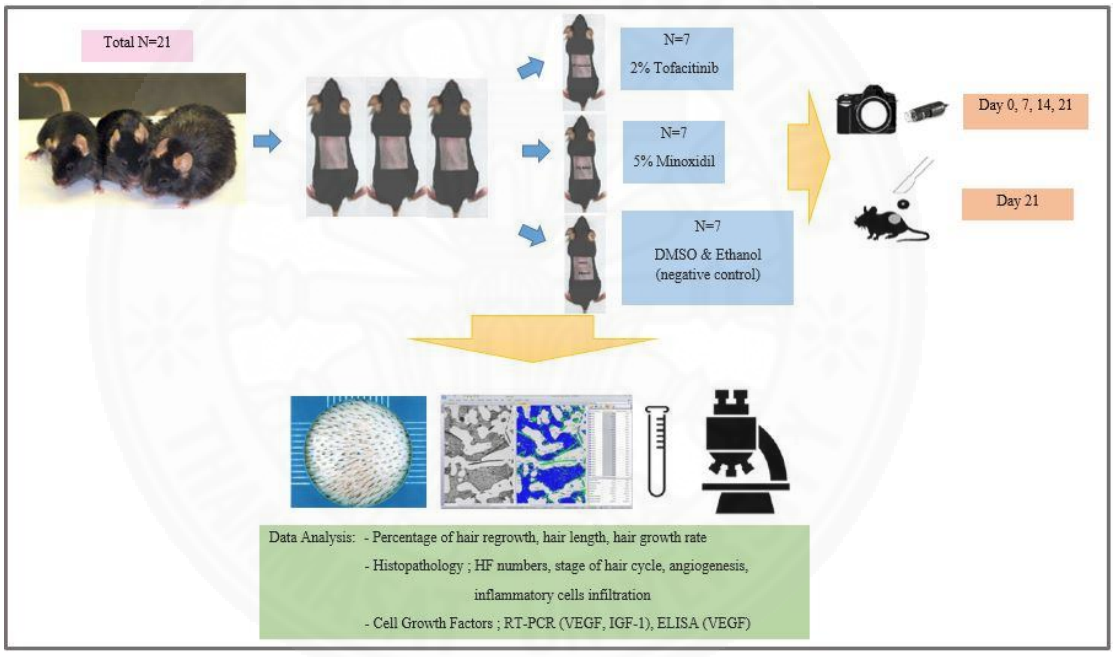

Figure 7.1 Flow chart of research methodology

Mice were anesthetized with inhaled isoflurane (Aerrane, Baxtar, USA) one day before the procedure. Hair on the dorsal skin (size 2.5x3.6 cm position just below to scapula) of all mice were gently coated under sterile conditions using an electric shaver to avoid injury.

Ref. code: 25595829040418WTR

Figure 7.2 Mice were gently coated under sterile conditions using an electric shaver.

After coating, the mice were randomly divided into group of seven, then numbering and labelling.

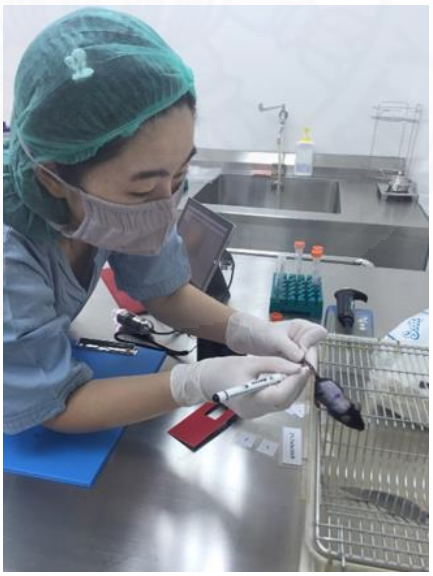

Figure 7.3 Numbering and labelling mice

Ref. code: 25595829040418WTR

Each labelled mouse was digitally photographed using digital camera and microscope, focused on the dorsal back coated skin. On the day on which the reagents were to be applied (day 1-21), each group were treated topically 0.1 mL/area once daily with 2% tofacitinib or 5% minoxidil. A digital image of the coated area was weekly recorded until three weeks. In case of minimized variations, we calculated area hair regrowth relatively from each mouse baseline. For hair regrowth study area, a window template size 2.5x3.6 cm was used to standardize the size of calculated area. And for microscopic area photographed by digital microscope, the mark point on a window template helped focusing on the same position while taking photo in each week.

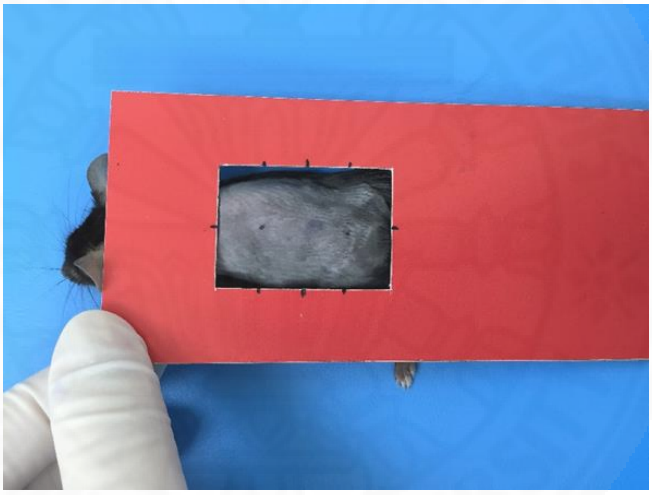

Figure 7.4 A digital image of the coated area was recorded at the same position.

At the experimental endpoint, tissues from the dorsal back coated area were collected from each treated mouse using sterile punch biopsy (6 mm in diameter) for histopathological study and cell growth factors analysis. Finally, mice were humanely euthanized with carbon dioxide (CO_2).

Ref. code: 25595829040418WTR

Figure 7.5 Tissues from the dorsal back coated area were collected using punch biopsy.

7.2.2 Outcome measurements

7.2.2.1 Hair growth observation

Hair growth was determined weekly by digital photograph using a digital camera (DSC-RX100M3, Sony Corporation, Japan). The photographic data was analyzed using Adobe Photoshop 6.0 software (Adobe Systems Incorporated, United States), performed by the same independent computer graphic administrator, without bias from recognizing the previous treatment information, to calculate the area of hair regrowth in percentage. Hair growth rate was evaluated using digital microscope (Dino-Lite AM7013MZT(R4), AnMo Electronics Corporation, Taiwan) at 65x magnification.

Ref. code: 25595829040418WTR

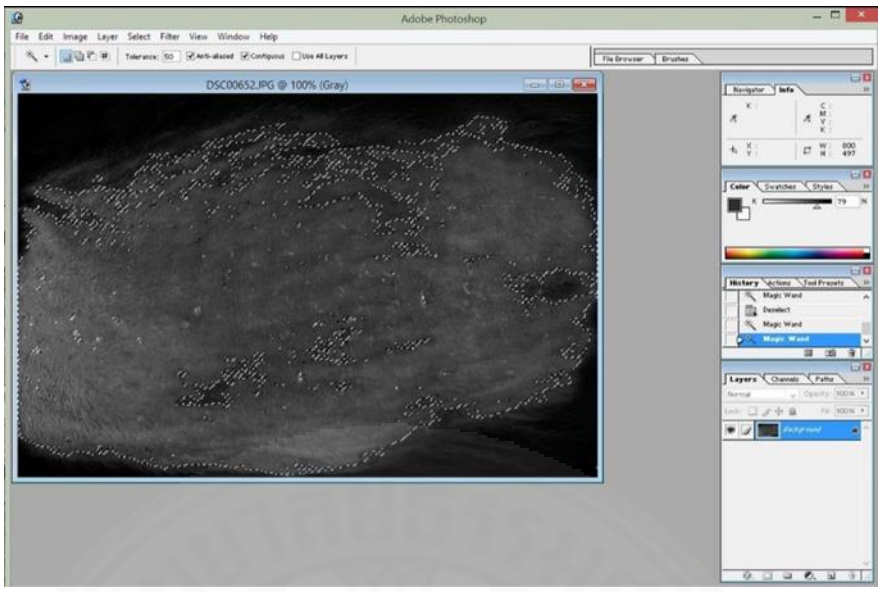

Figure 7.6 An example of the photographic data that was analysed using Adobe Photoshop 6.0 software to calculate the area of hair regrowth in percentage

Figure 7.7 An example of mean hair growth measurement using digital microscope in order to evaluate hair growth rate

Ref. code: 25595829040418WTR

7.2.2.2 Histopathological analysis

Tissues from the coated area were collected on day 21 using punch biopsy (6 mm in diameter) under inhaled isoflurane anaesthesia. The samples were fixed in 10% buffered formalin for 24 hours, embedded in paraffin wax, cut in vertical section at 3 µm-thickness, and stained with haematoxylin and eosin (H&E), to evaluate:

- Hair regrowth by comparing mean number of hair follicles in the examined area of 6 mm in diameter (approximately 28.27 mm^2) between control and treated groups.

- The hair follicle of the examined area was classified according to the stages of the hair growth cycle (anagen, catagen and telogen).

- Angiogenesis by determining newly formed and completely formed capillaries, then compared among the treated and control groups.

- The inflammatory cells were categorized and evaluated using an optical microscope comparing among the treated and control groups.

All histopathological analysis was done by veterinary pathologists under 4x and 10x magnification using optical microscopy.

7.2.2.3 Cell growth factors analysis

(1) Real-time polymerase chain reaction (RT-PCR)

The collected tissue samples were stored as fresh frozen at -80°C until use. VEGF and IGF-1, hypothesized important cell growth factors on hair growth promotion induced by tofacitinib, were analyzed by RT-PCR technique. RNeasy® Mini Kit (QIAGEN, Valencia, California, USA) was used for total RNA purification from the collected tissues. RNA isolation was performed according to the manufacturer's protocol.

Ref. code: 25595829040418WTR

Figure 7.8 RNeasy® Mini Kit for total RNA extraction

(1.1) Tissue samples were removed from the -80°C storage. According to this experimental research, we used entire unstable cryopreserved tissues placing directly into a suitable sized vessel for disruption and homogenization process.

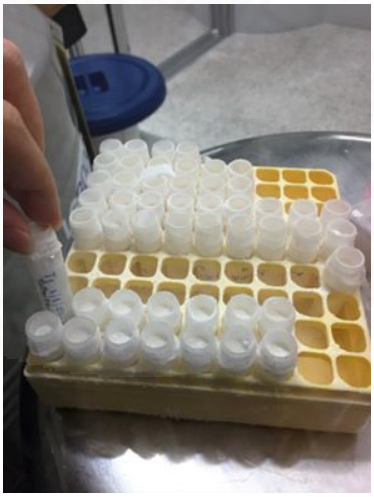

Figure 7.9 Tissue samples

(1.2) Mortar and pestle were used to destruct tissues. The frozen tissues were placed in mortar and added liquid nitrogen, then grinded with pestle into small grain. After liquid nitrogen was evaporated, the tissue grain was gently transferred into an RNase-free micro-centrifuge tube.

Ref. code: 25595829040418WTR

Figure 7.10 Tissue samples were destructed using mortar and pestle.

(1.3) The lysate was homogenized with 600 µL of RLT buffer and transferred into each 1.5 mL eppendorf tube by pipetting. Then, those prepared tubes were placed into provided shredder spin column and centrifuged at full speed for 2 minutes. Next, the supernatant was carefully pipetted to transfer into each new micro-centrifuge tube.

Figure 7.11 The lysate was centrifuged.

Ref. code: 25595829040418WTR

(1.4) Adding 600 µL of 70% ethanol into the lysate and immediately pipetted to mix it. Transferring 700 µL of the sample with any precipitate into the provided RNeasy spin column placed in a 2 mL collection tube, then, centrifuged for 15 seconds at 10,000 rpm, thereafter, discarding the flow-through.

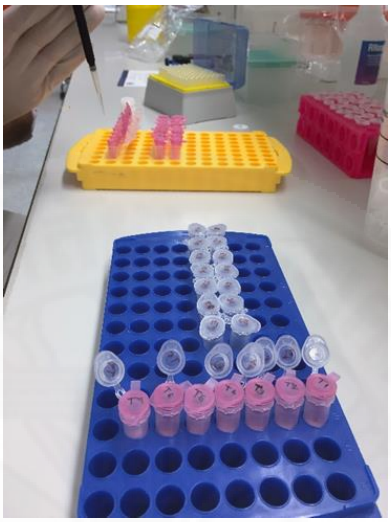

Figure 7.12 Transferring the sample with any precipitate into the provided RNeasy spin column placed in a 2 mL collection tube.

(1.5) The spin column membrane was washed 3 times with:

-700 µL Buffer RW1, then centrifuged for 15 seconds at 10,000 rpm.

-500 µL Buffer RPE, then centrifuged for 15 seconds at 10,000 rpm.

-500 µL Buffer RPE, then centrifuged for 2 minutes at 10,000 rpm.

(1.6) Transferring the RNeasy spin column into a new 1.5 mL collection tube. RNase-free water was then added directly to the spin column membrane in order to elute the RNA, and centrifuged for 1 minute at 10,000 rpm.

(1.7) The previous step was repeated using another 15 µL of RNase-free water to elute the RNA.

Ref. code: 25595829040418WTR

(1.8) RNA concentration was measured by NanoDrop spectrophotometer (Thermo Fisher Scientific Incorporation, Massachusetts, USA) in order to evaluate the RNA quantity and purity.

Figure 7.13 RNA concentration was measured using NanoDrop spectrophotometer.

Due to the concentration of RNA was too low or maybe error in some samples, we had to exclude those off, left over 22 samples (tofacitinib 7 samples, minoxidil 5 samples, DMSO 7 samples, and ethanol 3 samples) to further analyze by reverse transcription process.

In order to synthesis complementary DNA (cDNA), reverse transcription was performed using ImProm-II™ Reverse Transcription System (Promega Madison, USA). Before mixing with other reagents, RNA was heated at 70°C for 5 minutes, and left on ice 1-2 minutes, then the following components were added and mixed.

Ref. code: 25595829040418WTR

Figure 7.14 RNA was heated at 70°C for 5 minutes, before mixing with other reagents.

Finally, the mixture was placed in T100™ Thermal Cycler (BIO-RAD, Hercules, California, US) running the process of cDNA synthesis under control temperature at 25°C for 5 minutes, 42°C for 1 hour, and 70°C for 15 minutes.

- Oligo dT 1 µL
- dNTP mix 1 µL
- Buffer 4 µL
- Reverse transcriptase enzyme 1 µL
- Recombinant Rnasin 0.5 µL
- $MgCl_2$ 1.6
- RNA 0.582-10 µL (volume used is according to RNA concentration in each sample; 30-100 ng of RNA)
- RNase free water (titrate until total volume reach 20 µL)

Total volume = 20 µL

Ref. code: 25595829040418WTR

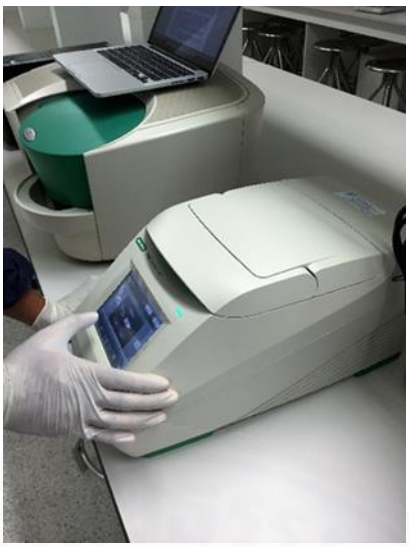

Figure 7.15 T100™ Thermal Cycler

We evaluated the mRNA expression of VEGF, IGF-1, and beta 2-microglobulin (as an internal control). The following primers were used:

- Mm.282184 for VEGF
- Mm.268521 for IGF-1
- Mm.163 for beta 2-microglobulin

One step RT-PCR was performed following the manufacturer's protocol using the QuantiNova Probe RT-PCR Kit (QIAGEN, Valencia, California, USA). The reverse transcription reaction mixture was prepared by combining the following components in a sterile 1.5 mL microcentrifuge tube on ice.

- 2x Probe RT-PCR Master mix 10 μL
- QN Probe RT mix 0.2 μL
- Primer 1-FAM 1 μL
- Primer 2-VIC 1 μL
- RNA (7 ng)
- RNase-free water

Ref. code: 25595829040418WTR

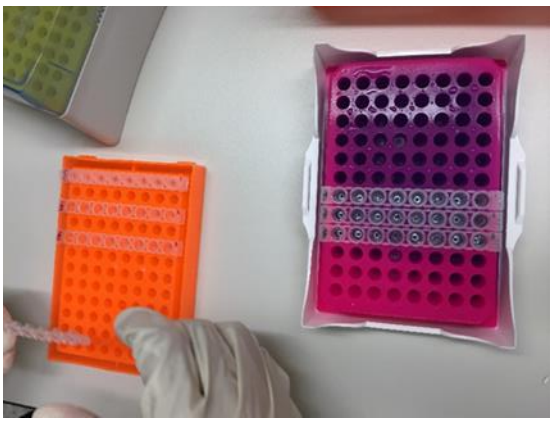

Figure 7.16 The reverse transcription reaction mixture

The reactions were placed in a C1000 Touch™ thermal cycler BIO-RAD CFX96™ Real-Time System (BIO-RAD, Hercules, California, US) that has been preheated to 95°C. An optimized program for amplification using the Upstream and Downstream Control Primers provided as 95°C for 10 minutes, 40 cycles of 95°C for 15 seconds denaturing, and 60°C for 1 minute annealing. Fluorescence dye was detected. The relative ratio of gene expression for each gene was determined by standard exponential curves. The internal control gene (beta 2-microglobulin) was used to normalize the target gene ratio.

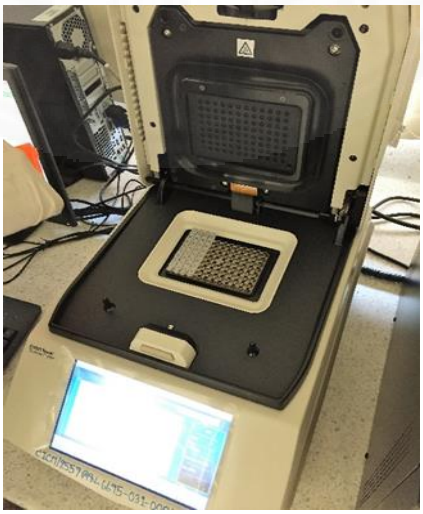

Figure 7.17 The reaction mixture plate was transferred in the thermal cycler, then RT-PCR was run.

Ref. code: 25595829040418WTR

(2) Enzyme-linked immunosorbent assay (ELISA)

Quantitative measurement of VEGF protein was done by ELISA technique using Abcam's VEGF Mouse ELISA kit (ab100752, Abcam, UK). Dermal levels of VEGF were determined in the biopsy tissue sample. The skin tissues were minced and homogenized in a polytron-type homogenizer using 2 mL of 1N acetic acid. Then the tissue homogenates were centrifuged (3,000 × g, 10 minutes, 4°C). The resulting supernatants were measured by Bradford method before using for ELISA.

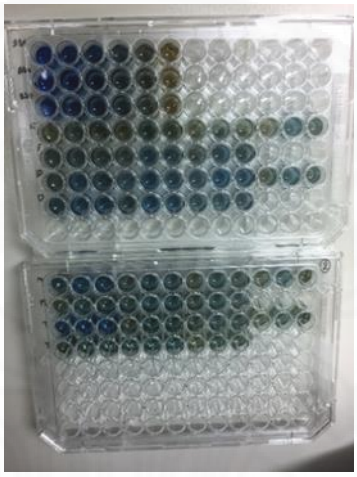

Figure 7.18 The supernatants were measured by Bradford method

The concentration of VEGF protein in the supernatants was measured using an Abcam's VEGF Mouse ELISA kit according to the manufacturer's instructions.

(2.1) Reagent preparation

Sample diluent buffer was diluted 5-fold, cell lysate buffer was diluted 2-fold, and assay diluent was diluted 5-fold with distilled water before use. Wash solution was diluted into 400 mL of 1-fold wash solution with distilled water. The Biotinylated VEGF anti-Mouse vial was spinned before use. Then 1-fold assay diluent 100 μL was added into the vial to prepare a detection antibody concentrate. Gently mixed with pipette. Before using in the assay procedure, the detection antibody concentrate was diluted to 80-fold with 1-fold sample diluent buffer. Prior to use in the assay procedure, the HRP-Streptavidin concentrate vial was spinned

Ref. code: 25595829040418WTR

and diluted to 160-fold with 1-fold sample diluent buffer. All reagents were equilibrated to room temperature (18-25°C) before using.

(2.2) Standard preparations

The vial of VEGF standard was grossly spinned, then added 400 µL of 1-fold assay diluent or 1-fold sample diluent buffer into the vial to prepare a 25 ng/mL VEGF stock standard. After gently mixed, the standards were prepared into 8 concentration. Standard #1 was prepared by adding 40 µL of 25 ng/mL stock standard to 960 µL of 1-fold assay diluent or 1-fold assay diluent into tube #1, then the tube was thoroughly and gently mixed. 300 µL of 1-fold assay diluent was pipetted into each tube. Standard #2 was prepared by transferring 200 µL of the mixture from tube #1 to #2, then mixed rigorously. As same as standard #2, other standards were prepared in serial as shown in the standard dilution preparation table below. 1-fold assay diluent or 1-fold sample diluent buffer was served as the zero standard (0 pg/mL).

Table 7.1 Standard dilution preparation table

Standard #	Volume to dilute (µL)	Diluent (µL)	Total volume (µL)	Starting conc. (pg/mL)	Final conc. (pg/mL)
1	40	960	1,000	25,000	1,000
2	200	300	500	1,000	400
3	200	300	500	400	160
4	200	300	500	160	64
5	200	300	500	64	25.6
6	200	300	500	25.6	10.2
7	200	300	500	10.2	4.1
8	0	300	300	0	0

(2.3) Sample preparation

Tissue lysate sample was diluted into 2- and 4-fold with 1-fold sample diluent buffer.

(2.4) Assay procedure

Before using, equilibrate all materials and prepared reagents to room temperature (18-25°C). 100 µL of each standard and sample were added into the appropriate wells, then incubate at 4°C overnight with gentle shaking.

Ref. code: 25595829040418WTR

Next, the wells were washed by filling each well with 300 μL of 1-fold wash solution for 4 times. After the last wash, any remaining solution was removed from wells by aspirating. The plate was inverted and blotted against clean paper towels. Then, 100 μL of 1-fold biotinylated VEGF detection antibody was added to each well and incubated at room temperature for 1 hour with gentle shaking. After that, the 4-time wash process with 1-fold wash solution was repeated again. 100 μL of 1-fold HRP-Streptavidin solution was added to each well prior to 45 minutes incubation at room temperature with gentle shaking. After the solution was discarded, the 4-time wash process was repeated again. 100 μL of TMB one-step substrate reagent was added to each well prior to 30 minutes incubation in the dark at room temperature with gentle shaking. Finally, 50 μL of stop solution was added to each well. The results was read at 450 nm immediately.

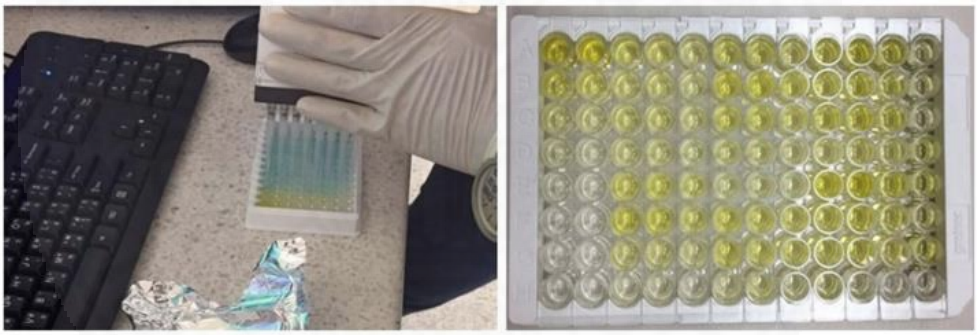

Figure 7.19 After adding stop solution, each well turned into vary yellow gradient up to its VEGF concentration.

(2.5) Calculations

The mean absorbance for each set of duplicate standards, controls and samples was calculated, and subtracted the average zero standard optical density (OD). Eventually, the standard curve was plotted in order to indicate VEGF concentration relating from the absorbance. The standard curve and the OD of each sample are demonstrated in Appendix J.

Ref. code: 25595829040418WTR

7.3 Data analysis

ANOVA with post-hoc Bonferroni test and independent t-test were run to compare the data obtained from the treatment groups, and all measured values were reported in means. In case of non-parametric data, the values were presented as median (range: min - max) and p-value was corresponded to Mann-Whitney U test. All statistical analyses were performed using Stata version 13 (StataCorp LP, USA). Statistical significance in all cases was considered to have a p-value <0.05.

Ref. code: 25595829040418WTR

CHAPTER 8
RESULTS

The total of 21 C57BL/6 male mice were enrolled in this research and all remained healthy until the experimental endpoint.

8.1 Hair growth

8.1.1 Significant hair regrowth in the topical tofacitinib-treated group compared to that in the topical minoxidil-treated group.

After 7 days of treatment, mice treated with tofacitinib showed initiation of hair regrowth on the coated area, while minoxidil-treated mice were still denuded with higher statistical significance for the tofacitinib-treated group (25.36%) as compared to minoxidil-treated group (18.23%) with 95% CI 7.13 (3.1-11.16), P=0.002. On day 14, more distinct hair regrowth was observed with tofacitinib treatment (64.62%) than with minoxidil (30.31%), with 95% CI 34.32 (14.5-54.13), P=0.004. At experimental endpoint on day 21, hair regrowth continued, and we could macroscopically observe almost complete regrowth of hair in tofacitinib-treated group (98.5%) as compared to partial regrowth seen in minoxidil-treated group (61.58%) with a statistically significant 95% CI 36.91 (11.35-62.48), P=0.012. As the data shown in Table 8.1 and Figure 8.1.

Table 8.1 Comparison of area hair growth (%) at day 0, 7, 14, and 21 between tofacitinib-treated group and minoxidil-treated group.

	Tofacitinib (n=7) Mean (95%CI)	Minoxidil (n=7) Mean (95%CI)	Mean difference (95%CI)	p-value (t-test)
Day 0	15.22 (11.86, 18.58)	14.42 (11.55, 17.29)	0.8 (-3.13, 4.73)	0.666
Day 7	25.36 (21.66, 29.06)	18.23 (15.63, 20.83)	7.13 (3.1, 11.16)	0.002**
Day 14	64.62 (45.08, 84.16)	30.31 (23, 37.62)	34.32 (14.5, 54.13)	0.004**
Day 21	98.5 (96.8, 100.2)	61.58 (36.02, 87.14)	36.91 (11.35, 62.48)	0.012**

Values presented as mean (95% confident interval of mean). P-value corresponds to Independent t-test. **P<0.05.

Ref. code: 25595829040418WTR

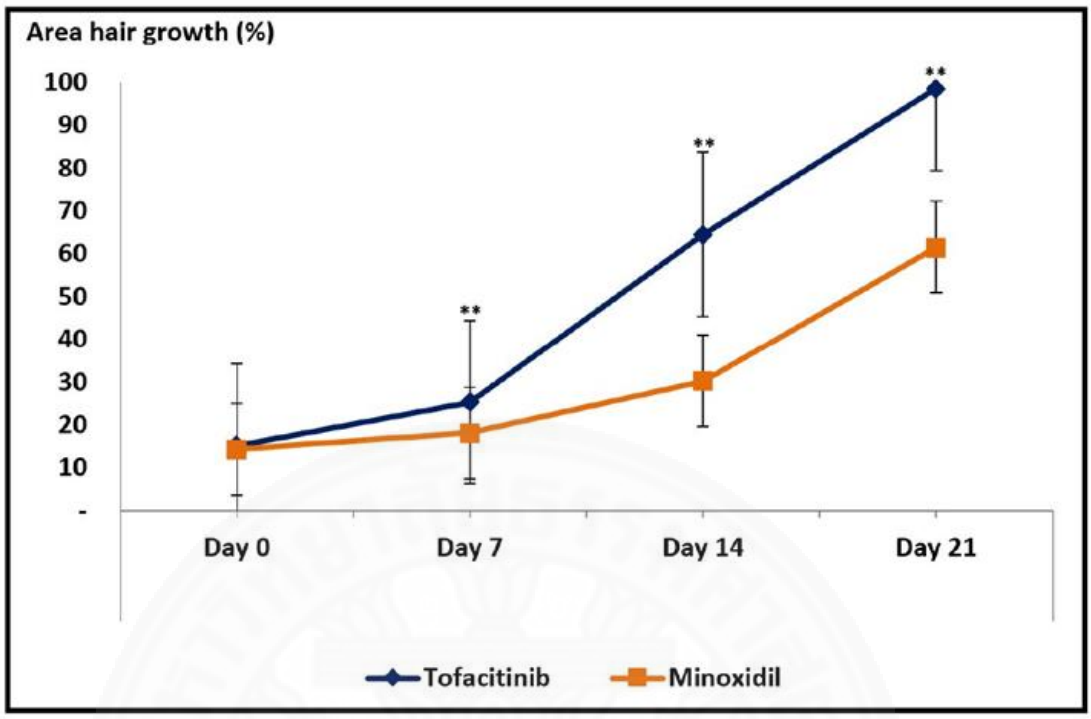

Figure 8.1 Comparison of area hair growth (%) at day 0, 7, 14, and 21 between tofacitinib-treated group and minoxidil-treated group. Mean ± Standard error of mean (SEM). **P<0.05.

In the same way, on day 14, tofacitinib showed more significant hair regrowth on the coated area (64.62%) when compared to DMSO-treated group (31.21%) and ethanol-treated group (31.48%), P<0.001. On day 21, tofacitinib also showed distinct hair regrowth on the coated area (98.5%) when compared to DMSO-treated group (66.59%) and ethanol-treated group (36.62%), P<0.001. Whereas minoxidil-treated group demonstrated no significant hair regrowth when compared to both vehicle-treated groups. Noticeably, on day 21, DMSO-treated group (66.59%) showed significant hair regrowth as compared to ethanol-treated group (36.62%), P<0.001.

Although, at baseline (day 0), the data showed significant difference of area hair growth between tofacitinib-treated versus (VS) ethanol-treated group and minoxidil-treated VS ethanol-treated group as a result from the error of hair shaving procedure, but in this study, we evaluated area hair regrowth relatively from each group

Ref. code: 25595829040418WTR

baseline, thus would compromise the results error. Area of hair growth at the beginning point (day 0) from each group was used as reference value in order to calculate the progression of area hair regrowth after continuing the treatment. At day 7, tofacitinib-treated group (10.14%) revealed higher progression of area hair regrowth as compared to that of minoxidil (3.82%) and ethanol (1.25%), P=0.003, while DMSO displayed quite high progression of area hair regrowth at 6.63%, despite statistically non-significant. Correspondingly, at day 14, tofacitinib-treated group (49.41%) demonstrated the highest progression of area hair regrowth as compared to minoxidil-treated (15.89%), DMSO-treated (9.59%), and ethanol-treated group (4.26%) with P<0.001. Finally, at day 21, tofacitinib-treated group (83.28%) also showed the greatest improvement of area hair regrowth in comparison to that of minoxidil (47.17%), DMSO (44.97%), and ethanol (9.4%) with P<0.001. As the data shown in Table 8.2 and Figure 8.2.

The raw data of area hair growth (%) on the dorsal back coated area of mice in each group is described in Appendix C.

Ref. code: 25595829040418WTR

Table 8.2 Comparison of area hair growth (%) and improvement of area hair regrowth (%) at day 0, 7, 14, and 21 among all treated groups.

	Tofaciti-nib (n=7)	Minoxi-dil (n=7)	Vehicle-DMSO (n=7)	Vehicle-ethanol (n=7)	p-value	
					ANOVA test	Bonferroni test
Area hair growth day 0	15.22 ± 3.63	14.42 ± 3.1	21.62 ± 4.16	27.22 ± 10.6	0.002*	c,e
Area hair growth day 7	25.36 ± 4	18.23 ± 2.81	28.25 ± 6.45	28.47 ± 8.72	0.012*	d,e
Area hair growth day 14	64.62 ± 21.13	30.31 ± 7.9	31.21 ± 7.39	31.48 ± 8.49	<0.001**	a,b,c
Area hair growth day 21	98.5 ± 1.84	61.58 ± 27.64	66.59 ± 25.29	36.62 ± 6.32	<0.001**	a,b,c,f
Improvement day 0	0	0	0	0	-	-
Improvement day 7	10.14 ± 5.14	3.82 ± 2.08	6.63 ± 4.9	1.25 ± 3.88	0.003*	a,c
Improvement day 14	49.41 ± 21.74	15.89 ± 9.96	9.59 ± 7.93	4.26 ± 5.45	<0.001**	a,b,c
Improvement day 21	83.28 ± 3.71	47.17 ± 29.54	44.97 ± 26.51	9.4 ± 8.07	<0.001**	a,b,c,e,f

Values presented as mean (95% confident interval of mean). P-value corresponds to ANOVA test and Post hoc test by Bonferroni. *P<0.05. **P<0.001.

(a) Tofacitinib VS Minoxidil, (b) Tofacitinib VS Vehicle-DMSO, (c) Tofacitinib VS Vehicle-ethanol, (d) Minoxidil VS Vehicle-DMSO, (e) Minoxidil VS Vehicle-ethanol, (f) Vehicle-DMSO VS Vehicle-ethanol

Ref. code: 25595829040418WTR

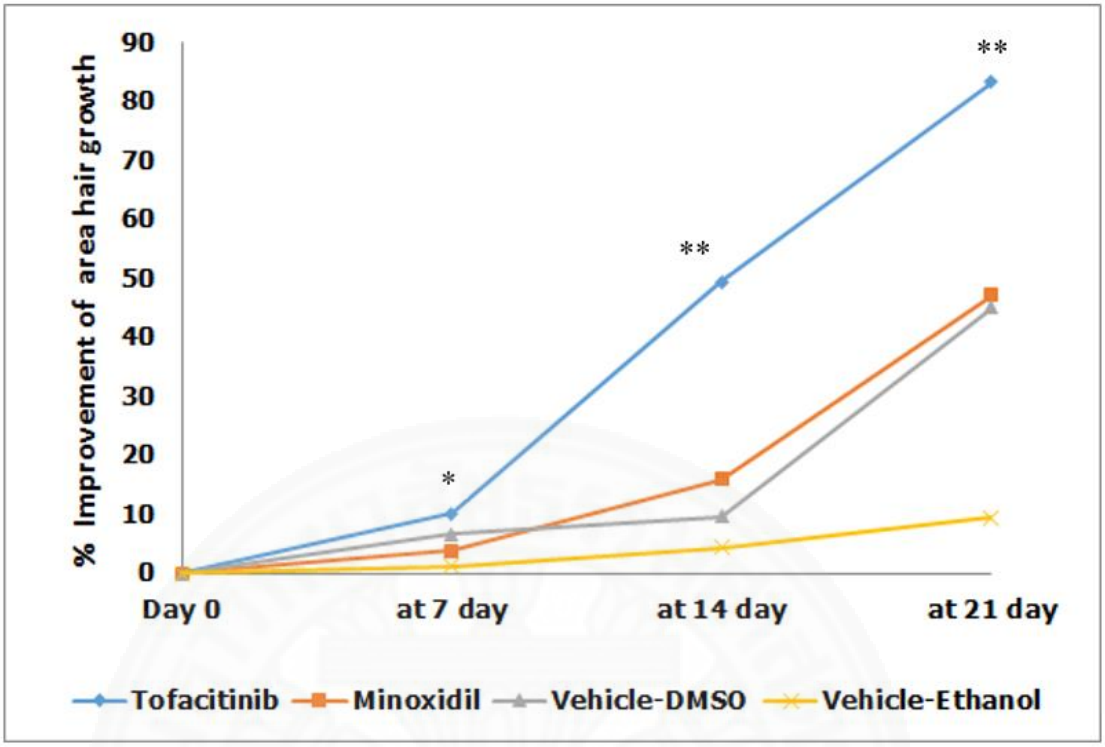

Figure 8.2 Comparison of area hair regrowth improvement (%) at day 0, 7, 14, and 21 among all treated groups. *P<0.05. ** P<0.001.

From observation, we could macroscopically see thinned-quality hair regrowth initiated on the dorsal back coated area of mice treated with tofacitinib approximately since day 7 after treatment, despite still denuded in minoxidil-treated group. With slower onset, we could observe hair regrowth initiation from minoxidil-treated group on day 11, and DMSO-treated group on day 14. Despite, no distinct hair regrowth observed from ethanol-treated group. Hair regrowth in mice treated with tofacitinib, minoxidil, and DMSO continue up to the end of the study (21 days) with gradually larger in hair diameter and density. Another unexpected findings recognized from the study was that mice in tofacitinib-treated group and DMSO-treated group developed dry erythematous skin on the dorsal back coated area after applying those reagents since day 7, but after continue to apply, erythema was gradually diminished, then the skin turned grey and replaced with regrown hair in tofacitinib-treated group following by DMSO-treated group. As the results of the hair regrowth model were represented in Figure 8.3. And for more figures, please see Appendix A.

Ref. code: 25595829040418WTR

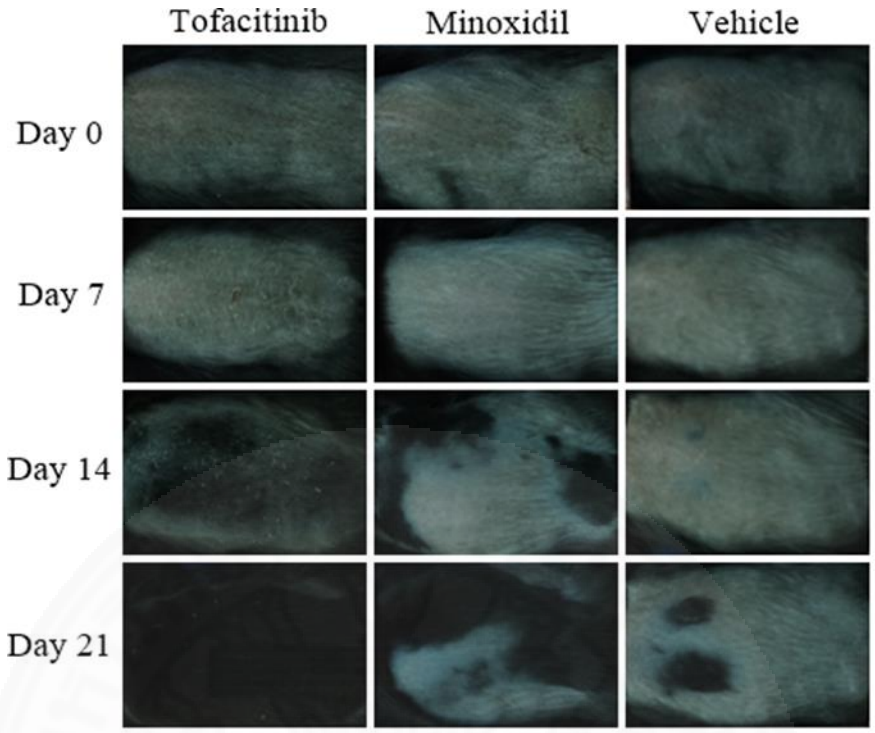

Figure 8.3 Hair regrowth model on day 0, 7, 14, and 21 after topical application of tofacitinib (left), minoxidil (middle), and vehicle (right); DMSO on left half and ethanol on right half. Tofacitinib-treated group displayed faster onset of hair regrowth since day 7, whereas minoxidil-treated and vehicle-treated group still denuded. On day 21, despite almost full area of hair regrowth showed in tofacitinib-treated group, partial hair regrowth observed in minoxidil-treated and vehicle-treated group.

Thus, the results suggest that tofacitinib promotes significantly more hair regrowth coupled with rapid onset than minoxidil and vehicle.

8.1.2 Mice treated with topical tofacitinib exhibited rapid rate of hair growth.

We examined hair growth rate, calculated from the mean hair length (mm) measured using a digital microscope from day 0 until day 14 of treatment (on day 21, hairs in tofacitinib-treated group were greater in length, which mostly beyond the microscopic field, so that it could not be measured), and found that mice treated with topical tofacitinib had a significant increase in the rate of hair growth compared with that of topical minoxidil at day 14, with 95% CI 0.03 (0.01-0.04), P=0.003, as shown

Ref. code: 25595829040418WTR

in Table 8.3 and Figure 8.4. And for digital microscope figures, please see Appendix B.

Table 8.3 Comparison of average rate of hair growth between tofacitinib-treated and minoxidil-treated groups calculated from mean hair length (mm) measured using digital microscope from day 0 until day 14 of treatment.

	Tofacitinib (n=7) Mean (95%CI)	Minoxidil (n=7) Mean (95%CI)	Mean difference (95%CI)	p-value (t-test)
Mean hair length (mm)				
Day 0	0.29 (0.25, 0.33)	0.28 (0.25, 0.31)	0.01 (-0.03, 0.05)	0.522
Day 7	0.33 (0.29, 0.37)	0.32 (0.29, 0.35)	0 (-0.04, 0.05)	0.818
Day 14	0.8 (0.56, 1.04)	0.41 (0.33, 0.49)	0.39 (0.16, 0.61)	0.003**
Hair growth rate (mm/day)				
Day 0-14	0.04 (0.02, 0.06)	0.01 (0, 0.02)	0.03 (0.01, 0.04)	0.003**

Values presented as mean (95% confident interval of mean). P-value corresponds to Independent t-test. **P<0.05.

Ref. code: 25595829040418WTR

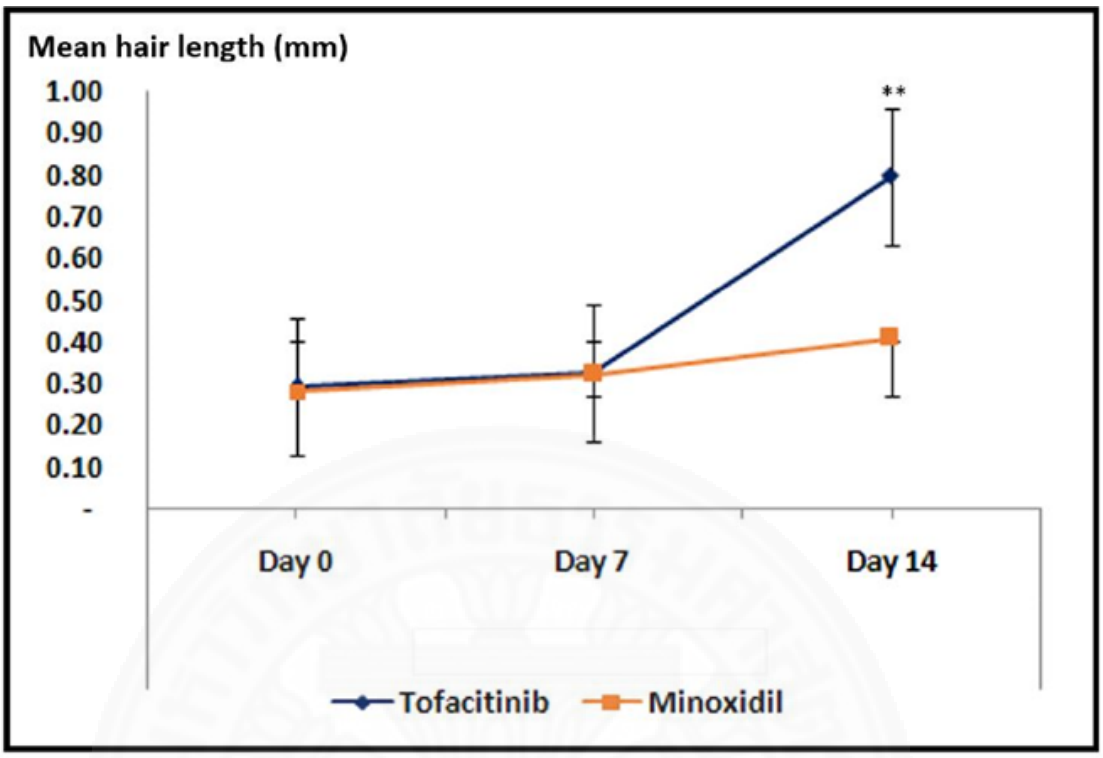

Figure 8.4 Comparison of mean hair length (mm) from day 0 until day 14 after treatment between tofacitinib-treated group and minoxidil-treated group. Mean ± SEM. **P<0.05.

Overall, mice treated with topical tofacitinib had a significant increase in the rate of hair growth compared with that of minoxidil and vehicle at day 14, with P<0.001. Mean hair growth rate of tofacitinib-treated group, minoxidil-treated group, DMSO-treated group, and ethanol-treated group were 0.04, 0.01, 0.01, and 0 mm/day, respectively, as shown in Table 8.4 and Figure 8.5.

The raw data of mean hair length (mm) and hair growth rate (mm/day) of each treated mouse is demonstrated in Appendix D.

Ref. code: 25595829040418WTR

Table 8.4 Comparison of average rate of hair growth among all treated groups calculated from mean hair length (mm) measured using digital microscope from day 0 until day 14 of treatment.

	Tofacitinib (n=7)	Minoxidil (n=7)	Vehicle-DMSO (n=7)	Vehicle-ethanol (n=7)	p-value	
					ANOVA test	Bonferroni test
Mean hair length (mm)						
Day 0	0.29 (0.25, 0.33)	0.28 (0.25, 0.31)	0.33 (0.31, 0.35)	0.37 (0.34, 0.4)	<0.001**	c,d,e
Day 7	0.33 (0.29, 0.37)	0.32 (0.29, 0.35)	0.38 (0.35, 0.41)	0.39 (0.35, 0.43)	0.001*	c,d,e
Day 14	0.8 (0.56, 1.04)	0.41 (0.33, 0.49)	0.44 (0.35, 0.53)	0.41 (0.37, 0.45)	<0.001**	a,b,c
Hair growth rate (mm/day)						
Day 0-14	0.04 (0.02, 0.06)	0.01 (0, 0.02)	0.01 (0, 0.02)	0 (0, 0)	<0.001**	a,b,c

Values presented as mean (95% confident interval of mean). P-value corresponds to ANOVA test and Post hoc test by Bonferroni. *P<0.05. **P<0.001.

(a) Tofacitinib VS Minoxidil, (b) Tofacitinib VS Vehicle-DMSO, (c) Tofacitinib VS Vehicle-ethanol, (d) Minoxidil VS Vehicle-DMSO, (e) Minoxidil VS Vehicle-ethanol, (f) Vehicle-DMSO VS Vehicle-ethanol

Ref. code: 25595829040418WTR

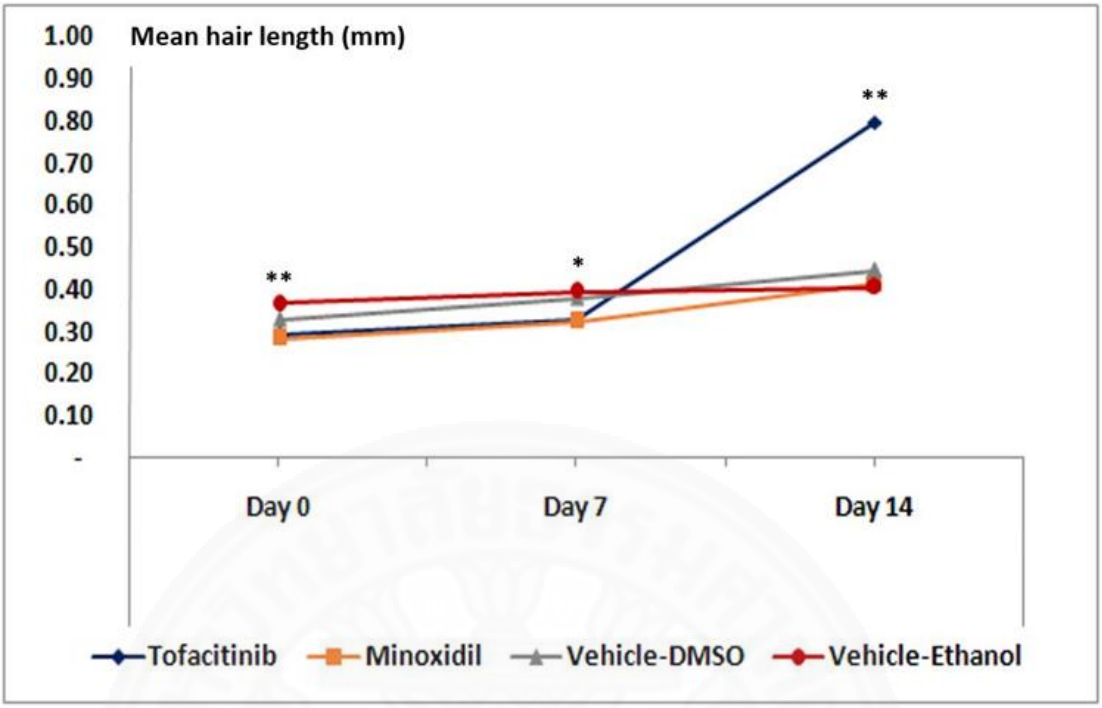

Figure 8.5 Comparison of mean hair length (mm) from day 0 until day 14 after treatment among all groups. *P<0.05. **P<0.001.

8.2 Histopathology

8.2.1 Most of the hair follicles in tofacitinib-treated group were in late anagen stage, while those of minoxidil-treated group were in catagen and anagen stages.

As corresponded to clinical, it was observed that the number of hair follicles in tofacitinib-treated group was distinctly increased and mainly classified in mature/late anagen phase in hypodermis, followed by some early anagen hair follicles in superficial dermis, but rarely catagen or telogen hair follicles were found. Meanwhile, less number of hair follicles was found in minoxidil-treated group as compared to that of tofacitinib and mostly classified in catagen phase in deep dermis and late anagen phase in deep dermis and hypodermis. Interestingly, quite high number of hair follicles was found in DMSO-treated group and largely classified as late anagen hairs in deep dermis and hypodermis, followed by catagen hairs in deep dermis and telogen hairs in superficial dermis. Whereas hair follicles in ethanol-treated group were

Ref. code: 25595829040418WTR

the least found and mainly demonstrated to be in telogen phase in superficial dermis and catagen phase in deep dermis. As expected, anagen hairs were scarcely reported in ethanol-treated group.

The model results of H&E staining of the dorsal skin tissue after 21 days of topical tofacitinib, minoxidil, DMSO, and ethanol application are shown in Figure 8.6. All tissues were well epithelialization with keratinization. The granulation was seen well organized with abundant collagen bundles and fibroblast infiltration. And for more histopathological figures, please see Appendix E.

Ref. code: 25595829040418WTR

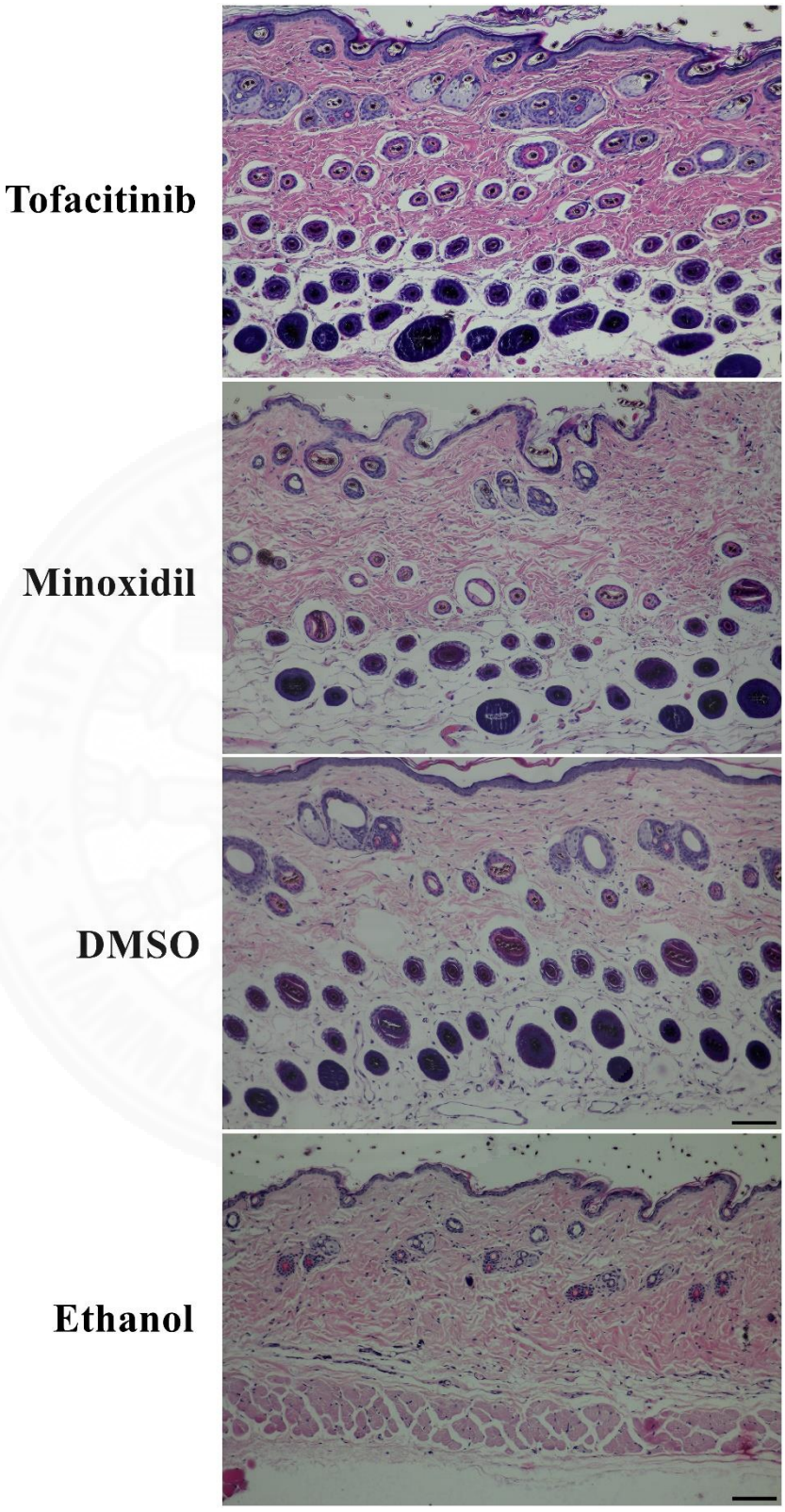

Figure 8.6 The model results of H&E staining of the dorsal skin tissue after 21 days of topical tofacitinib, minoxidil, DMSO, and ethanol application.

Ref. code: 25595829040418WTR

8.2.2 Tofacitinib-treated group revealed to have more newly formed capillary numbers.

Observations revealed of multiple newly formed small-sized capillaries in tofacitinib-treated group, whereas completely formed capillaries were less found. Contrastingly, plenty completely formed dilated capillaries were found in minoxidil-treated group, but newly formed capillaries were less found as compared to that of tofacitinib-treated group. In the same way, DMSO-treated group also demonstrated of less newly formed capillaries, though completely formed capillaries were relatively more often found. As expected, ethanol-treated group had less both newly and completely formed capillaries. The model results of H&E staining of the dorsal skin tissue after 21 days of topical tofacitinib, minoxidil, DMSO, and ethanol application focusing on the capillaries are demonstrated in Figure 8.7.

Ref. code: 25595829040418WTR

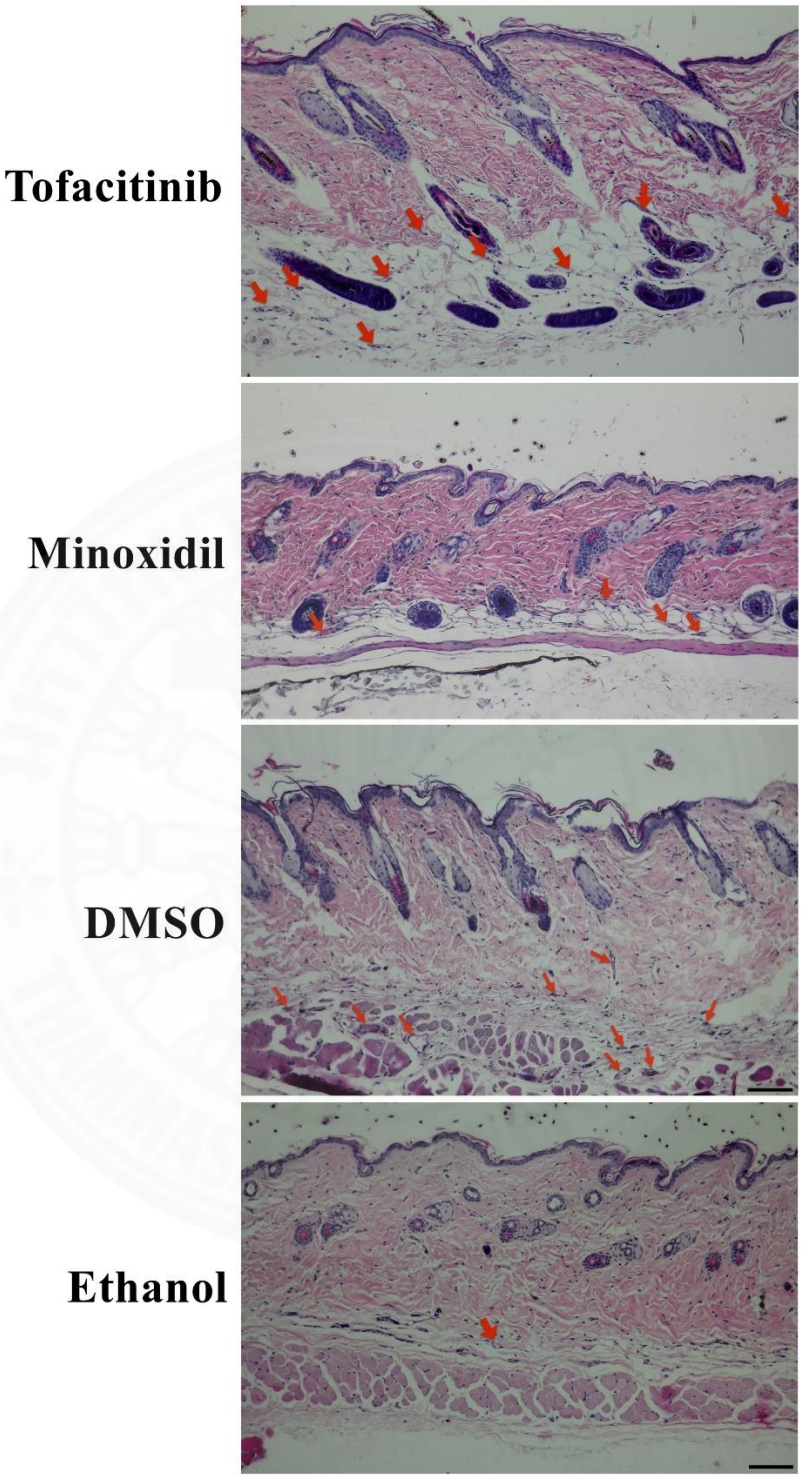

Figure 8.7 Demonstration of the model results of H&E staining under 10x magnification of the dorsal skin tissue after topical tofacitinib, minoxidil, DMSO, and ethanol application focusing on the newly and completely formed capillaries. The capillaries are labelled in red arrows.

Ref. code: 25595829040418WTR

8.2.3 Tofacitinib-treated group demonstrated less inflammatory cells infiltration.

Among all treatment groups, tofacitinib-treated and ethanol-treated seemed having the least inflammatory cells infiltrated in tissues. As in tofacitinib-treated group, this detection was correlated to the clinical that its inflammatory sign was lessen after continue applying tofacitinib, and having hair regrowth instead. In minoxidil-treated group, mononuclear inflammatory cells were found to be infiltrated, even though slightly, but still more than that of tofacitinib and ethanol. In DMSO-treated group, as corresponded to the development of dry scaly erythematous skin, demonstrated of having the most mononuclear inflammatory cells infiltration in comparison to all treated groups. The model results of H&E staining of the dorsal skin tissue after 21 days of topical tofacitinib, minoxidil, DMSO, and ethanol application focusing on the infiltration of inflammatory cells are demonstrated in Figure 8.8.

Ref. code: 25595829040418WTR

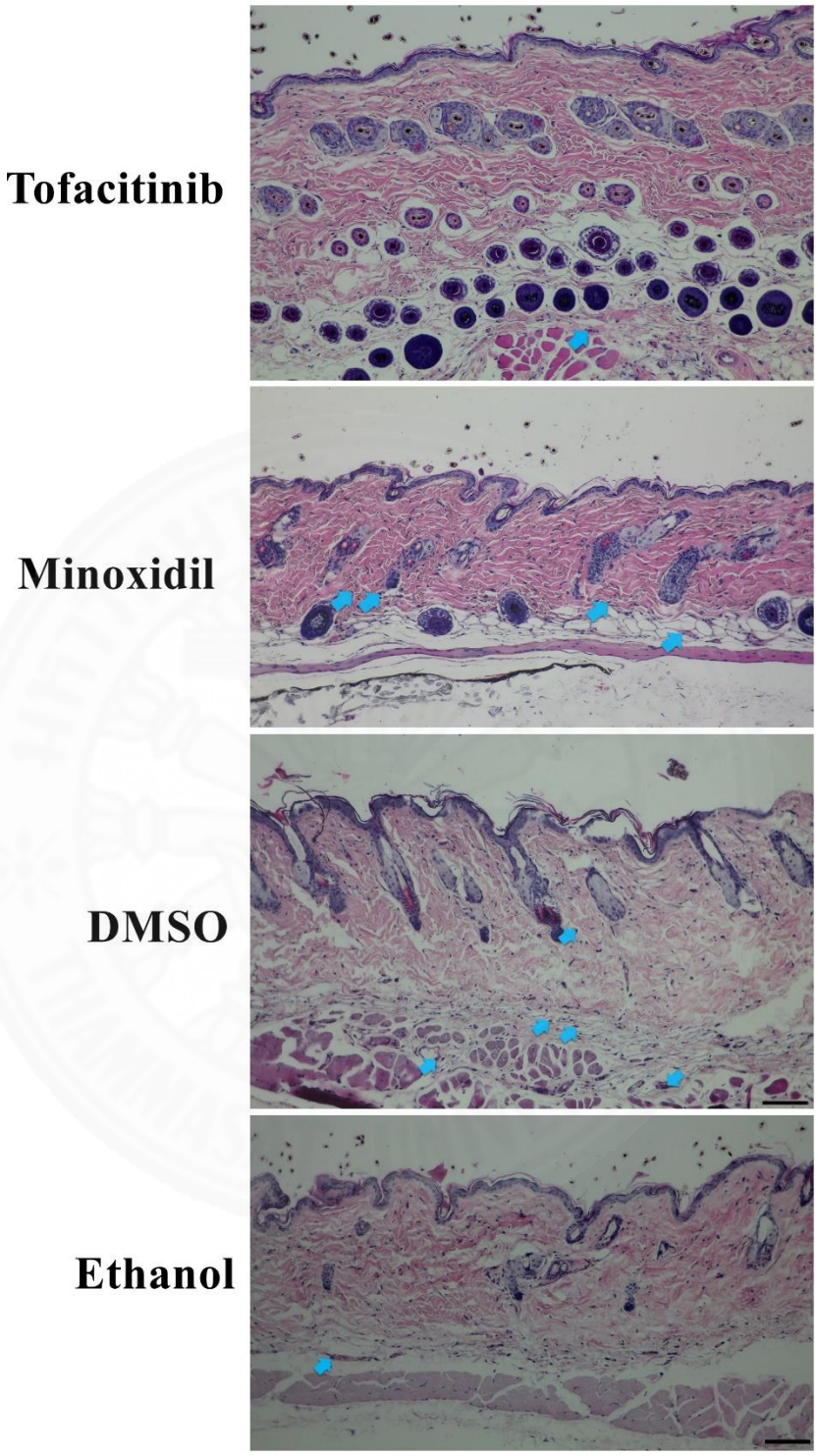

Figure 8.8 Demonstration of the model results of H&E staining under 10x magnification of the dorsal skin tissue after topical tofacitinib, minoxidil, DMSO, and ethanol application focusing on the infiltration of inflammatory cells. The infiltrated inflammatory cells are labelled in blue arrows.

Ref. code: 25595829040418WTR

8.3 Cell growth factors

8.3.1 RT-PCR

8.3.1.1 VEGF

According to either laboratory error or the quantity of cell growth factor expression was too low, hence, some values were not be able to evaluate and to be odded out. 6 samples of tofacitinib-treated group were left to be calculated for the VEGF mRNA expression, while 4, 7, and 3 samples of minoxidil-treated, DMSO-treated, and ethanol-treated groups, respectively, were to be included in calculation for the VEGF mRNA expression.

The median expression of VEGF mRNA in tofacitinib-treated group (117.45) showed significantly higher in value when comparing to minoxidil-treated group (25.415), P=0.033. As well as vehicle-treated group, the median expression of VEGF mRNA in tofacitinib-treated group (117.45) was markedly higher as compared to DMSO-treated group (28.33), P=0.032, and to ethanol-treated group (9.15), P=0.02. In contrast, although minoxidil-treated group demonstrated quite large quantity of the median expression of VEGF mRNA as compared to ethanol-treated group, but still not that high to be statistically significant. And surprisingly, the median expression of VEGF mRNA in DMSO-treated group showed even slightly higher than in minoxidil-treated group, though not statistically significant. As the data shown in Table 8.5 and Figure 8.9.

Table 8.5 The median expression of VEGF mRNA evaluated from RT-PCR.

Treated group	n	Median	Min	Max	p-value		
Tofacitinib	6	117.45	20.01	189.13	Ref		
Minoxidil	4	25.415	10.32	63.21	0.033*	Ref	
Vehicle-DMSO	7	28.33	4.32	45.01	0.032*	1	Ref
Vehicle-ethanol	3	9.15	5.17	13.39	0.02*	0.157	0.087

Values presented as median (range: min - max). P-value corresponds to Mann-Whitney U test. Ref, reference group. *P<0.05.

Ref. code: 25595829040418WTR

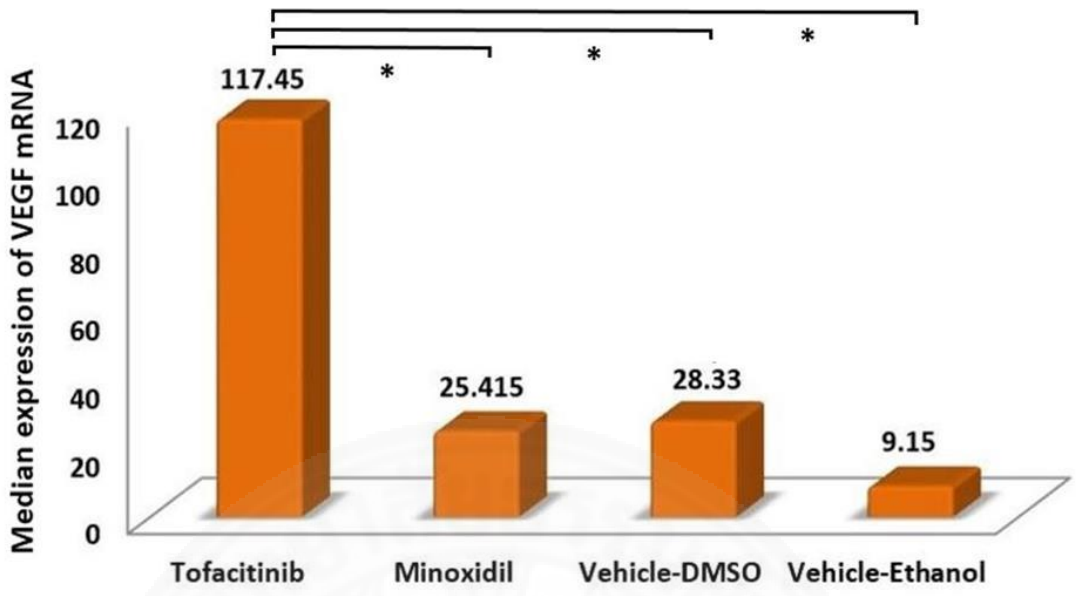

Figure 8.9 Comparison of the median expression of VEGF mRNA evaluated from RT-PCR. *P<0.05.

8.3.1.2 IGF-1

Similarly to the VEGF mRNA evaluation, in case of the IGF-1, either laboratory error or the quantity of cell growth factor expression was too low, thus, some values were not be able to evaluate and to be odded out. 6 samples of tofacitinib-treated group were left for calculating the IGF-1 mRNA expression, whereas 3, 7, and 3 samples of minoxidil-treated, DMSO-treated, and ethanol-treated groups, respectively, were to be included in calculation for the IGF-1 mRNA expression.

The median expression of the IGF-1 mRNA in minoxidil-treated group (175.46) showed the greatest value as compared to others with statistically significant with P=0.039, 0.03, and 0.037 for tofacitinib-treated, DMSO-treated, and ethanol-treated reference groups, respectively. The median expression of the IGF-1 mRNA in tofacitinib-treated group (15.23) was significantly higher when comparing to ethanol-treated group (too low to be evaluated, imputation as 1), P=0.043. DMSO-treated group (27.13) also had significantly higher value of the median expression of the IGF-1 mRNA as compared to ethanol-treated group (too low to be evaluated, imputation as 1), P=0.015. Surprisingly, DMSO-treated group (27.13) revealed higher

Ref. code: 25595829040418WTR

value of the median expression of the IGF-1 mRNA when comparing to tofacitinib-treated group (15.23), but yet was not that high to be statistically significant. As shown in Table 8.6 and Figure 8.10.

Table 8.6 The median expression of the IGF-1 mRNA evaluated from RT-PCR.

Treated group	n	Median	Min	Max	p-value		
Tofacitinib	6	15.23	1	81.81	Ref		
Minoxidil	3	175.46	73.76	236.09	0.039*	Ref	
Vehicle-DMSO	7	27.13	1.04	129.38	0.317	0.03*	Ref
Vehicle-ethanol	3	1	1	1	0.043*	0.037*	0.015*

Values presented as median (range: min - max). P-value corresponds to Mann-Whitney U test. 1, too low to be evaluated. Ref, reference group. *P<0.05.

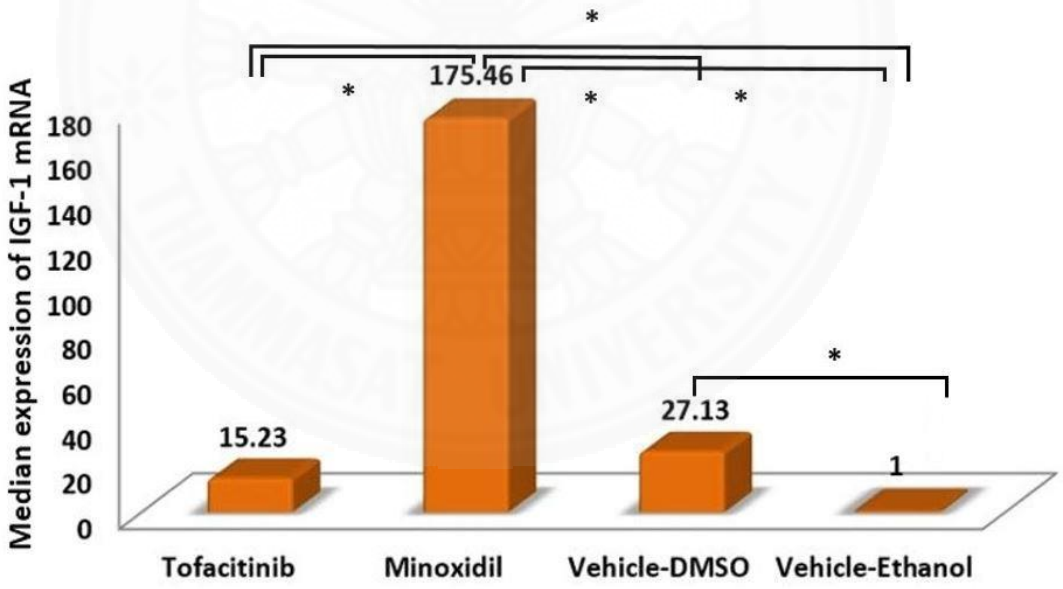

Figure 8.10 Comparison of the median expression of IGF-1 mRNA evaluated from RT-PCR. *P<0.05.

Ref. code: 25595829040418WTR

8.3.2 ELISA

8.3.2.1 VEGF

According to RT-PCR results, the median expression of VEGF mRNA in tofacitinib-treated group showed significantly higher when comparing to others, thus, in order to determine protein concentration of VEGF, the ELISA technique was used. The standard dilutions were duplicated and placed on the first two column of well plate. Overall 28 samples with duplication and triplication were included in ELISA process, despite some outlier concentrations were odded out. 5 samples of tofacitinib-treated group were left for calculating mean VEGF concentration, whereas 4, 5, and 7 samples of minoxidil-treated, DMSO-treated, and ethanol-treated groups, respectively, were to be included in calculation for mean VEGF concentration. Mean VEGF concentration of tofacitinib-treated group (904.77 pg/mL), corresponding with the mRNA expression results, showed significantly higher as compared to that of minoxidil-treated group (562.20 pg/mL) with P=0.046. As expected, mean VEGF concentration of tofacitinib-treated group (904.77 pg/mL) also demonstrated significantly higher than DMSO-treated (554.30 pg/mL) and ethanol-treated (372.13 pg/mL) group with P=0.025 and 0.004, respectively. Correlating with RT-PCR results, mean VEGF concentration of minoxidil-treated group (562.20 pg/mL) was not significantly increased when compared to those of vehicle groups, while mean VEGF concentration of DMSO-treated group (554.30 pg/mL) revealed significantly higher than that of ethanol-treated group (372.13 pg/mL) with P=0.014. As shown in Table 8.7 and Figure 8.11.

Table 8.7 Mean VEGF concentration (pg/mL) evaluated from ELISA.

Treated group	n	Mean	SD	p-value		
Tofacitinib	5	904.77	230.17	Ref		
Minoxidil	4	562.20	182.47	0.046*	Ref	
Vehicle-DMSO	5	554.30	60.10	0.025*	0.929	Ref
Vehicle-Ethanol	7	372.13	125.26	0.004**	0.128	0.014*

Values presented as mean and standard deviation (SD). P-value corresponds to Independent t-test. Ref, reference group. *P<0.05. **P<0.005.

Ref. code: 25595829040418WTR

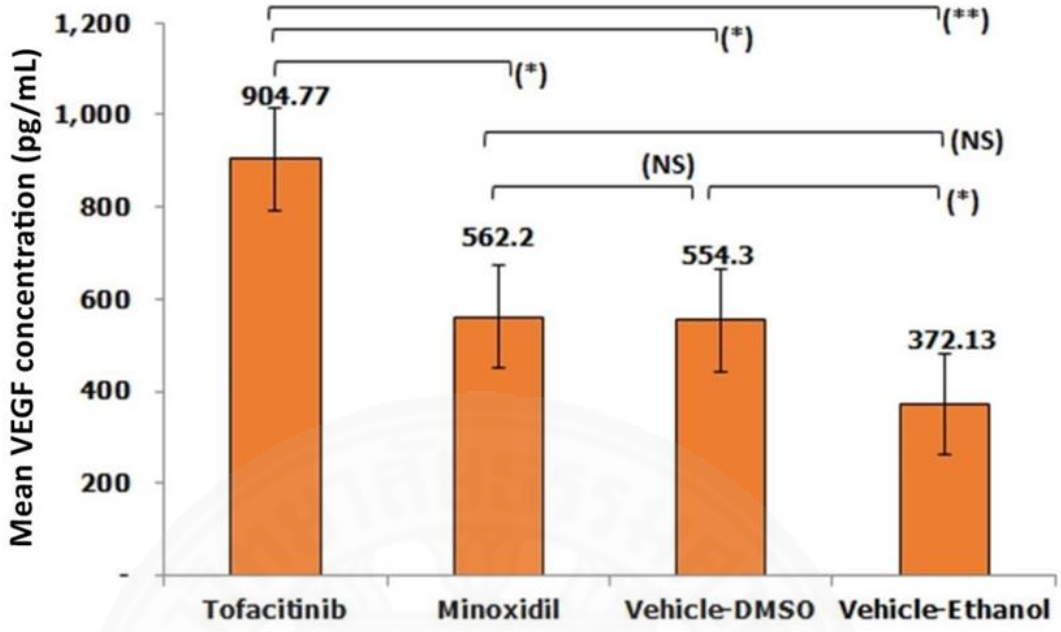

Figure 8.11 Comparison of mean VEGF concentration (pg/mL) evaluated from ELISA. NS, non-significant. *P<0.05. **P<0.005.

Ref. code: 25595829040418WTR

CHAPTER 9
DISCUSSION AND RECOMMENDATIONS

9.1 Discussion

Currently approved medication for AGA includes oral finasteride and topical minoxidil, both still limited in efficacy and many have untoward side effects. Tofacitinib has been proven of its stimulatory effect towards hair growth (3, 15). Treatment of JAK inhibitors in topical form resulted in more robust hair growth than did systemic form, possibly because it increases the local drug concentration in the hair follicle microenvironment, allowing interactions to occur (3) as well as lesser side effect achieved in topical treated. Thus, this study intends to demonstrate the efficacy in promoting hair growth of topical tofacitinib compared with topical minoxidil conducting in mice model.

From our data, topical application of tofacitinib led to hair regrowth initiation since day 7 after treatment, whereas minoxidil and DMSO also led to hair regrowth but with slower onset, on day 11 and 14 respectively, despite no obvious hair regrowth initiation was observed in ethanol-treated group for the entire experiment. Moreover, area hair regrowth according to tofacitinib application demonstrated almost full area of the dorsal back previously coated, despite partial hair regrowth area in minoxidil-treated and DMSO-treated group, even though till day 21 which was the experimental endpoint. Corresponding with clinical, histopathological observations also revealed distinctly more hair follicles in tofacitinib-treated group compared to that of others. Another interesting outcome, we measured mean hair length using Dino-Lite microscope on day 0 until day 14 (the hair length of tofacitinib-treated group on day 21 was too long to be evaluated, thus we used the data till day 14) and used to calculate average hair growth rate. The results showed that mice treated with topical tofacitinib had significantly more rapid rate of hair regrowth as compared to others.

A further interesting histopathological findings was that most hair follicles in tofacitinib-treated group were classified as anagen hairs, while nearly half of the hair follicles in minoxidil-treated group were classified in catagen phase, which indicates

Ref. code: 25595829040418WTR

and reaffirms that tofacinib could accelerate transition to anagen phase (3, 15) in greater magnitude. An additional evidence was that after continue treating with tofacitinib, we observed skin darkening, which indicated the migration of melanin to the skin surface during telogen to anagen conversion (162).

Furthermore, another feasible effect of tofacitinib that supports the results is that of its anti-inflammatory property (2, 4) confirming by the experimental findings that during the first week after the application of tofacitinib and DMSO, the dorsal skin of mice turned erythema with dry scales due to the exorbitant concentration of DMSO (100% concentration using as tofacitinib's vehicle and control), but after continue applying, the erythema and scales were lessened with new hair regrowth recognized instead in tofacitinib-treated group, whereas still some dry scaly erythematous skin observed in DMSO-treated group. Concurrently, according to the histopathological results, tofacitinib-treated group revealed less inflammatory cells infiltration, while more inflammatory cells still observed in minoxidil-treated and DMSO-treated groups. The findings suggest that an anti-inflammatory effect of tofacitinib may be an additional potential in promotion of hair growth by inhibiting the process of hair follicle microinflammation, which can lead to hair follicle apoptosis and play a crucial role in the pathogenesis of follicle miniaturization (163, 164). While the histopathological findings in minoxidil-treated group, which demonstrated of having more mononuclear inflammatory cells infiltration, reaffirm the former knowledge that minoxidil alone has limited in anti-inflammatory effect (165).

Overall, our experimental results could ascertain the previous study, which has been reported that tofacitinib leads to hair growth promotion according to the mechanism of WNT and SHH signaling pathways activation, even though the process of stimulation has not been clearly known, together with stimulatory effect of hair follicle stem cells activation and/or proliferation (3). Whereof the processes are evidenced from the repression of receptors that involved in the modulation of dermal papilla inductivity, such as FGFR1, ACVRL1, IGFR1, OSMR, and PTGFR (20–23) collocate with down-regulation of proapoptotic genes included BAX, Bcl2L11 and CASP12. In addition, genes up-regulation induced by tofacitinib involving the members of the TGF-β and BMP pathway, which formerly has been shown to play an important role in DP inductivity (23–26). Besides, LEF1, another key regulator of the

Ref. code: 25595829040418WTR

WNT pathway, together with the NOTCH pathway members are also overexpressed during the treatment with tofacitinib (3).

Meanwhile, minoxidil induces several cell growth factors, such as VEGF, HGF, and IGF-1, together with activates uncoupled sulfonylurea receptor on DP plasma membrane. It also inhibits TGF-β, which acts as hair matrix cells apoptosis inducer. And lastly, minoxidil performs as hair follicle vasodilator, thereby increasing blood flow to the dermal papillae, resulting in an anagen phase extension (48, 166, 167).

Curiously, in accordance with the study, we found that one of the possible potential mechanisms leading to hair growth of tofacitinib might be that of VEGF expression, which revealed the highest level within tofacitinib-treated group among others. Although, we have previously known that VEGF expression shows high in minoxidil treatment, but according to our results, tofacitinib could even induce more. The expression of VEGF has been projected to angiogenesis, but apart from this, it also has direct action on hair DP cells as an autocrine growth factor (168). Correlatively, our histopathological results also proved VEGF promoting angiogenesis by demonstrating that the newly formed capillaries were the most found in tofacitinib-treated tissue in comparison to all treated groups. Therefore, this suggests that overexpression of VEGF induced by JAK-STAT inhibitory effect of tofacitinib might play another important role in hair growth promotion according to the angiogenic process evidenced by the observations of new forming capillaries, which leads to anagen extension and hair regrowth. In case of minoxidil, the completely formed or mature capillaries with slightly dilation were found in relatively greater quantity, while the newly formed capillaries were also demonstrated, but fewer, corresponding with VEGF expression of minoxidil, which exhibited lower. This indicates that during minoxidil application, the angiogenesis, which refers from a number of new forming capillaries, was lowered comparing with tofacitinib, despite a number of slightly dilated mature capillaries were more found. The possible reason may help explaining is that beside VEGF, there are several other minoxidil-induced cell growth factors performing in angiogenesis. Previous knowledge demonstrated that VEGF is not the only factors, but bFGF, angiopoietins, IL-8, placental growth factor (PlGF), and PDGF also play an important role as angiogenic promoters (169). Hence, apart from VEGF, we consider that

Ref. code: 25595829040418WTR

minoxidil may additionally up-regulate other cell growth factors assisting in angiogenesis.

Aside from VEGF, tofacitinib has previously been proved of its stimulatory effect on multiple hair follicle growth factors and inhibitory effect on apoptotic signal inducers resulting in better hair regrowth outcome.

Moreover, from observations, we surprisingly recognized distinct hair regrowth from DMSO-treated group, although tofacitinib-treated group still revealed more significant hair regrowth area, but at the experimental endpoint, mice treated with DMSO demonstrated high percentage of hair regrowth area as nearly to that of the minoxidil-treated group. Correspondingly, the median expression of VEGF mRNA in DMSO-treated group showed even slightly higher, though not statistically significant, than in minoxidil-treated group and mean VEGF concentration of DMSO-treated group also demonstrated in quite large volume as nearly to that of minoxidil. The explanation is that during the application of DMSO, the dorsal coated skin of mice showed the characteristic sign of irritant contact dermatitis by turning erythema with dry scales. According to previous knowledge, the protein kinase C (PKC)-α inducing by skin irritation or allergic contact dermatitis has been implicated in the growth of mouse hair (170, 171). Additionally, the expression level of VEGF, one of the hair growth promoting factors, has been reported to be greatly increased after inducing irritant contact dermatitis in mouse skin (172), which our results displayed in the same way. Therefore, in this setting, DMSO application in mouse skin resulting in irritant contact dermatitis might lead to hair growth due to similar condition.

Even though DMSO was used as vehicle for tofacitinib and we could also observe characteristic sign of dermatitis in tofacitinib-treated mice, but as continue treating, the inflammatory sign lessened and hair regrowth was observed instead. The percentage of area hair growth collocate with VEGF expression in tofacitinib-treated group revealed strikingly highest among all treated groups, this might be implicated that though dermatitis reaction could more or less influence on hair regrowth in tofacitinib-treated group, but other mechanisms that have been discussed above according to hair growth inductive property of tofacitinib still be substantially more advantageous.

Ref. code: 25595829040418WTR

In contrast to VEGF expression that found high in tofacitinib application, the expression of IGF-1 was exhibited low suggesting that the IGF-1 gene expression cascade might be less concern in the mechanism of hair growth promotion of tofacitinib.

In conclusion, according to macroscopic, histopathologic, and immunologic results could underscore the statistically significant of tofacitinib effect as hair growth promoter with greater in efficacy as compared to minoxidil which has been approved as therapeutic agent and generally use in non-scarring alopecia.

Tofacitinib has been approved in rheumatoid arthritis treatment by the US FDA and currently in clinical trials for treatment of psoriasis (13), vitiligo (14), and AA (15, 16). The successful treatment of AU with topical ruxolitinib as JAK inhibitor (173) together with the report of significantly hair regrowth regarding the use of oral tofacitinib in AA, AT, and AU (160, 174) has been demonstrated.

Our study raises another crucial therapeutic effect in addition to immune-driven conditions, tofacitinib proved to be advantageous in having significantly greater in hair growth promoting efficacy comparing to minoxidil with faster onset, more rapid rate of hair regrowth and better outcome. These findings would probably beneficial in open access to apply in human clinical trials in further study.

Ref. code: 25595829040418WTR

9.2 Recommendations

- Further studies with using vary concentration of tofacitinib in order to determine its dose dependent effect.

- Further studies in long term duration are pursued in order to examine tofacitinib adverse events and to determine whether its therapeutic effect on hair growth can be maintain throughout after treatment cessation or not.

- Further studies with initiating age of mice variation to achieve the data on reproducibility of hair growth resulting from tofacitinib treatment on hair stage variation, whether tofacitinib can abrogate the quiescence-promoting microenvironment at the early stages of telogen or not.

- Further studies in other cell growth factors expression according to tofacitinib treatment which will benefit in providing further information on hair growth promoted mechanism.

- Further studies in human clinical trials.

Ref. code: 25595829040418WTR

REFERENCES

1. Cetkovic-Cvrlje M TH. Therapeutic potential of Janus kinase 3 (JAK3) inhibitors. Curr Pharm Des. 2004;10(15):1767–84.

2. O'Shea JJ, Kontzias A, Yamaoka K, Tanaka Y, Laurence A. Janus kinase Inhibitors in autoimmune diseases. Ann Rheum Dis. 2013;72(2):ii111–ii115.

3. Harel S, Higgins CA, Cerise JE, Dai Z, Chen JC, Clynes R, et al. Pharmacologic inhibition of JAK-STAT signaling promotes hair growth. Sci Adv. 2015;1(9):e1500973.

4. Ghoreschi K, Jesson MI, Li X, Lee JL, Ghosh S, Alsup JW, et al. Modulation of Innate and Adaptive Immune Responses by Tofacitinib (CP-690,550). J Immunol. 2011;186(7):4234–43.

5. Fleischmann R, Kremer J, Cush J, Schulze-Koops H, Connell CA, Bradley JD, et al. Placebo-Controlled Trial of Tofacitinib Monotherapy in Rheumatoid Arthritis. N Engl J Med. 2012;367:495–507.

6. Boyce EG, Vyas D, Rogan EL, Valle-Oseguera CS, O'Dell KM. Impact of tofacitinib on patient outcomes in rheumatoid arthritis - review of clinical studies. Patient Relat Outcome Meas. 2016;14(7):1–12.

7. Migita K, Izumi Y, Jiuchi Y, Kozuru H, Kawahara C, Izumi M, et al. Effects of Janus kinase inhibitor tofacitinib on circulating serum amyloid A and interleukin-6 during treatment for rheumatoid arthritis. Clin Exp Immunol. 2014;175(2):208–14.

8. Sandborn WJ, Ghosh S, Panes J, Vranic I, Su C, Rousell S, et al. Tofacitinib, an oral Janus kinase inhibitor in active ulcerative colitis. New Engl J Med. 2012;367(7):616–24.

9. Boy MG, Wang C, Wilkinson BE, Chow VF, Clucas AT, Krueger JG, et al. Double-blind, placebo-controlled, dose-escalation study to evaluate the pharmacologic effect of CP-690,550 in patients with psoriasis. J Invest Dermatol. 2009;129(9):2299–302.

10. van Gurp E, Weimar W, Gaston R, Brennan D, Mendez R, Pirsch J, et al. Phase 1 dose-escalation study of CP-690550 in stable renal allograft recipients: preliminary findings of safety, tolerability, effects on lymphocyte subsets and pharmacokinetics. Am J Transpl. 2008;8:1711–8.

Ref. code: 25595829040418WTR

11. Sakimoto T IA. Anti-inflammatory effect of topical administration of tofacitinib on corneal inflammation. Exp Eye Res. 2015;12(145):110–7.

12. Liew SH, Nichols KK, Klamerus KJ, Li JZ, Zhang M FG. Tofacitinib (CP-690550), a Janus Kinase Inhibitor for Dry Eye Disease: Results from a Phase 1/2 Trial. Ophthalmology. 2012;119(7):1328–35.

13. Bachelez H, van de Kerkhof PC, Strohal R, Kubanov A, Valenzuela F, Lee JH, et al. Tofacitinib versus etanercept or placebo in moderate-to-severe chronic plaque psoriasis: A phase 3 randomised non-inferiority trial. Lancet. 2015;386(9993):552–61.

14. Craiglow BG, King BA. Tofacitinib citrate for the treatment of vitiligo: A pathogenesis-directed therapy. JAMA Dermatol. 2015;151(10):1110–2.

15. Xing L, Dai Z, Jabbari A, Cerise JE, Higgins CA, Gong W, et al. Alopecia areata is driven by cytotoxic T lymphocytes and is reversed by JAK inhibition. Nat Med. 2014;20:1043–9.

16. Craiglow BG, King BA. Killing two birds with one stone: oral tofacitinib reverses alopecia universalis in a patient with plaque psoriasis. J Invest Dermatol. 2014;134(12):2988–90.

17. Paladini RD, Saleh J, Qian C, Xu GX, Rubin LL. Modulation of hair growth with small molecule agonists of the hedgehog signaling pathway. J Invest Dermatol. 2005;125:638–46.

18. Alonso L, Fuchs E. The hair cycle. J Cell Sci. 2006;119:391–3.

19. Greco V, Chen T, Rendl M, Schober M, Pasolli HA, Stokes N, et al. A two-step mechanism for stem cell activation during hair regeneration. Cell Stem Cell. 2009;4:155–69.

20. Kawano M, Komi-Kuramochi A, Asada M, Suzuki M, Oki J, Jiang J, et al. Comprehensive analysis of FGF and FGFR expression in skin: FGF18 is highly expressed in hair follicles and capable of inducing anagen from telogen stage hair follicles. J Invest Dermatol. 2005;124:877–85.

21. Kamp H, Geilen CC, Sommer C, Blume-Peytavi U. Regulation of PDGF and PDGF receptor in cultured dermal papilla cells and follicular keratinocytes of the human hair follicle. Exp Dermatol. 2003;12(5):662–72.

22. Rendl M, Lewis L, Fuchs E. Molecular dissection of mesenchymal–epithelial interactions in the hair follicle. PLOS Biol. 2005;3:e331.

Ref. code: 25595829040418WTR

23. Rendl M, Polak L, Fuchs E. BMP signaling in dermal papilla cells is required for their hair follicle-inductive properties. Genes Dev. 2008;22:543–57.

24. Paus R, Foitzik K, Welker P, Bulfone-Paus S, Eichmüller S. Transforming growth factor-β receptor type I and type II expression during murine hair follicle development and cycling. J Invest Dermatol. 1997;109:518–26.

25. Foitzik K, Paus R, Doetschman T, Dotto GP. The TGF-β2 isoform is both a required and sufficient inducer of murine hair follicle morphogenesis. Dev Biol. 1999;212:278–89.

26. Oshimori N, Fuchs E. Paracrine TGF-β signaling counterbalances BMP-mediated repression in hair follicle stem cell activation. Cell Stem Cell. 2012;10:63–75.

27. Zhou P, Byrne C, Jacobs J, Fuchs E. Lymphoid enhancer factor 1 directs hair follicle patterning and epithelial cell fate. Genes Dev. 1995;9:700–13.

28. Kratochwil K, Dull M, Farinas I, Galceran J, Grosschedl R. LEF-1 expression is activated by BMP-4 and regulates inductive tissue interactions in tooth and hair development. Genes Dev. 1996;10:1382–94.

29. Ambler CA, Watt FM. Expression of Notch pathway genes in mammalian epidermis and modulation by β-catenin. Dev Dyn. 2007;236:1595–601.

30. Craiglow BG, Tavares D, King BA. Topical Ruxolitinib for the Treatment of Alopecia Universalis. JAMA Dermatol. 2016;152(4):490–1.

31. Gordon KA, Tosti A. Alopecia: evaluation and treatment. Clin Cosmet Investig Dermatol. 2011;4:101–6.

32. Pathomvanich D, Pongratananukul S, Thienthaworn P, Manoshai S. A random study of Asian male androgenetic alopecia in Bangkok, Thailand. Dermatol Surg. 2002;28:804–7.

33. Tru¨eb RM. Mini-Review Molecular mechanisms of androgenetic alopecia. Exp Gerontol. 2002;37:981–90.

34. Inui S, Itami S. Molecular basis of androgenetic alopecia: From androgen to paracrine mediators through dermal papilla. J Dermatol Sci. 2011;61(1):1–6.

35. Jamin C. Androgenetic alopecia. Ann Dermatol Venereol. 2002;129(5 Pt 2):801–3.

Ref. code: 25595829040418WTR

36. Jaworsky C, Kligman AM, Murphy GF. Characterisation of inflammatory infiltrates in male pattern alopecia: implication for pathogenesis. Br J Dermatol. 1992;127:239–46.

37. Rudman SM, Philpott MP, Thomas GA, Kealey T. The role of IGF1 in human skin and its appendages-morphogen as well as mitogen. J Invest Dermatol. 1997;109:770–7.

38. Ozeki M, Tabata Y. Promoted growth of murine hair follicles through controlled release of basic fibroblast growth factor. Tissue Eng. 2002;8(3):359–66.

39. Li W, Li C, Lu Z. Vascular endothelial growth factor and its receptor may be one molecular mechanism for androgenetic alopecia. Med Hypotheses. 2009;72(3):366–7.

40. Stenn KS, Paus R. Controls of hair follicle cycling. Physiol Rev. 2001;81(1):449–94.

41. Olsen EA. Finasteride (1 mg) in the treatment of androgenetic alopecia in men. Aust J Dermatol. 1997;38:A316.

42. Chhipa RR, Halim D, Cheng J, Zhang HY, Mohler JL, Ip C, et al. The Direct Inhibitory Effect of Dutasteride or Finasteride on Androgen Receptor Activity is Cell Line Specific. Prostate. 2013;73(14):1483–94.

43. Mella JM, Perret MC, Manzotti M, Catalano HN, Guyatt G. Efficacy and safety of finasteride therapy for androgenetic alopecia: A systematic review. Arch Dermatol. 2010;146:1141–50.

44. Erdemir F, Harbin A, Hellstrom WJ. 5-alpha reductase inhibitors and erectile dysfunction: The connection. J Sex Med. 2008;5:2917–24.

45. Thompson IM, Goodman PJ, Tangen CM, Lucia MS, Miller GJ, Ford LG, et al. The influence of finasteride on the development of prostate cancer. N Engl J Med. 2003;17(349):215–24.

46. Thompson IM Jr, Goodman PJ, Tangen CM, Parnes HL, Minasian LM, Godley PA, et al. Long-term survival of participants in the prostate cancer prevention trial. N Engl J Med. 2013;369:603–10.

47. Kaufman KD, Olsen EA, Whiting D, Savin R, DeVillez R, Bergfeld W, et al. Finasteride in the treatment of men with androgenetic alopecia. J Am Acad Dermatol. 1998;39:578–89.

Ref. code: 25595829040418WTR

48. Li M, Marubayashi A, Nakaya Y, Fukui K, Arase S. Minoxidil-induced hair growth is mediated by adenosine in cultured dermal papilla cells: possible involvement of sulfonylurea receptor 2B as a target of minoxidil. J Invest Dermatol. 2001;117(6):1594–600.

49. Olsen EA, Dunlap FE, Funicella T, Koperski JA, Swinehart JM, Tschen EH, et al. A randomized clinical trial of 5% topical minoxidil versus 2% topical minoxidil and placebo in the treatment of androgenetic alopecia in men. J Am Acad Dermatol. 2002;47:377–85.

50. La Placa M, Balestri R, Bardazzi F, Vincenzi C. Scalp Psoriasiform Contact Dermatitis with Acute Telogen Effluvium due to Topical Minoxidil Treatment. Skin Appendage Disord. 2016;1(3):141–3.

51. Brown MP. Cytokines, Jaks, Stats, health and disease. Aust NZ J Med. 1999;29(1):73–8.

52. Leonard WJ, O'Shea JJ. JAKS AND STATS: Biological Implications∗. Annu Rev Immunol. 1998;16:293–322.

53. Lai KS, Jin Y, Graham DK, Witthuhn BA, Ihle JN, Liu ET. A kinase-deficient splice variant of the human JAK3 is expressed in hematopoietic and epithelial cancer cells. J Biol Chem. 1995;270(42):25028–36.

54. Wilks AF, Harpur AG, Kurban RR, Ralph SJ, Zürcher G, Ziemiecki A. Two novel protein-tyrosine kinases, each with a second phosphotransferase-related catalytic domain, define a new class of protein kinase. Mol Cell Biol. 1991;11(4):2057–65.

55. Feng J, Witthuhn BA, Matsuda T, Kohlhuber F, Kerr IM, Ihle JN. Activation of Jak2 catalytic activity requires phosphorylation of Y1007 in the kinase activation loop. Mol Cell Biol. 1997;17(5):2497–501.

56. Lindauer K, Loerting T, Liedl KR, Kroemer RT. Prediction of the structure of human Janus kinase 2 (JAK2) comprising the two carboxy-terminal domains reveals a mechanism for autoregulation. Protein Eng. 2001;14(1):27–37.

57. Hornakova T, Chiaretti S, Lemaire MM, Foà R, Ben Abdelali R, Asnafi V, et al. ALL-associated JAK1 mutations confer hypersensitivity to the antiproliferative effect of type I interferon. Blood. 2010;115(16):3287–95.

Ref. code: 25595829040418WTR

58. Funakoshi-Tago M, Tago K, Kasahara T, Parganas E, Ihle JN. Negative regulation of Jak2 by its auto-phosphorylation at tyrosine 913 via the Epo signaling pathway. Cell Signal. 2008;20(11):1995–2001.

59. Zhou YJ, Chen M, Cusack NA, Kimmel LH, Magnuson KS, Boyd JG, et al. Unexpected effects of FERM domain mutations on catalytic activity of Jak3: structural implication for Janus kinases. Mol Cell. 2001;8(5):959–69.

60. Pellegrini S, Dusanter-Fourt I. The structure, regulation and function of the Janus kinases (JAKs) and the signal transducers and activators of transcription (STATs). Eur J Biochem. 1997;248:615–33.

61. Funakoshi-Tago M, Pelletier S, Matsuda T, Parganas E, Ihle JN. Receptor specific downregulation of cytokine signaling by autophosphorylation in the FERM domain of Jak2. EMBO J. 2006;25:4763–72.

62. Darnell JEJ, Kerr IM, Stark GR. Jak-STAT pathways and transcriptional activation in response to IFNs and other extracellular signaling proteins. Science (80-). 1994;264:1415–21.

63. Witthuhn BA, Quelle FW, Silvennoinen O, Yi T, Tang B, Miura O, et al. JAK2 associates with the erythropoietin receptor and is tyrosine phosphorylated and activated following stimulation with erythropoietin. Cell. 1993;74:227–36.

64. Argetsinger LS, Campbell GS, Yang X, Witthuhn BA, Silvennoinen O, Ihle JN, et al. Identification of JAK2 as a growth hormone receptor-associated tyrosine kinase. Cell. 1993;74:237–44.

65. Stahl N, Boulton TG, Farruggella T, Ip NY, Davis S, Witthuhn BA, et al. Association and activation of Jak-Tyk kinases by CNTF-LIF-OSMIL- 6 beta receptor components. Science (80-). 1994;263:92–5.

66. Quelle FW, Sato N, Witthuhn BA, Inhorn RC, Eder M, Miyajima A, et al. JAK2 associates with the beta c chain of the receptor for granulocyte-macrophage colony-stimulating factor, and its activation requires the membrane-proximal region. Mol Cell Biol. 1994;14:4335–41.

67. Russell SM, Johnston JA, Noguchi M, Kawamura M, Bacon CM, Friedmann M, et al. Interaction of IL-2R beta and gamma c chains with Jak1 and Jak3: implications for XSCID and XCID. Science (80-). 1994;266:1042–5.

Ref. code: 25595829040418WTR

68. Colamonici OR, Uyttendaele H, Domanski P, Yan H, Krolewski JJ. p135tyk2, an interferon-alpha-activated tyrosine kinase, is physically associated with an interferon-alpha receptor. J Biol Chem. 1994;269:3518–22.

69. Zou J, Presky DH, Wu CY, Gubler U. Differential associations between the cytoplasmic regions of the interleukin- 12 receptor subunits beta1 and beta2 and JAK kinases. J Biol Chem. 1997;272:6073–7.

70. Baker SJ, Rane SG, Reddy EP. Hematopoietic cytokine receptor signaling. Oncogene. 2007;26(47):6724–37.

71. Jatiani SS, Baker SJ, Silverman LR, Reddy EP. JAK/STAT Pathways in Cytokine Signaling and Myeloproliferative Disorders. Genes Cancer. 2010;1(10):979–93.

72. Schindler C, Strehlow I. Cytokines and STAT signaling. Adv Pharmacol. 2000;47:113–74.

73. Rodig SJ, Meraz MA, White JM, Lampe PA, Riley JK, Arthur CD, et al. Disruption of the Jak1 gene demonstrates obligatory and nonredundant roles of the Jaks in cytokine-induced biologic responses. Cell. 1998;93:373–83.

74. Ware CB, Horowitz MC, Renshaw BR, Hunt JS, Liggitt D, Koblar SA, et al. Targeted disruption of the low-affinity leukemia inhibitory factor receptor gene causes placental, skeletal, neural and metabolic defects and results in perinatal death. Development. 1995;121:1283–99.

75. von Freeden-Jeffry U, Vieira P, Lucian LA, McNeil T, Burdach SE, Murray R. Lymphopenia in interleukin (IL)-7 gene-deleted mice identifies IL-7 as a nonredundant cytokine. J Exp Med. 1995;181:1519–26.

76. Kisseleva T, Bhattacharya S, Braunstein J, Schindler CW. Signaling through the JAK/STAT pathway, recent advances and future challenges. Gene. 2002;285(1–2):1–24.

77. Neubauer H, Cumano A, Mueller M, Wu H, Huffstadt U, Pfeffer K. Jak2 deficiency defines an essential developmental checkpoint in definitive hematopoiesis. Cell. 1998;93:397–409.

78. O'Shea JJ, Gadina M, Schreiber RD. Cytokine Signaling in 2002: New Surprises in the Jak/Stat Pathway. 2002;109(2):121–31.

Ref. code: 25595829040418WTR

79. Velazquez L, Fellous M, Stark GR, Pellegrini S. A protein tyrosine kinase in the Interferon α/β signaling pathway. Cell. 1992;70:313–22.

80. Karaghiosoff M, Neubauer H, Lassnig C, Kovarik P, Schindler H, Pircher H, et al. Partial impairment of cytokine responses in Tyk2-deficient mice. Immunity. 2000;13:549–60.

81. Bogdan C, Rollinghoff M, Diefenbach A. The role of nitric oxide in innate immunity. Immunol Rev. 2000;173:17–26.

82. Cao X, Shores EW, Hu-Li J, Anver MR, Kelsall BL, Russell SM, et al. Defective lymphoid development in mice lacking expression of the common cytokine receptor gamma chain. Immunity. 1995;223–38.

83. Saijo K, Park SY, Ishida Y, Arase H, Saito T. Crucial role of Jak3 in negative selection of self-reactive T cells. J Exp Med. 1997;185:351–6.

84. O'Shea JJ, Holland SM, Staudt LM. JAKs and STATs in immunity, immunodeficiency, and cancer. N Engl J Med. 2013;368(2):161–70.

85. O'Shea JJ, Schwartz DM, Villarino AV, Gadina M, McInnes IB, Laurence A. The JAK-STAT Pathway: Impact on Human Disease and Therapeutic Intervention*. Annu Rev Med. 2015;66:311–28.

86. Murray PJ. The JAK-STAT signaling pathway: input and output integration. J Immunol. 2007;178(5):2623–9.

87. Schaefer TS, Sanders LK, Nathans D. Cooperative transcriptional activity of Jun and Stat3 beta, a short form of Stat3. Proc Natl Acad Sci USA. 1995;92:9097–101.

88. Lin JX, Mietz J, Modi WS, John S, Leonard WJ. Cloning of human Stat5B: reconstitution of interleukin-2-induced Stat5A and Stat5B DNA binding activity in COS-7 cells. J Biol Chem. 1996;271:10738–44.

89. Mertens C, Zhong M, Krishnaraj R, Zou W, Chen X, Darnell JE Jr. Dephosphorylation of phosphotyrosine on STAT1 dimers requires extensive spatial reorientation of the monomers facilitated by the N-terminal domain. Genes Dev. 2006;20(24):3372–81.

90. Khwaja A. The role of Janus kinases in haemapoiesis and haematological malignancy. Br J Haematol. 2006;134:366–84.

91. Horvath CM, Darnell JE. The state of STATs: recent developments in the study of signal transduction to the nucleus. Curr Opin Cell Biol. 1997;9:233–9.

Ref. code: 25595829040418WTR

92. Ihle JN. The Stat family in cytokine signaling. Curr Opin Cell Biol. 2001;13:211–7.

93. Shankaran V, Ikeda H, Bruce AT, White JM, Swanson PE, Old LJ, et al. IFNgamma and lymphocytes prevent primary tumour development and shape tumour immunogenicity. Nature. 2001;410:1107–11.

94. Chin YE, Kitagawa M, Kuida K, Flavell RA, Fu XY. Activation of the STAT signaling pathway can cause expression of caspase 1 and apoptosis. Mol Cell Biol. 1997;17:5328–37.

95. Kumar A, Commane M, Flickinger TW, Horvarth CM, Stark GR. Defective TNF-α induced apoptosis in Stat1 null cells due to low constitutive levels of caspases. Science (80-). 1997;278:1630–2.

96. Park C, Li S, Cha E, Schindler C. Immune response in Stat2 knockout mice. Immunity. 2000;13:795–804 a.

97. Akira S. Roles of STAT3 defined by tissue-specific gene targeting. Oncogene. 2000;19:2607–11.

98. Sano S, Takahama Y, Sugawara T, Kosaka H, Itami S, Yoshikawa K, et al. Stat3 in thymic epithelial cells is essential for postnatal maintenance of thymic architecture and thymocyte survival. Immunity. 2001;15:261–73.

99. Wurster AL, Tanaka T, Grusby MJ. The biology of Stat4 and Stat6 . Oncogene. 2000;19:2577–84.

100. Chitnis T, Najafian N, Benou C, Salama AD, Grusby MJ, Sayegh MH, et al. Effect of targeted disruption of STAT4 and STAT6 on the induction of experimental autoimmune encephalomyelitis. J Clin Invest. 2001;108:739–47.

101. Farrar JD, Smith JD, Murphy TL, Leung S, Stark GR, Murphy KM. Selective loss of type I interferon-induced STAT4 activation caused by a minisatellite insertion in mouse Stat2. Nat Immunol. 2000;1:65–9.

102. Bunting KD, Bradley HL, Hawley TS, Moriggl R, Sorrentino BP, Ihle JN. Reduced lymphomyeloid repopulating activity from adult bone marrow and fetal liver of mice lacking expression of STAT5. Blood. 2002;99:479–87.

103. Snow JW, Abraham N, Ma MC, Abbey NW, Herndier B, Goldsmith MA. STAT5 promotes multilineage hematolymphoid development in vivo through effects on early hematopoietic progenitor cells. Blood. 2002;99:95–101.

Ref. code: 25595829040418WTR

104. Kieslinger M, Woldman I, Moriggl R, Hofmann J, Marine JC, Ihle JN, et al. Antiapoptotic activity of Stat5 required during terminal stages of myeloid differentiation. Genes Dev. 2000;14:232–44.

105. Okamura H, Rao A. Transcriptional regulation in lymphocytes. Curr Opin Cell Biol. 2001;13:239–43.

106. Terabe M, Matsui S, Noben-Trauth N, Chen H, Watson C, Donaldson DD, et al. NKT cell-mediated repression of tumor immunosurveillance by IL-13 and the IL-4R-STAT6 pathway. Nat Immunol. 2000;1:515–20.

107. Irie-Sasaki J, Sasaki T, Matsumoto W, Opavsky A, Cheng M, Welstead G, et al. CD45 is a JAK phosphatase and negatively regulates cytokine receptor signaling. Nature. 2001;409:349–54.

108. Samadi A, Ahmad Nasrollahi S, Hashemi A, Nassiri Kashani M, Firooz A. Janus kinase (JAK) inhibitors for the treatment of skin and hair disorders: A review of literature. J Dermatolog Treat. 2017;1–11.

109. Ortiz-Ibáñez K, Alsina MM, Muñoz-Santos C. Tofacitinib and Other Kinase Inhibitors in the Treatment of Psoriasis. Actas Dermosifiliogr. 2013;104:304–10.

110. Harrison C, Kiladjian JJ, Al-Ali HK, Gisslinger H, Waltzman R, Stalbovskaya V, et al. JAK inhibition with ruxolitinib versus best available therapy for myelofibrosis. N Engl J Med. 2012;366:787–98.

111. Mesa RA. Ruxolitinib, a selective JAK1 and JAK2 inhibitor for the treatment of myeloproliferative neoplasms and psoriasis. IDrugs. 2010;13(6):394–403.

112. Mackay-Wiggan J, Jabbari A, Nguyen N, Cerise JE, Clark C, Ulerio G. Oral ruxolitinib induces hair regrowth in patients with moderate-to-severe alopecia areata. JCI Insight. 2016;1(15):e89790.

113. Papp KA, Menter MA, Raman M, Disch D, Schlichting DE, Gaich C, et al. A randomized phase 2b trial of baricitinib, an oral Janus kinase (JAK) 1/JAK2 inhibitor, in patients with moderate-to-severe psoriasis. Br J Dermatol. 2016;174(6):1266–76.

114. Changelian PS, Flanagan ME, Ball DJ, Kent CR, Magnuson KS, Martin WH, et al. Prevention of organ allograft rejection by a specific Janus kinase 3 inhibitor. Science (80-). 2003;302(5646):875–8.

Ref. code: 25595829040418WTR

115. Meyer DM, Jesson MI, Li X, Elrick MM, Funckes-Shippy CL, Warner JD, et al. Anti-inflammatory activity and neutrophil reductions mediated by the JAK1/JAK3 inhibitor, CP-690,550, in rat adjuvant-induced arthritis. J Inflamm. 2010;7:41.

116. Villarino AV, Tato CM, Stumhofer JS, Yao Z, Cui YK, Hennighausen L, et al. Helper T cell IL-2 production is limited by negative feedback and STAT-dependent cytokine signals. J Exp Med. 2007;204:65–71.

117. Kudlacz E, Conklyn M, Andresen C, Whitney-Pickett C, Changelian P. The JAK-3 inhibitor CP-690550 is a potent anti-inflammatory agent in a murine model of pulmonary eosinophilia. Eur J Pharmacol. 2008;582:154–61.

118. Ghoreschi K, Laurence A, Yang XP, Tato CM, McGeachy MJ, Konkel JE, et al. Generation of pathogenic T(H)17 cells in the absence of TGF-beta signaling. Nature. 2010;467:967–71.

119. Ghoreschi K, Laurence A, O'Shea JJ. Selectivity and therapeutic inhibition of kinases: to be or not to be? Nat Immunol. 2009;10(4):356–60.

120. Papp KA, Menter A, Strober B, Langley RG, Buonanno M, Wolk R, et al. Efficacy and safety of tofacitinib, an oral Janus kinase inhibitor, in the treatment of psoriasis: a Phase 2b randomized placebo-controlled dose-ranging study. Br J Dermatol. 2012;167(3):668–77.

121. Bissonnette R, Iversen L, Sofen H, et al. Tofacitinib withdrawal and retreatment in moderate-to-severe chronic plaque psoriasis: a randomized controlled trial. Br J Dermatol. 2015;172:1395–406.

122. Papp KA, Krueger JG, Feldman SR, Langley RG, Thaci D, Torii H, et al. Tofacitinib, an oral Janus kinase inhibitor, for the treatment of chronic plaque psoriasis: Long-term efficacy and safety results from 2 randomized phase-III studies and 1 open-label long-term extension study. J Am Acad Dermatol. 2016;74(5):841–50.

123. Ports WC, Feldman SR, Gupta P, Tan H, Johnson TR, Bissonnette R. Randomized Pilot Clinical Trial of Tofacitinib Solution for Plaque Psoriasis: Challenges of the Intra-Subject Study Design. J Drugs Dermatol. 2015;14(8):777–84.

124. Papp KA, Bissonnette R, Gooderham M, Feldman SR, Iversen L, Soung J, et al. Treatment of plaque psoriasis with an ointment formulation of the Janus kinase inhibitor, tofacitinib: a Phase 2b randomized clinical trial. BMC Dermatol. 2016;16:15.

Ref. code: 25595829040418WTR

125. Craiglow BG, King BA. Tofacitinib Citrate for the Treatment of Vitiligo A Pathogenesis-Directed Therapy. JAMA Dermatol. 2015;151(10):1110–2.

126. Bissonnette R, Papp KA, Poulin Y, Gooderham M, Raman M, Mallbris L, et al. Topical tofacitinib for atopic dermatitis: a phase IIa randomized trial. Br J Dermatol. 2016;175(5):902–11.

127. Kao L, Chung L, Fiorentino DF. Pathogenesis of dermatomyositis: role of cytokines and interferon. Curr Rheumatol Rep. 2011;13(3):225–32.

128. O'Shea JJ, Schwartz DM, Villarino AV, Gadina M, McInnes IB, Laurence A. The JAK-STAT pathway: impact on human disease and therapeutic intervention. Annu Rev Med. 2015;66:311–28.

129. Morgan BA. The Dermal Papilla: An Instructive Niche for Epithelial Stem and Progenitor Cells in Development and Regeneration of the Hair Follicle. Cold Spring Harb Perspect Med. 2014;4(7):a015180.

130. Westgate GE, Tobin NVB, Desmond J. Review Article The biology of hair diversity. Int J Cosmet Sci. 2013;35(4):329–36.

131. Kishimoto J, Burgeson RE, Morgan BA. Wnt signaling maintains the hair-inducing activity of the dermal papilla. Genes Dev. 2000;14(10):1181–5.

132. Botchkarev VA, Paus R. Molecular biology of hair morphogenesis: development and cycling. J Exp Zool B Mol Dev Evol. 2003;298(1):164–80.

133. Lavker RM, Sun TT, Oshima H, Barrandon Y, Akiyama M, Ferraris C, et al. Hair follicle stem cells. J Investig Dermatol Symp Proc. 2003;8(1):23–8.

134. Andl T, Ahn K, Kairo A, Chu EY, Wine-Lee L, Reddy ST, et al. Epithelial Bmpr1a regulates differentiation and proliferation in postnatal hair follicles and is essential for tooth development. Development. 2004;131(10):2257–68.

135. Mak KK, Chan SY. Epidermal Growth Factor as a Biologic Switch in Hair Growth Cycle. J Biol Chem. 2003;278(28):26120–6.

136. Schmidt-Ullrich R, Paus R. Molecular principles of hair follicle induction and morphogenesis. Bioassays. 2005;27(3):247–61.

137. Foitzik K, Lindner G, Mueller-Roever S, Maurer M, Botchkareva N, Botchkarev V, et al. Control of murine hair follicle regression (catagen) by TGF-beta1 in vivo. FASEB J. 2000;14(5):752–60.

Ref. code: 25595829040418WTR

138. Lindner G, Botchkarev VA, Botchkareva NV, Ling G, van der Veen C, Paus R. Analysis of apoptosis during hair follicle regression (catagen). Am J Pathol. 1997;151(6):1601–17.

139. Oshima H, Rochat A, Kedzia C, Kobayashi K, Barrandon Y. Morphogenesis and Renewal of Hair Follicles from Adult Multipotent Stem Cells. Cell. 2001;104(2):233–45.

140. Tumbar T, Guasch G, Greco V, Blanpain C, Lowry WE, Rendl M, et al. Defining the epithelial stem cell niche in skin. Science (80-). 2004;303(5656):359–63.

141. Kulessa H, Turk G, Hogan BLM. Inhibition of Bmp signaling affects growth and differentiation in the anagen hair follicle. EMBO J. 2000;19(24):6664–74.

142. Müller-Röver S, Handjiski B, van der Veen C, Eichmüller S, Foitzik K, McKay IA, et al. A comprehensive guide for the accurate classification of murine hair follicles in distinct hair cycle stages. J Invest Dermatol. 2001;117(1):3–15.

143. Kos L, Conlon J. An update on alopecia areata. Curr Opin Pediatr. 2009;21(4):475–80.

144. MacDonald Hull SP, Wood ML, Hutchinson PE, Sladden M, Messenger AG. Guidelines for the management of alopecia areata. Br J Dermatol. 2003;149(4):692–9.

145. Friedli A, Labarthe MP, Engelhardt E, Feldmann R, Salomon D, Saurat JH. Pulse methylprednisolone therapy for severe alopecia areata: an open prospective study of 45 patients. J Am Acad Dermatol. 1998;39(4 Pt 1):597–602.

146. Alkhalifah A, Alsantali A, Wang E, McElwee KJ, Shapiro J. Alopecia areata update: part II. Treatment. J Am Acad Dermatol. 2010;62(2):191–202.

147. Tosti A, Bellavista S, Iorizzo M. Alopecia areata: a long term follow-up study of 191 patients. J Am Acad Dermatol. 2006;55(3):438–41.

148. Singh G, Lavanya MS. Topical Immunotherapy in Alopecia Areata. Int J Trichology. 2010;2(1):36–9.

149. Bas Y, Seckin HY, Kalkan G, Takci Z, Citil R, Önder Y, et al. Prevalence and types of androgenetic alopecia in north Anatolian population: A community-based study. J Pak Med Assoc. 2015;65(8):806–9.

150. Nuwaihyd R, Redler S, Heilmann S, Drichel D, Wolf S, Birch P, et al. Investigation of four novel male androgenetic alopecia susceptibility loci: no association with female pattern hair loss. Arch Dermatol Res. 2014;306(4):413–8.

Ref. code: 25595829040418WTR

151. Heilmann S, Kiefer AK, Fricker N, Drichel D, Hillmer AM, Herold C, et al. Androgenetic Alopecia: Identification of Four Genetic Risk Loci and Evidence for the Contribution of WNT Signaling to Its Etiology. J Invest Dermatol. 2013;133(6):1489–96.

152. Rinaldi S, Bussa M, Mascaro A. Update on the treatment of androgenetic alopecia. Eur Rev Med Pharmacol Sci. 2016;20(1):54–8.

153. Divito SJ, Kupper TS. Inhibiting Janus kinases to treat alopecia areata. Nat Med. 2014;20:989–90.

154. Geyfman M, Plikus MV, Treffeisen E, Andersen B, Paus R. Resting no more: re-defining telogen, the maintenance stage of the hair growth cycle. Biol Rev Camb Philos Soc. 2015;90(4):1179–96.

155. Schmidt-Ullrich R, Tobin DJ, Lenhard D, Schneider P, Paus R, Scheidereit C. NF-kB transmits Eda A1/EdaR signaling to activate Shh and cyclin D1 expression, and controls post-initiation hair placode down growth. Development. 2006;133:1045–57.

156. Kellenberger AJ, Tauchi M. Mammalian target of rapamycin complex 1 (mTORC1) may modulate the timing of anagen entry in mouse hair follicles. Exp Dermatol. 2013;22:77–80.

157. Legrand JMD, Roy E, Ellis JJ, Francois M, Brooks AJ, Khosrotehrani K. STAT5 activation in the dermal papilla is important for hair follicle growth phase induction. J Invest Dermatol. 2016;136:1781–91.

158. Stenn KS, Paus R. Control of hair follicle cycling. Physiol Rev. 2001;81(1):449–94.

159. Plikus MV, Mayer JA, de la Cruz D, Baker RE, Maini PK, Maxson R, et al. Cyclic dermal BMP signaling regulates stem cell activation during hair regeneration. Nature. 2008;451:340–4.

160. Jabbari A, Nguyen N, Cerise JE, Ulerio G, de Jong A, Clynes R, et al. Treatment of an alopecia areata patient with tofacitinib results in regrowth of hair and changes in serum and skin biomarkers. Exp Derm. 2016;25(8):642–3.

161. Faul F, Erdfelder E, Lang A, Buchner A. G*Power 3: A flexible statistical power analysis program for the social, behavioural, and biomedical sciences. Behav Res Methods. 2007;39(2):175–91.

Ref. code: 25595829040418WTR

162. Kim EJ, Choi JY, Park BC, Lee B. Platycarya strobilacea S. et Z. Extract Has a High Antioxidant Capacity and Exhibits Hair Growth-promoting Effects in Male C57BL/6 Mice. Prev Nutr Food Sci. 2014;19(3):136–44.

163. Ramos PM, Brianezi G, Martins AC, da Silva MG, Marques ME, Miot HA. Apoptosis in follicles of individuals with female pattern hair loss is associated with perifollicular microinflammation. Int J Cosmet Sci. 2016;38(6):651–4.

164. Mahe´ YF, Michelet J, Billoni N, Jarrousse F, Buan B, Commo S, et al. Androgenetic alopecia and microinflammation. Int J Dermatol. 2000;39(8):576–84.

165. Sakr FM, Gado AM, Mohammed HR, Adam AN. Preparation and evaluation of a multimodal minoxidil microemulsion versus minoxidil alone in the treatment of androgenic alopecia of mixed etiology: a pilot study. Drug Des Devel Ther. 2013;7:413–23.

166. Otomo S. Hair growth effect of minoxidil. Nippon Yakurigaku Zasshi. 2002;119(3):167–74.

167. Messenger AG, Rundegren J. Minoxidil: mechanisms of action on hair growth. Br J Dermatol. 2004;150(2):186–94.

168. Lachgar S, Moukadiri H, Jonca F, Charveron M, Bouhaddioui N, Gall Y, et al. Vascular endothelial growth factor is an autocrine growth factor for hair dermal papilla cells. J Invest Dermatol. 1996;106(1):17–23.

169. Kerbel RS. Therapeutic implications of intrinsic or induced angiogenic growth factor redundancy in tumors revealed. Cancer Cell. 2005;8(4):269–71.

170. Li LF, Guo J GZ. Overexpression of skin protein kinase C-alpha in anagen hair follicles during induced growth of mouse hair. Clin Exp Dermatol. 2003;28(4):429–33.

171. Li LF, Fiedler VC, Kumar R. The potential role of skin protein kinase C isoforms alpha and delta in mouse hair growth induced by diphencyprone-allergic contact dermatitis. J Dermatol. 1999;26(2):98–105.

172. Bae CJ, Shim SB, Jee SW, Lee SH, Kim MR, Lee JW, et al. IL-6, VEGF, KC and RANTES are a major cause of a high irritant dermatitis to phthalic anhydride in C57BL/6 inbred mice. Allergol Int. 2010;59(4):389–97.

173. Craiglow BG, Tavares D, King BA. Topical Ruxolitinib for the Treatment of Alopecia Universalis. JAMA Dermatology. 2016;152(4):490–1.

Ref. code: 25595829040418WTR

174. Gupta AK, Carviel JL, Abramovits W. Efficacy of tofacitinib in treatment of alopecia universalis in two patients. J Eur Acad Dermatol Venereol. 2016;30(8):1373–8.

Ref. code: 25595829040418WTR

APPENDICES

Ref. code: 25595829040418WTR

APPENDIX A
DIGITAL IMAGES OF TREATED AREA

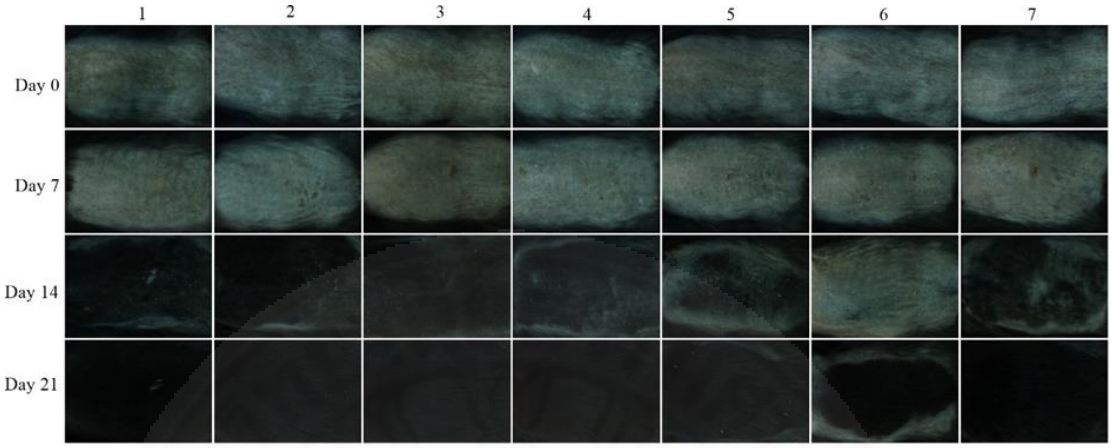

Figure A1 Digital images of treated area: tofacitinib-treated group

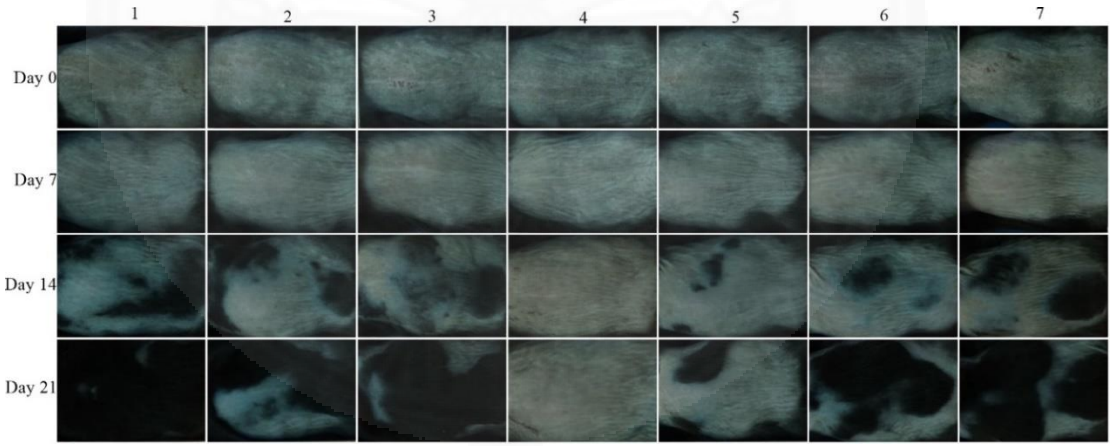

Figure A2 Digital images of treated area: minoxidil-treated group

Ref. code: 25595829040418WTR

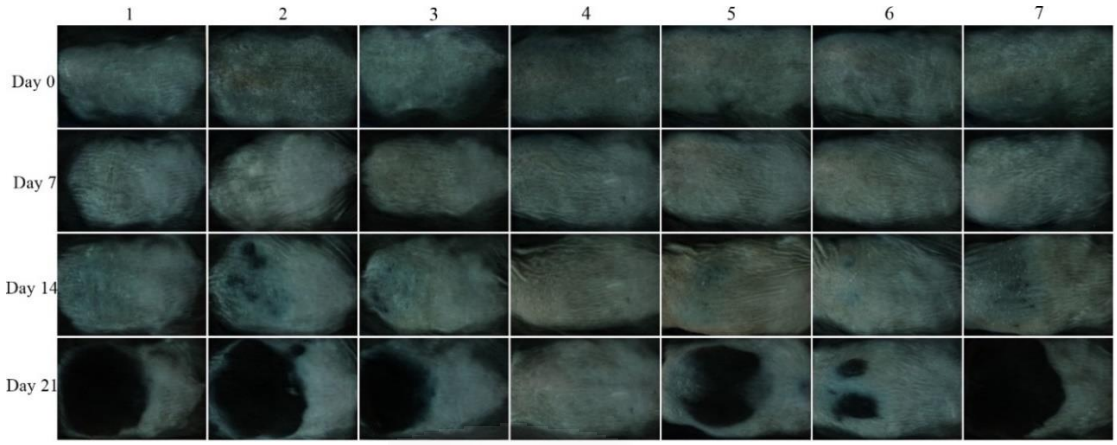

Figure A3 Digital images of treated area: vehicle-treated group (left half: DMSO, right half: ethanol)

Ref. code: 25595829040418WTR

APPENDIX B

DIGITAL MICROSCOPE IMAGES OF TREATED AREA

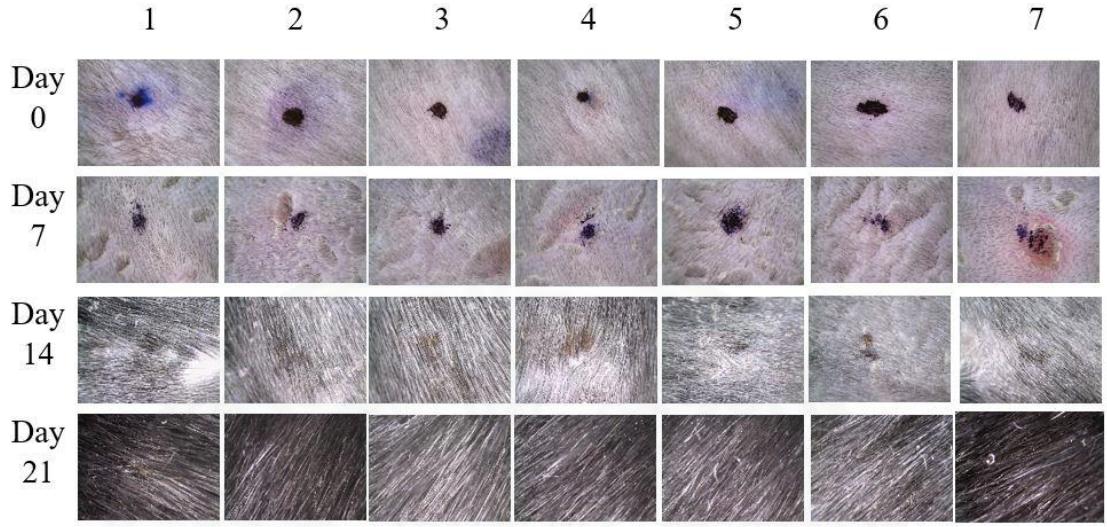

Figure B1 Digital microscope images of treated area: tofacitinib-treated group

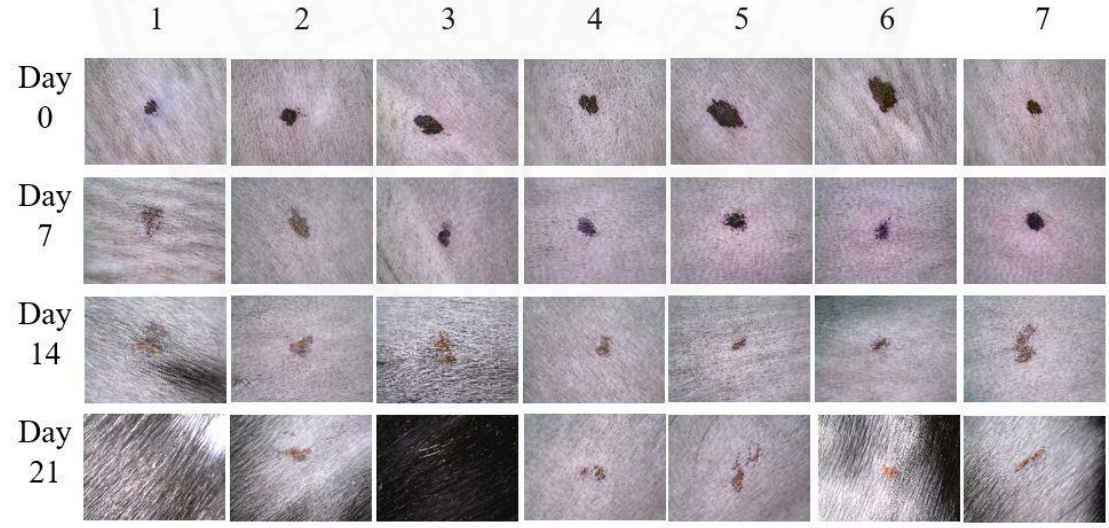

Figure B2 Digital microscope images of treated area: minoxidil-treated group

Ref. code: 25595829040418WTR

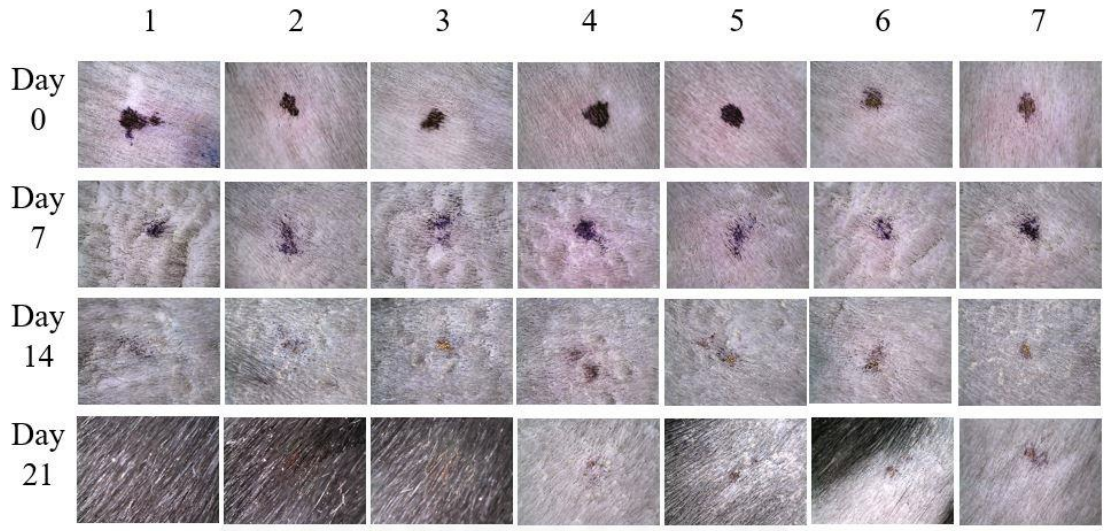

Figure B3 Digital microscope images of treated area: DMSO-treated group

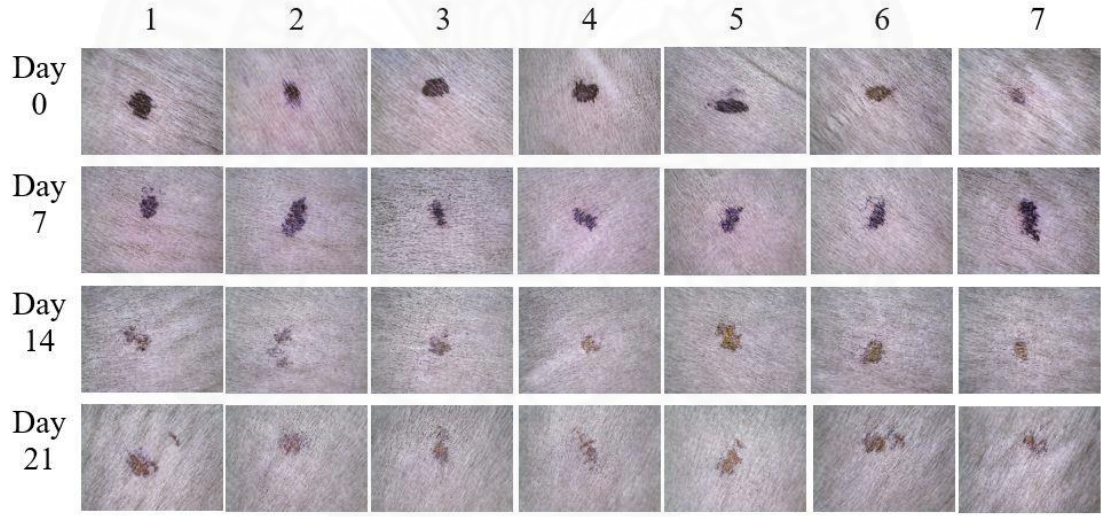

Figure B4 Digital microscope images of treated area: ethanol-treated group

Ref. code: 25595829040418WTR

APPENDIX C

AREA HAIR GROWTH (%)

Table C1 Area hair growth (%)

Treatment group	No.	Area hair growth day 0	Area hair growth day 7	Area hair growth day 14	Area hair growth day 21
Tofacitinib	1	17.55330189	26.21320755	83.60778302	99.85613208
	2	15.69599057	21.22476415	81.49080189	99.97995283
	3	9.473349057	23.79198113	84.88938679	100
	4	20.12051887	30.47641509	69.85141509	100
	5	11.5245283	29.87830189	56.12523585	96.23372642
	6	15.27570755	25.96132075	30.23537736	96.33396226
	7	16.86721698	19.98113208	46.1745283	97.08089623
Minoxidil	1	10.66438679	12.92877358	33.98820755	96.8990566
	2	16.32759434	19.20283019	29.15330189	72.31320755
	3	13.28938679	18.04457547	35.87358491	77.34599057
	4	13.96108491	16.60471698	17.30023585	17.25660377
	5	18.92995283	21.54599057	23.78773585	33.96650943
	6	16.81816038	20.22641509	30.98325472	56.80801887
	7	10.93301887	19.07924528	41.08089623	76.50165094
DMSO	1	27.1754717	36.04009434	36.66226415	82.5009434
	2	16.30377358	24.23396226	40.41226415	83.2509434
	3	23.40943396	37.47688679	38.24622642	74.52311321
	4	22.48254717	30.06179245	30.41415094	33.30660377
	5	16.49716981	23.00283019	24.37924528	59.5254717
	6	25.20377358	25.89198113	27.11556604	34.22264151
	7	20.26745283	21.06745283	21.22216981	98.79622642
Ethanol	1	31.06132075	31.11933962	38.88349057	45.43113208
	2	19.525	21.09528302	27.03867925	34.31415094
	3	47.02216981	43.01415094	44.79669811	45.26839623
	4	31.0990566	34.22971698	32.75801887	33.92216981
	5	17.85849057	16.64009434	18.61084906	32.34528302
	6	16.98443396	25.3754717	30.32877358	35.91132075
	7	27.02311321	27.84528302	27.95235849	29.14575472

No., mouse number

Ref. code: 25595829040418WTR

APPENDIX D

MEAN HAIR LENGTH AND HAIR GROWTH RATE

Table D1 Mean hair length (mm) and hair growth rate (mm/day)

Treatment group	Mouse no.	Mean hair length day 0	Mean hair length day 7	Mean hair length day 14	Mean hair length day 21	Hair growth rate day 0-14
Tofacitinib	1	0.358	0.394	1.063	No	0.0503571
	2	0.285	0.319	1.025	No	0.0528571
	3	0.318	0.337	0.895	No	0.0412143
	4	0.233	0.242	0.886	No	0.0466429
	5	0.275	0.334	0.755	No	0.0342857
	6	0.271	0.325	0.326	No	0.0039286
	7	0.319	0.34	0.63	No	0.0222143
Minoxidil	1	0.269	0.363	0.551	No	0.0201429
	2	0.32	0.326	0.363	0.665	0.0030714
	3	0.278	0.342	0.535	No	0.0183571
	4	0.31	0.334	0.344	0.347	0.0024286
	5	0.264	0.323	0.401	0.424	0.0097857
	6	0.248	0.265	0.33	0.636	0.0058571
	7	0.286	0.304	0.352	0.698	0.0047143
DMSO	1	0.359	0.435	0.453	No	0.0067143
	2	0.288	0.368	0.667	No	0.0270714
	3	0.315	0.381	0.447	No	0.0094286
	4	0.326	0.392	0.403	0.407	0.0055
	5	0.352	0.367	0.377	0.46	0.0017857
	6	0.34	0.353	0.407	No	0.0047857
	7	0.321	0.349	0.353	0.397	0.0022857
Ethanol	1	0.407	0.451	0.478	0.48	0.0050714
	2	0.383	0.411	0.423	0.417	0.0028571
	3	0.357	0.423	0.426	0.422	0.0049286
	4	0.33	0.385	0.389	0.397	0.0042143
	5	0.341	0.337	0.348	0.357	0.0005
	6	0.356	0.384	0.388	0.402	0.0022857
	7	0.383	0.373	0.384	0.397	0.0000714

No, can’t be evaluated

Ref. code: 25595829040418WTR

APPENDIX E
HISTOPATHOLOGICAL IMAGES

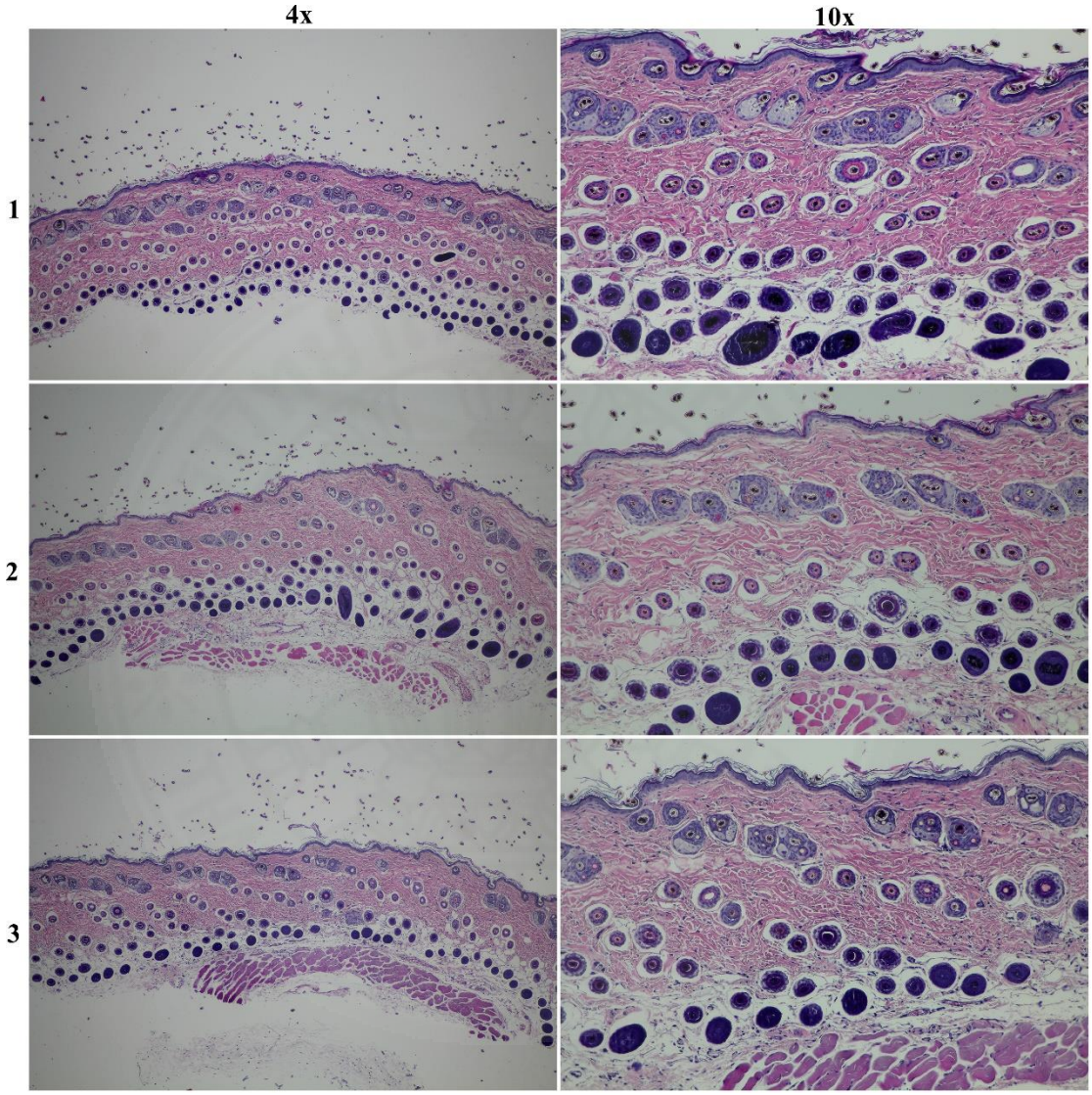

Figure E1 Histopathological images of tofacitinib-treated mice number 1-3

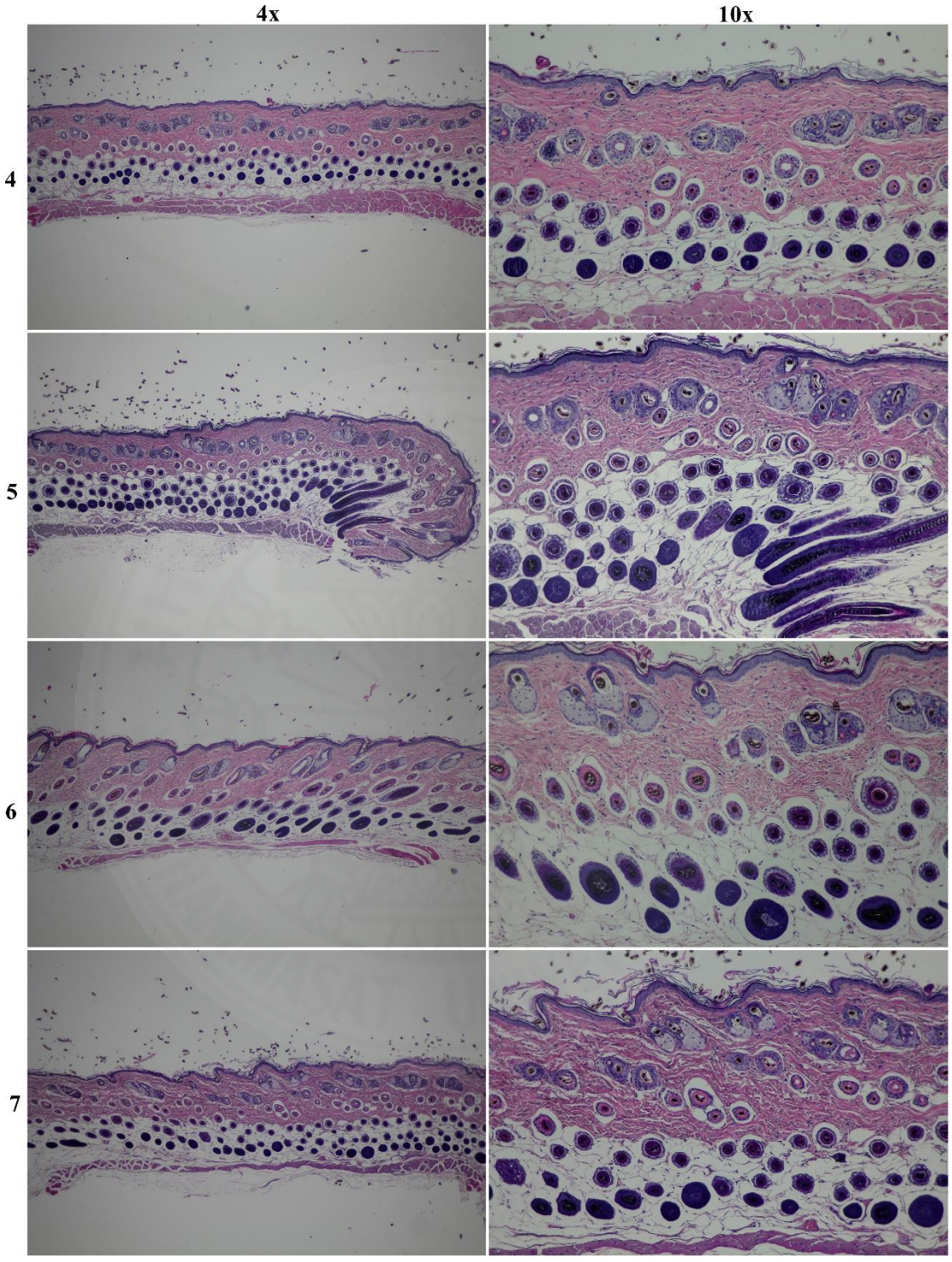

Figure E2 Histopathological images of tofacitinib-treated mice number 4-7

Ref. code: 25595829040418WTR

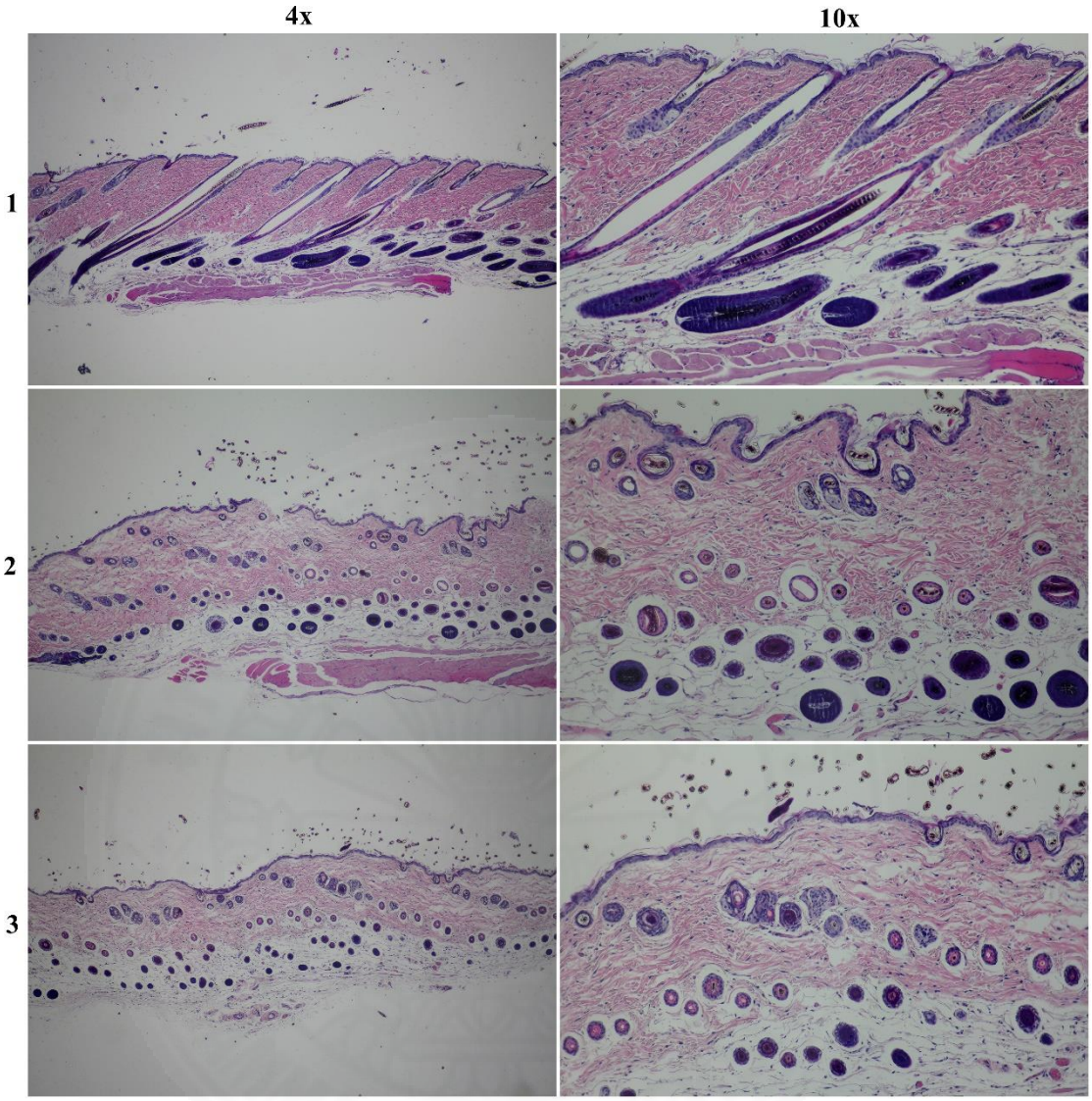

Figure E3 Histopathological images of minoxidil-treated mice number 1-3

Ref. code: 25595829040418WTR

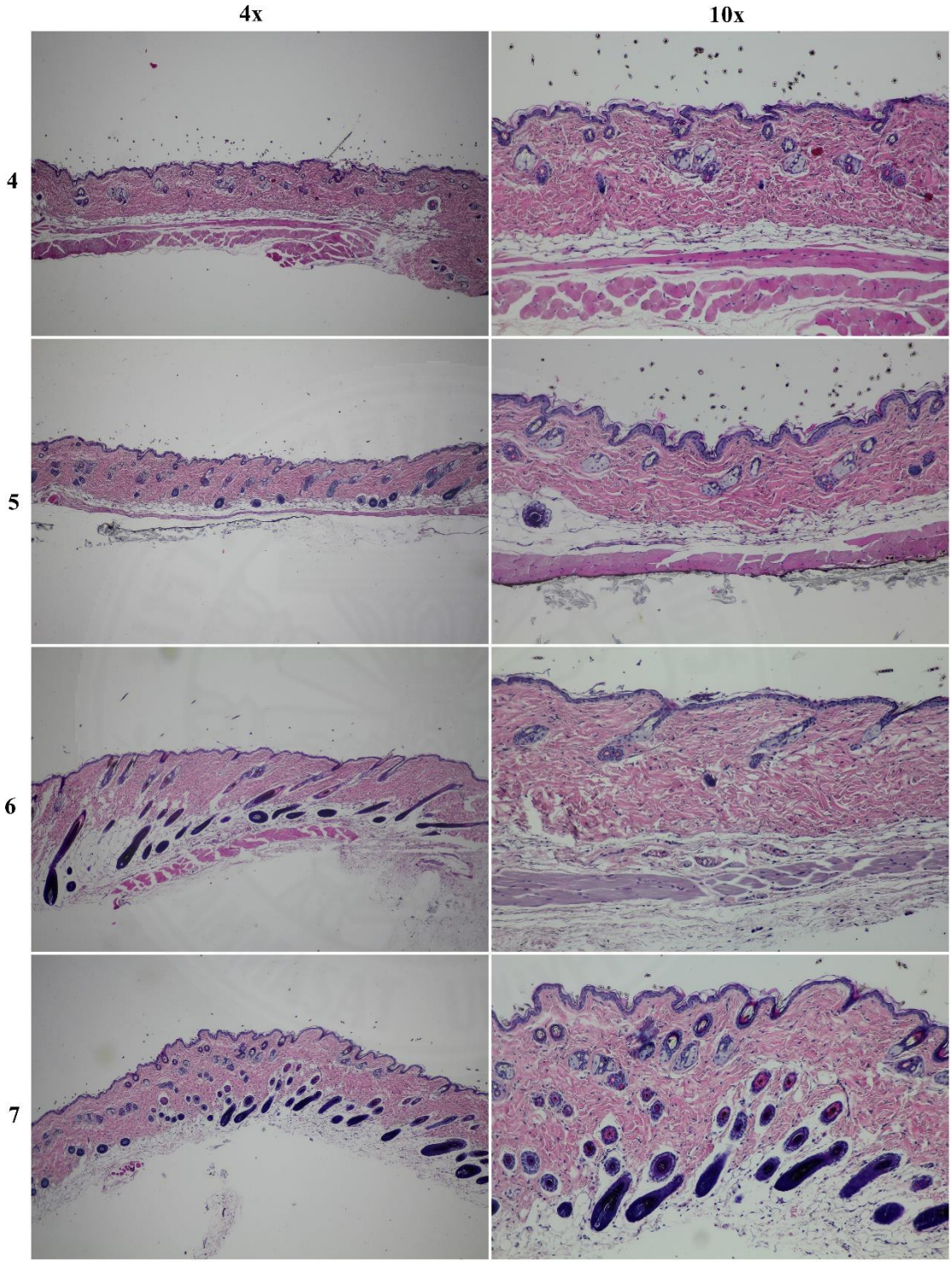

Figure E4 Histopathological images of minoxidil-treated mice number 4-7

Ref. code: 25595829040418WTR

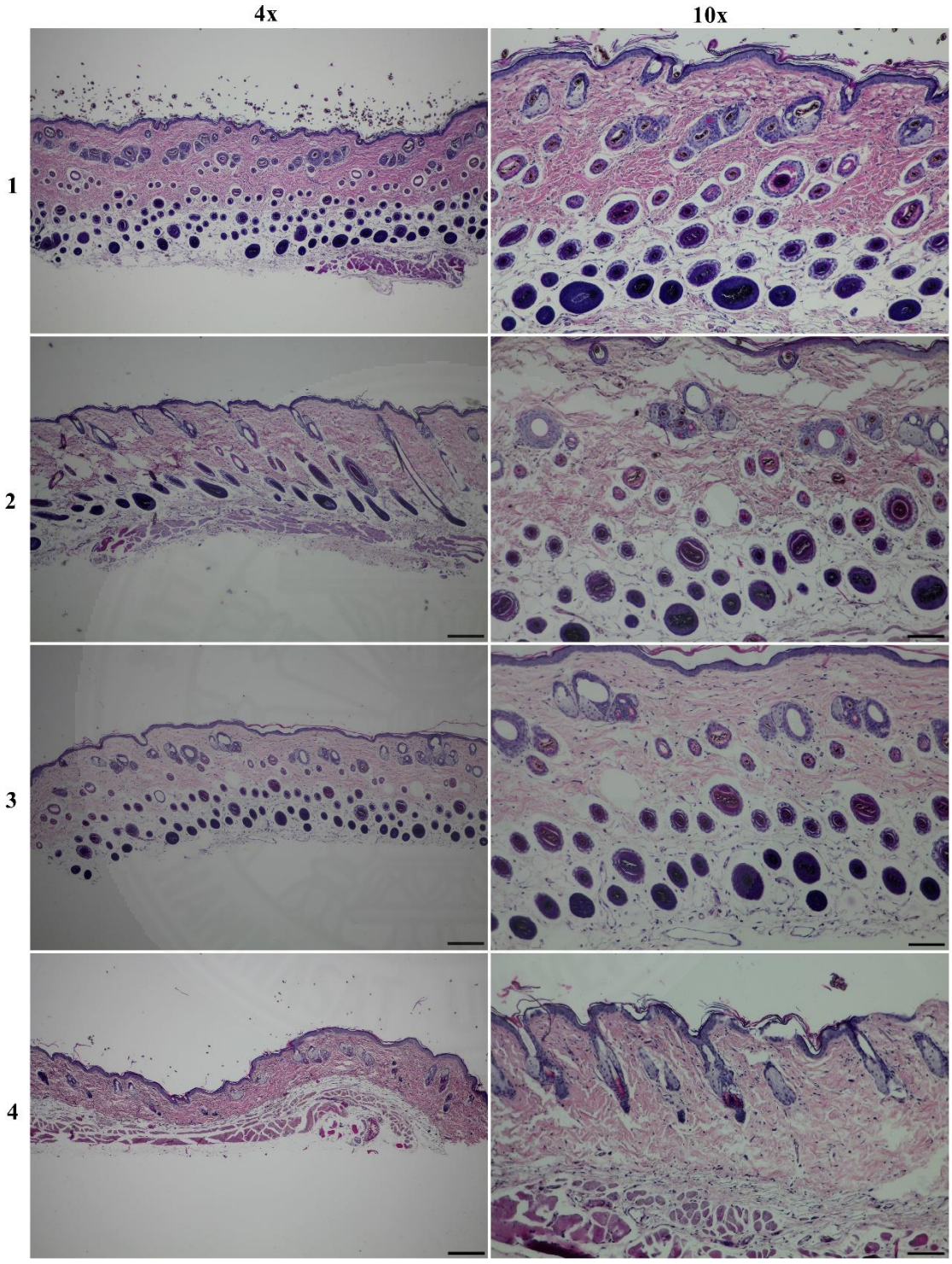

Figure E5 Histopathological images of DMSO-treated mice number 1-4

Ref. code: 25595829040418WTR

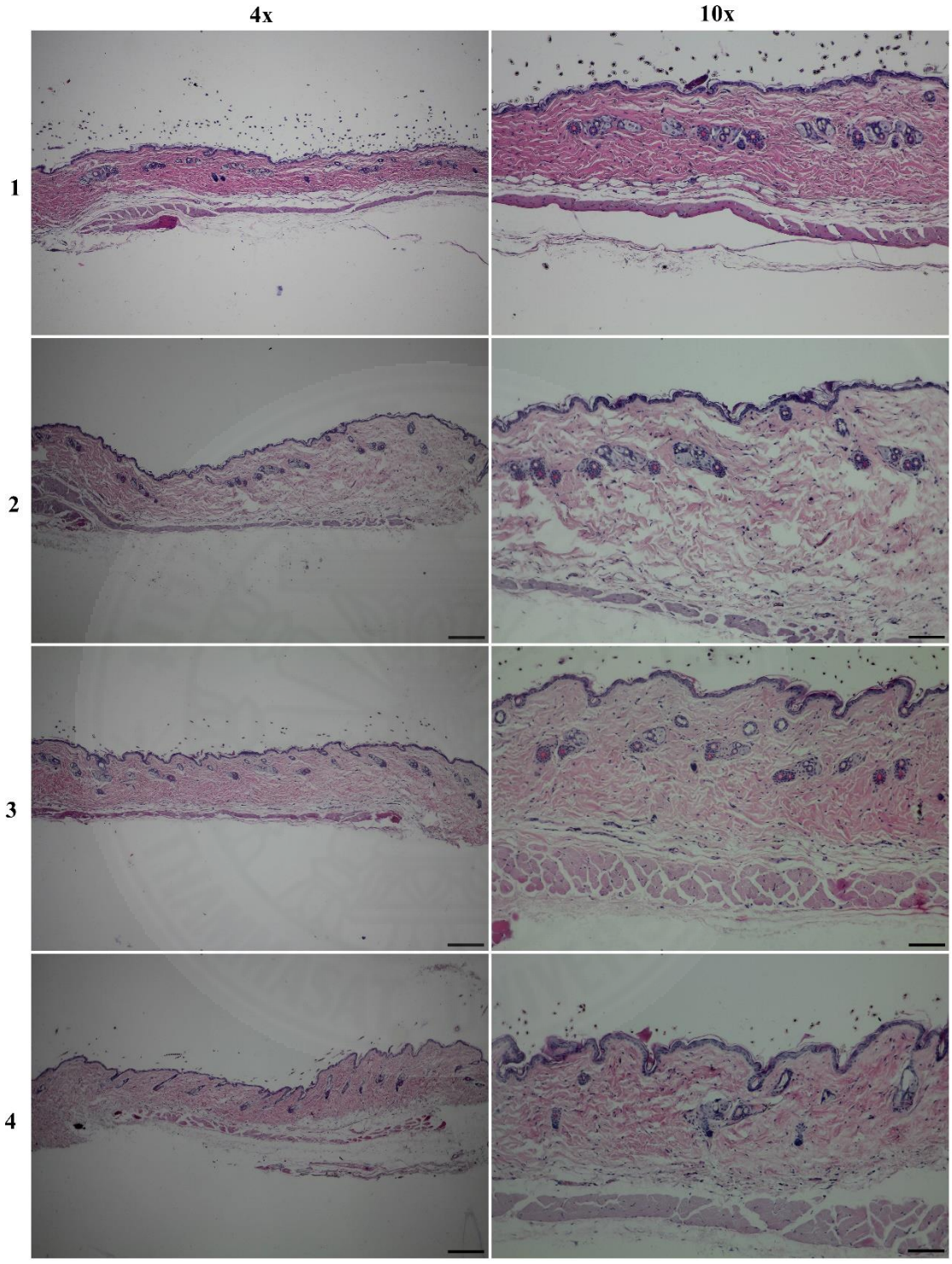

Figure E6 Histopathological images of ethanol-treated mice number 1-4

Ref. code: 25595829040418WTR

APPENDIX F

MAINLY HAIR STAGE

Table F1 Hair stage mainly found in each treated tissue

Treatment	No.	Hair stage (1st tissue)	Hair stage (2nd tissue)
Tofacitinib	1	anagen	anagen
	2	anagen	anagen
	3	anagen	anagen
	4	anagen	anagen
	5	anagen	anagen
	6	anagen	anagen
	7	anagen	anagen
Minoxidil	1	anagen	anagen
	2	anagen	anagen
	3	anagen	anagen
	4	catagen	catagen
	5	catagen	catagen
	6	anagen	catagen
	7	anagen	anagen
DMSO	1	anagen	anagen
	2	anagen	anagen
	3	anagen	anagen
	4	telogen	catagen
Ethanol	1	catagen	catagen
	2	telogen	telogen
	3	telogen	telogen
	4	catagen	catagen

No., mouse number

Ref. code: 25595829040418WTR

APPENDIX G

RNA CONCENTRATION

Table G1 RNA concentration (ng/µL)

Treatment	Mouse no.	RNA Concentration (ng/µL)
Tofacitinib	1	45.35
	2	58.96
	3	115.99
	4	121.07
	5	49.38
	6	29.91
	7	34.73
Minoxidil	1	101.9
	2	117.43
	3	0.16
	4	0.28
	5	1.6
	6	2.59
	7	79.64
DMSO	1	171.87
	2	88.94
	3	62.95
	4	15.42
	5	37.86
	6	4.17
	7	67.9
Ethanol	1	1.06
	2	-3.27
	3	0.23
	4	-0.14
	5	16.08
	6	1.12
	7	-0.26

Ref. code: 25595829040418WTR

APPENDIX H

VEGF AND IGF-1 mRNA EXPRESSION

Table H1 VEGF and IGF-1 mRNA expression

Treatment	Mouse no.	VEGF	IGF-1	VEGF imputation	IGF-1 imputation
Tofacitinib	1	189.13	min A	189.13	1.00
	2	1.00	31.72	.	31.72
	3	129.78	17.89	129.78	17.89
	4	20.01	4.01	20.01	4.01
	5	116.30	81.81	116.30	81.81
	6	118.60	92.85	118.60	.
	7	68.17	12.57	68.17	12.57
Minoxidil	1	10.32	236.09	10.32	236.09
	2	151.27	73.76	.	73.76
	3	min B	min B	.	.
	4	min B	min B	.	.
	5	10.66	1.00	10.66	.
	6	40.17	5.26	40.17	.
	7	63.21	175.46	63.21	175.46
DMSO	1	27.71	36.12	27.71	36.12
	2	28.33	30.24	28.33	30.24
	3	30.00	18.77	30.00	18.77
	4	4.32	1.04	4.32	1.04
	5	41.86	129.38	41.86	129.38
	6	45.01	22.39	45.01	22.39
	7	24.38	27.13	24.38	27.13
Ethanol	1	5.17	min A	5.17	1.00
	2	min B	min B	.	.
	3	min B	min B	.	.
	4	min B	min B	.	.
	5	13.39	min A	13.39	1.00
	6	9.15	min A	9.15	1.00
	7	min B	min B	.	.

min A, very low to be interpreted, imputation with 1.00

min B, too low to be interpreted or error, imputation with . (excluded from calculation)

Outstanding values are imputated with . (excluded from calculation)

Ref. code: 25595829040418WTR

APPENDIX I

EXTRACTED PROTEIN CONCENTRATION

Table I1 Standard curve calculation (for extracted protein concentration)

OD of blank	0.281646	0.296904	0.293871	Average OD of blank = 0.291
OD of standard1	net OD of standard1	OD of standard2	net OD of standard2	Average OD of standard
1.28851	0.998	1.27318	0.982	0.990
0.990283	0.699	0.979236	0.688	0.694
0.715609	0.425	0.715056	0.424	0.425
0.527749	0.237	0.522957	0.232	0.235
0.385115	0.094	0.390836	0.100	0.097
Average OD of standard: y axis			Protein concentration (ug/µL): x axis	
0.990			1	
0.694			0.5	
0.425			0.25	
0.235			0.125	
0.097			0.0625	

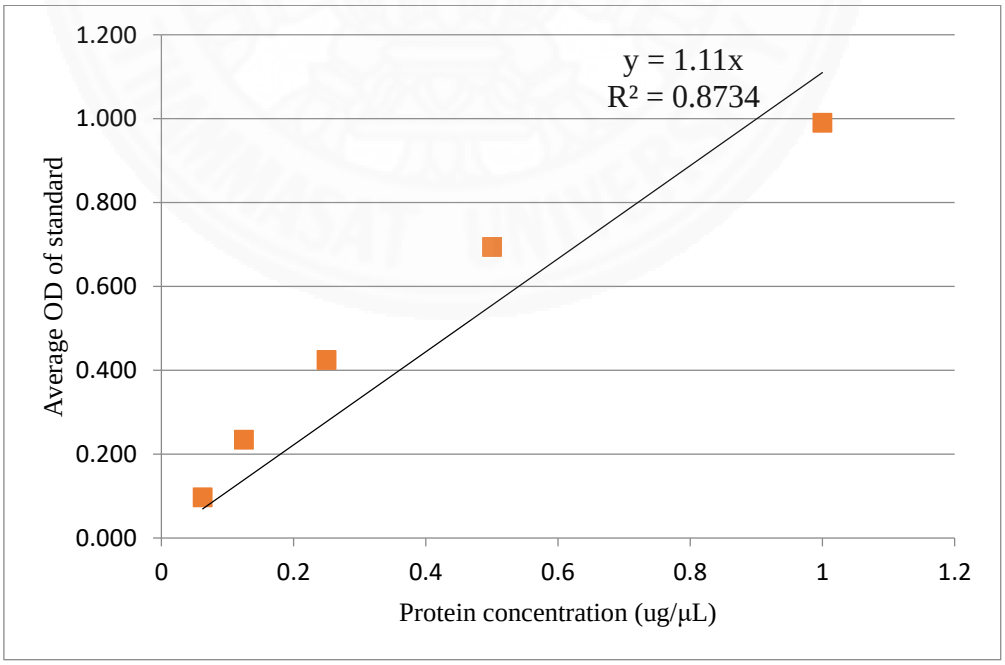

Figure I1 Standard curve for extracted protein concentration calculation

Ref. code: 25595829040418WTR

Table I2 Final protein concentration (μg/μL)

		Raw OD			Net OD			Av OD	x = y/1.11	
Triplicate	df	1	2	3	1	2	3		prot (μg/μL)	*df (μg/μL)
E1	01:10	0.380399	0.586733	0.45747	0.088399	0.294733	0.16547	0.182867	0.164745	1.647453
E2	01:10	0.367874	0.617218	0.471185	0.075874	0.325218	0.179185	0.193426	0.174257	1.742574
E3	01:10	0.399698	0.543046	0.510485	0.107698	0.251046	0.218485	0.19241	0.173342	1.73342
E4	01:10	0.379523	0.733157	0.565468	0.087523	0.441157	0.273468	0.267383	0.240885	2.408853
E5	01:10	0.582552	0.694055	0.638284	0.290552	0.402055	0.346284	0.346297	0.311979	3.119793
E6	01:10	0.534942	0.846764	0.725492	0.242942	0.554764	0.433492	0.410399	0.369729	3.697291
E7	01:10	0.532249	0.6739	0.616614	0.240249	0.3819	0.324614	0.315588	0.284313	2.843132
D1	01:10	0.577999	0.986345	0.757158	0.285999	0.694345	0.465158	0.481834	0.434085	4.340847
D2	01:10	0.535653	0.891549	0.827869	0.243653	0.599549	0.535869	0.45969	0.414135	4.141354
D3	01:10	0.64406	0.920605	0.837129	0.35206	0.628605	0.545129	0.508598	0.458196	4.581964
D4	01:10	0.441385	0.726271	0.605094	0.149385	0.434271	0.313094	0.298917	0.269294	2.692943
D5	01:10	0.769341	0.898267	0.936816	0.477341	0.606267	0.644816	0.576141	0.519046	5.190462
D6	01:10	0.658396	0.936122	0.927394	0.366396	0.644122	0.635394	0.548637	0.494268	4.942679
D7	01:10	0.611472	0.67031	0.74566	0.319472	0.37831	0.45366	0.383814	0.345778	3.457784
M1	01:10	0.641135	0.957999	0.885711	0.349135	0.665999	0.593711	0.536282	0.483137	4.831366
M2	01:10	0.477327	0.587142	0.521422	0.185327	0.295142	0.229422	0.23663	0.21318	2.131805
M3	01:10	0.390138	0.610721	0.519702	0.098138	0.318721	0.227702	0.214854	0.193562	1.935619
M4	01:10	0.420623	0.692873	0.450864	0.128623	0.400873	0.158864	0.229453	0.206715	2.067147
M5	01:10	0.433517	0.601984	0.535564	0.141517	0.309984	0.243564	0.231688	0.208728	2.087282
M6	01:10	0.538191	0.62343	0.544862	0.246191	0.33143	0.252862	0.276828	0.249394	2.493943

Ref. code: 25595829040418WTR

Table I2 Final protein concentration (µg/µL) (Cont.)

		Raw OD			Net OD			Av OD	x = y/1.11	
Triplicate	df	1	2	3	1	2	3		prot (µg/µL)	*df (µg/µL)
M7	01:10	0.519792	0.660831	0.598654	0.227792	0.368831	0.306654	0.301092	0.271254	2.712544
T1	01:10	0.890653	1.03638	1.03268	0.598653	0.74438	0.74068	0.694571	0.62574	6.257396
T2	01:10	0.466611	0.633978	0.526644	0.174611	0.341978	0.234644	0.250411	0.225595	2.255955
T3	01:10	0.490731	0.618093	0.552403	0.198731	0.326093	0.260403	0.261742	0.235804	2.358039
T4	01:10	0.430104	0.566254	0.532893	0.138104	0.274254	0.240893	0.21775	0.196171	1.961715
T5	01:10	0.453313	0.56101	0.537744	0.161313	0.26901	0.245744	0.225356	0.203023	2.030231
T6	01:10	0.559798	0.584699	0.546941	0.267798	0.292699	0.254941	0.271813	0.244876	2.448763
T7	01:10	0.366595	0.452318	0.437845	0.074595	0.160318	0.145845	0.126919	0.114342	1.143417

df, dilution factor. Av, average. prot, protein. OD, optical density. T, tofacitinib. M, minoxidil. D, DMSO. E, ethanol.

Ref. code: 25595829040418WTR

APPENDIX J
VEGF CONCENTRATION

Table J1 Standard optical density

VEGF concentration (pg/mL): x axis	OD (STD)	OD-BLK (0): y axis
1000	1.24975	1.197781
400	0.51673	0.464761
160	0.260802	0.260802
64	0.142683	0.090714
25.6	0.085006	0.033038
10.2	0.064663	0.012694
4.1	0.054404	0.002436
0	0.051969	

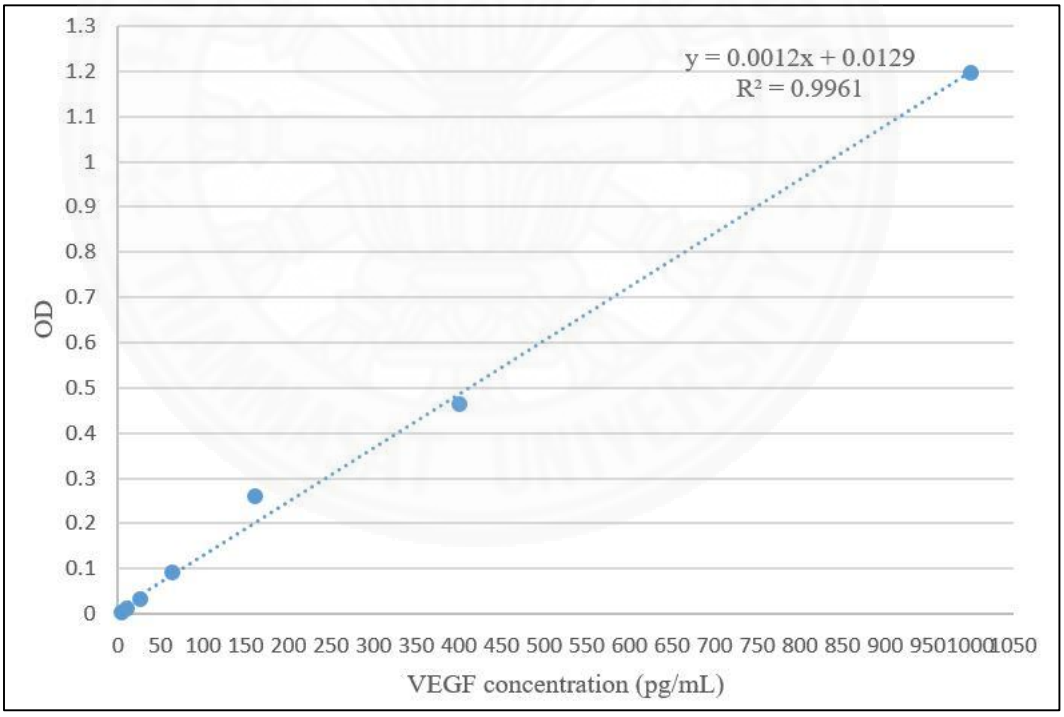

Figure J1 Standard curve for VEGF concentration calculation. STD, standard. OD, optical density.

Equation: x = (y-0.0129)/0.0012

Table J2 VEGF concentration of samples (pg/mL)

Treatment	No.	VEGF concentration (pg/mL)
Tofacitinib	1	331.32625
	2	676.655794
	3	631.330592
	4	530.4940171
	5	1056.200641
	6	1058.740203
	7	1100.910668
Minoxidil	1	488.1499315
	2	1573.358135
	3	1170.26977
	4	561.917333
	5	385.3184998
	6	911.8981421
	7	813.4322101
DMSO	1	638.2722663
	2	603.8049896
	3	598.5002272
	4	504.4120216
	5	793.4571637
	6	474.9747312
	7	589.8269809
Ethanol	1	328.489358
	2	375.4728182
	3	197.1010799
	4	482.860746
	5	460.4622419
	6	236.3826628
	7	524.1306423

No., mouse number

BIOGRAPHY

Name	Miss Jindapa Thummakriengkrai
Date of Birth	January 2, 1988
Educational Attainment	Academic Year 2011: Doctor of Medicine, Mahidol University, Thailand
Work Experiences	2012-2013: General Practice Internship Singburi and Chai Badan Hospital, Thailand

Ref. code: 25595829040418WTR